

QUANTUM SPIN LIQUIDS AND CONNECTIONS WITH NONLINEAR σ MODELS

Thesis submitted in
Partial Fulfilment of the
Degree of Doctor of Philosophy (Ph.D.)
by

Naveen Surendran

Institute of Mathematical Sciences
Madras

UNIVERSITY OF MADRAS

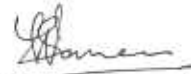
MADRAS 600 005

OCTOBER 2003



DECLARATION

I declare that the thesis entitled *Quantum Spin Liquids and connections with Nonlinear Sigma models*, submitted by me for the Degree of Doctor of Philosophy is the record of work carried out by me during the period from August 1998 to July 2003 under the guidance of Prof. R. Shankar and has not formed the basis for the award of any degree, diploma, associateship, fellowship, titles in this or any other University or other similar institution of higher learning.



Naveen Surendran.

THE INSTITUTE OF MATHEMATICAL SCIENCES

C I T CAMPUS, TARAMANI, CHENNAI 600 113, INDIA

R. Shankar
Professor

Phone: (044)2254 1856, (044)2254 2588

Fax: (044)2254 1586

E-Mail: shankar@imsc.res.in

October 8, 2003

CERTIFICATE

I certify that the thesis entitled **Quantum Spin Liquids and connections with Nonlinear σ models** submitted for the Degree of Doctor of Philosophy by Naveen Surendran is the record of research work carried out by him during the period from August 1998 to July 2003 under my guidance and supervision, and that this work has not formed the basis for the award of any Degree, Diploma, Associateship, Fellowship or other titles in this University or any other university or institution of higher learning. It is further certified that the thesis represents independent work by the candidate and collaboration was necessitated by the nature and scope of the problems dealt with.



Prof. R. Shankar
Thesis Supervisor

October 2003

ACKNOWLEDGEMENTS

Shankar took great interest in the problems that we worked on, always made an effort to get me involved and spend loads of time with me . It was a pleasure working with him and I thank him for everything.

I thank Aad Pruiken who was also involved in the work that forms part of the thesis.

Naveen Surendran.

Contents

1	Introduction	1
1.1	One dimensional systems	3
1.1.1	Uniform chain and Haldane conjecture	5
1.1.2	Dimerised spin chain and the θ term	8
1.1.3	Quantum Hall effect and the physics of θ term	9
1.1.4	Dimerised spin chain and strong coupling NLSM	11
1.2	Two dimensional systems	11
1.2.1	$SrCu_2(BO_3)_2$ and the Shastry-Sutherland model	16
1.3	Magnetisation plateaus	18
1.4	An outline of subsequent chapters	19
2	Haldane mapping for dimerised $SU(2)$ spin chains	21
2.1	Path integral for a single spin in a magnetic field	22
2.1.1	The coherent state basis	22
2.1.2	The generating functional	23
2.1.3	The path integral representation	24
2.2	The dimer system	24
2.2.1	The rotor	25
2.3	Haldane mapping for semi-infinite dimerised spin chain	26
2.3.1	Change of variables	28
2.3.2	Nonlinear sigma model	30
2.4	Nonlinear σ model for a generalised ladder	31
2.5	Validity of Haldane mapping	35

3	Strong coupling NLSM and the edge spin	37
3.1	The edge theory	37
3.2	Edge spin	39
3.3	Correspondence between NLSM edge theory and DSC	41
4	Real space RG for $s = 1/2$ dimerised spin chain.	43
4.1	The decimation scheme	44
4.1.1	The first RG step	44
4.1.2	$s = \frac{1}{2}$ dimer system	45
4.1.3	The free energy for the dimer	47
4.1.4	Fixed points neglecting the time derivatives	48
4.1.5	The derivative expansion and the effective action	49
4.2	RG for the fermionic rotor chain	50
4.2.1	The strong coupling fixed points	52
4.3	NLSM for the fermionic rotor chain	53
4.4	Discussion	54
5	Effective $s = \frac{1}{2}$ models for higher spin dimerised chains	58
5.1	Spin- s dimerised chain	59
5.2	The effective spin- $\frac{1}{2}$ model	59
5.2.1	Schwinger bosons	60
5.2.2	The effective model	63
5.3	Real space RG for the ladder	64
5.3.1	The recurrence relations and the strong coupling fixed point	65
5.4	RG flow in the $1/g - \theta$ plane	67
5.5	Effective model for $s = 1$ chain and the gapless points	67
6	Grassmann σ models and $SU(N)$ spin chains	70
6.1	Grassmannian coherent states	71
6.1.1	$U(N_1 + N_2)$ generators	71
6.1.2	The replica fermion representation	72

6.1.3	Coherent states and the path integral	73
6.1.4	Correlation functions	75
6.2	Haldane mapping for dimerised $SU(N)$ spin chain	76
6.2.1	Change of variables	77
6.2.2	Effective action	78
7	Generalised Shastry-Sutherland models	80
7.1	Generalised Majumdar-Ghosh models	81
7.2	The generalised SSM	82
7.3	Experimental feasibility of the $3 - d$ lattice	85
7.4	Mean field theory for dimer-Néel transition	87
8	Exact magnetisation plateaus for spin- s models	91
8.1	Magnetisation plateaus of generalized SSM	91
8.2	Gelfand ladder	93
8.2.1	Ground state at $B = 0$	94
8.2.2	Magnetisation plateaus	95
8.3	Higher dimensional models	100
8.3.1	A general dimerised model	101
9	Conclusions	103
A	Solid angle for a dimer	106
B	Dimer perturbation theory to all orders	109
B.1	Free Energy	109
B.2	Effective hamiltonian	111

Chapter 1

Introduction

The low energy properties of many strongly correlated electronic systems can be described by an effective theory in terms of just the spin degrees of freedom. Heisenberg model, one of the simplest interacting model, has been successfully used to describe many such systems. It has also been studied as a theoretical model on its own right. The hamiltonian has the form,

$$H = \sum_{ij} J_{ij} \mathbf{S}_i \cdot \mathbf{S}_j . \quad (1.1)$$

where \mathbf{S}_i 's obey the $SU(2)$ algebra; $[S_i^a, S_j^b] = i \delta_{ij} \epsilon^{abc} S_i^c$. The above interaction has its origin in Pauli's exclusion principle and depending on the form of the electronic wave functions, J_{ij} 's can be either positive (antiferromagnetic) or negative (ferromagnetic).

At low temperatures the system will predominantly be in its low energy states. The first question then one asks is, what is the ground state? Classically, the ferromagnetic ground state consists of all spins pointing in the same direction - the fully ferromagnetic state. This is independent of the structure of the lattice or the range of the interactions. The quantum ground state also consists of all spins polarised in the same direction. This state breaks the rotational symmetry of the hamiltonian and there is a degenerate set of ground states connected to each other through rotations. In the thermodynamic limit, the system gets frozen into one of these states and we have a spontaneously broken symmetry.

For the antiferromagnetic case, say, for a bipartite lattice, the classical ground state consists of all spins of one sub-lattice pointing in one direction and the spins in the other sub-lattice in the opposite direction (Néel state). For non-bipartite lattices, the classical ground state can be more complex. It can be easily seen that in all the cases, the classical ground state is not even an eigen state of the quantum hamiltonian. The determination of the ground state of the Heisenberg antiferromagnet (HAFM) for even the simplest of cases is a highly non-trivial problem.

What one would like to know first about the ground state is whether the rotational symmetry is broken or not. The nature of low energy excitations and hence the low temperature properties depend crucially on this. A broken symmetry would imply the existence of excitations arbitrarily close in energy to the ground state. In the case of a bipartite lattice, spontaneously broken symmetry, or equivalently long range order, means that,

$$\langle P_i S_i \rangle \neq 0 \quad \text{and} \quad \lim_{|i-j| \rightarrow 0} \langle P_i S_i \cdot P_j S_j \rangle \neq 0 ,$$

where P_i is +1 for sub-lattice A and -1 for sub-lattice B .

The tendency of pairs of antiferromagnetically interacting spins to align anti-parallel opens up the interesting possibility of competing interactions. It may not always be possible to saturate every bond to its minimum energy, even classically, and the system is then said to be frustrated. The interplay of frustration and quantum fluctuations can lead to novel ground states and excitations, especially in low dimensions. Frustration, in general, favors disorder and in combination with low dimensionality can give rise to a variety of 'Spin liquids' in which the spins are not correlated over long distances.

There are some frustrated systems which have a macroscopic degeneracy for the classical ground state. This degeneracy is unrelated to any symmetry of the hamiltonian and is expected to manifest itself in peculiar ways in the quantum case. The quantum fluctuations may lift this degeneracy by picking out a unique ground state. Heisenberg antiferromagnet on the two dimensional Kagomé lattice is a famous example of such a system. For $s = \frac{1}{2}$, the system is known to have a unique singlet ground state with a gap to spin excitations [1], even though the

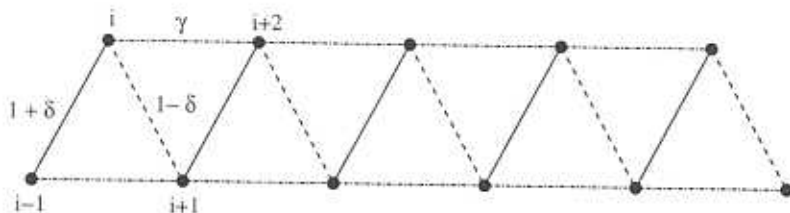


Figure 1.1: Dimerised spin chain with frustrating next-nearest neighbour interaction. The classical ground state has a huge macroscopic degeneracy. The latter property shows up in the form of a continuum of singlets filling up the triplet gap.

In this thesis we have studied the Heisenberg antiferromagnet (HAFM) on various lattices and in different dimensions. In the rest of this chapter we briefly review the systems that have been studied and summarize the work done in the thesis.

1.1 One dimensional systems

At lower dimensions, quantum fluctuations play a greater role. It is known that in one dimension, the ground state is always disordered. But some systems can have ‘quasi long-range order’, in which case the spin correlations fall off as a power-law in the asymptotic limit and the system is gapless. *i.e.*,

$$\langle S_i \rangle = 0; \text{ but, } S_i \cdot S_j \sim \frac{1}{|i-j|^\alpha},$$

where α is some positive fraction.

We will use ‘ $J_1 - J_2 - \delta$ ’ model as a prototype to describe various phases of one dimensional systems. The model has the hamiltonian (see Fig. 1.1),

$$H = J_1 \sum_i [1 + (-1)^i \delta] S_i \cdot S_{i+1} + \gamma J_1 \sum_i S_i \cdot S_{i+2} \quad (1.2)$$

where $\gamma \equiv J_2/J_1$.

Classically, the ground state exists in three phases (see Fig. 1.2). The system is in the Néel phase for weak frustration. For a given δ , beyond a critical value of the frustration, the system goes into a spiral phase. In the spiral phase, adjacent spins make angles θ_1 or θ_2 , depending on whether the bond is weaker or stronger,

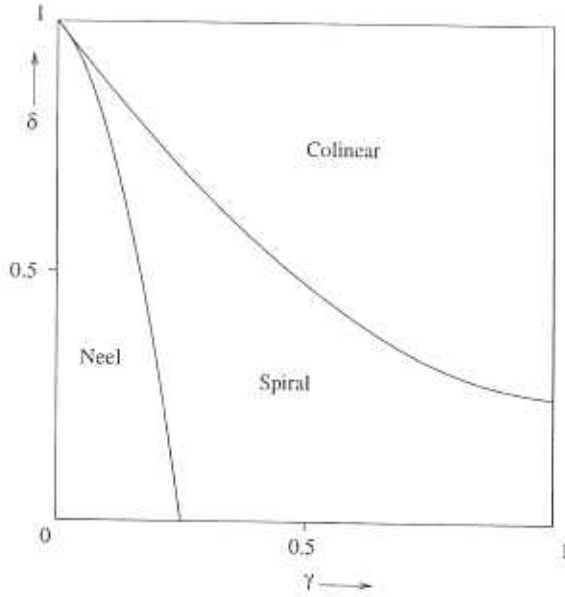


Figure 1.2: Classical phase diagram for the $J_1 - J_2 - \delta$ model.

with the angles determined by δ and γ . At an even stronger frustration, the ground state again becomes collinear in which the spins within each sub-lattice has an anti-parallel arrangement (see Fig. 1.3).

Though the quantum system does not have a broken symmetry, it has some short range order which can distinguish between various 'phases'. Also, in certain regime it has quasi long-range order which makes it gapless.

This model has been studied numerically for $s = \frac{1}{2}$ [2] and $s = 1$ [3] which are the extreme quantum cases. The 'phase diagram' is obtained from the short range correlations of the spin (see Figs. 1.4 and 1.5). The line $1 - \delta = 2\gamma$ demarcates the Néel and spiral phases. For $s = \frac{1}{2}$, the ground state is exactly solvable on this line.

Let (i, j) denote the singlet state, $\frac{1}{\sqrt{2}}(|\uparrow\downarrow\rangle - |\downarrow\uparrow\rangle)$, formed by the spins at sites i and j . Then the state,

$$\dots (-2, -1) (0, 1) (2, 3) (4, 5) \dots \quad (1.3)$$

is the exact ground state on the above line. This state is an extreme case of a spin liquid with zero correlation between spins in different dimers. When $\delta = 0$ (Majumdar-Ghosh point) [4, 5], the system becomes translationally invariant and

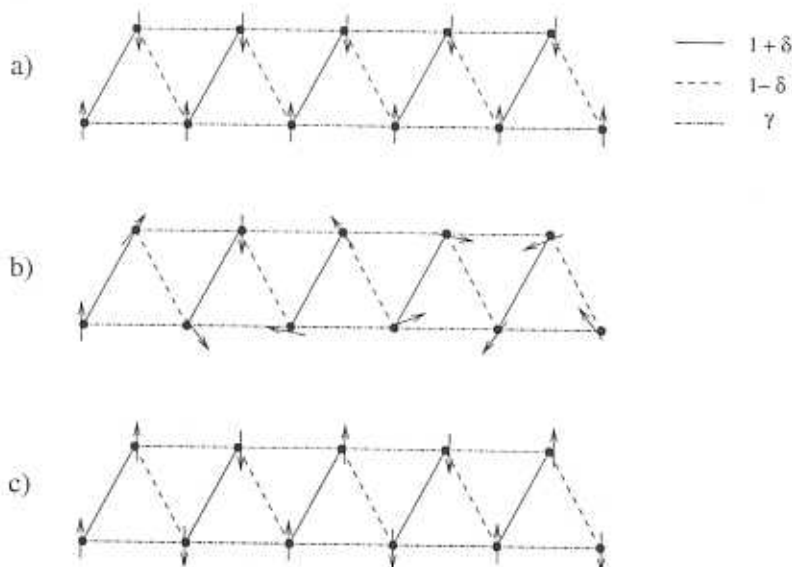


Figure 1.3: a) Néel, b) Spiral and c) Collinear phases.

the translated state

$$\dots (-1, 0) (1, 2) (3, 4) (5, 6) \dots \quad (1.4)$$

becomes degenerate with the state (1.3).

For spin 1, the state (1.3) remains the ground state on the line $1 - \delta = 2\gamma$ for δ greater than a certain critical value (see Fig. 1.5). In general, for spin s , (1.3) is the ground state for $\delta \geq \delta_{cr}(s)$.

1.1.1 Uniform chain and Haldane conjecture

The uniform chain ($\delta = \gamma = 0$) for $s = \frac{1}{2}$ was exactly solved by Bethe using what is now known as Bethe ansatz [6]. From Bethe's solution, it follows that the system is gapless and has quasi long-range order. At that time there was no reason to suspect that spin 1 chain will behave any differently. If anything, $s = 1$ is 'more' towards the classical limit and hence was expected to retain the quasi long-range order and gaplessness. Thus it came as a big surprise when Haldane made the conjecture that all integer spin chains are gapped.

Haldane's conjecture was based on his mapping of the Heisenberg chain in the

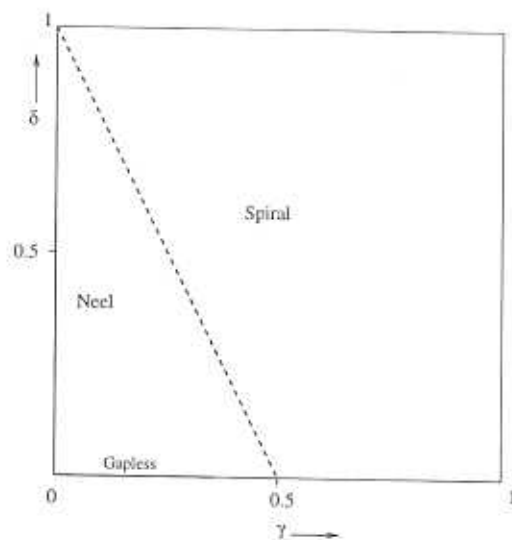


Figure 1.4: Phase diagram for $s = \frac{1}{2} J_1 - J_2 - \delta$ model. The solid line is gapless and on the dashed line, dimer singlet is the exact ground state.

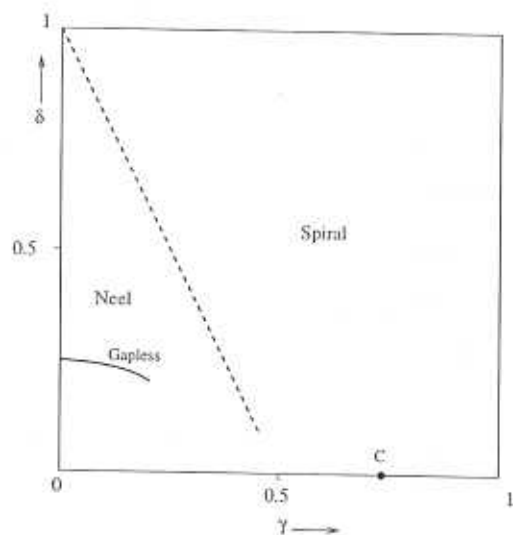


Figure 1.5: Phase diagram for $s = 1 J_1 - J_2 - \delta$ model. The solid curve and the point C are gapless. On the dashed line, dimer singlet is the exact ground state.

long wave-length limit to $O(3)$ nonlinear σ model (NLSM) with the topological θ -term [7, 8]. NLSM has the action,

$$S = \int dx dt \left[\frac{1}{2g} \left(\frac{1}{c} \partial_t \hat{\mathbf{n}} \cdot \partial_t \hat{\mathbf{n}} + c \partial_x \hat{\mathbf{n}} \cdot \partial_x \hat{\mathbf{n}} \right) - \frac{i\theta}{4\pi} \hat{\mathbf{n}} \cdot \partial_t \hat{\mathbf{n}} \times \partial_x \hat{\mathbf{n}} \right], \quad (1.5)$$

$$g = \frac{1}{s}; \quad c = Js \quad \text{and} \quad \theta = 2\pi s. \quad (1.6)$$

For the action to be finite, we have to impose the condition that on the boundary of space-time $\hat{\mathbf{n}}(x, t)$ is a constant, *i.e.*, space-time is topologically a sphere. Then the topological term normalised by 4π is the winding number which counts the number of times the field configuration wraps around the target space S^2 .

Note that,

- For integer s the topological term contributes a phase which is an integer multiple of 2π to the action, which is irrelevant for the path integral. NLSM without θ -term is known to be massive [9, 10].
- For half-integer s the topological term is significant and adds a phase π for configurations in the sectors with odd winding number. And $s = \frac{1}{2}$ chain is known to be gapless from Bethe's solution.

Based on the above facts Haldane made the conjecture that the *uniform chain is gapped for all integer spins and is gapless for all half-integer spins.*

There is a spin-1 model of Affleck, Kennedy, Lieb and Tasaki (AKLT) for which the ground state can be solved exactly [11]. In addition to the Heisenberg term, the hamiltonian also contains a quartic term.

$$H_{aklt} = \sum_i \left[\mathbf{S}_i \cdot \mathbf{S}_{i+1} + \frac{1}{3} (\mathbf{S}_i \cdot \mathbf{S}_{i+1})^2 \right] \quad (1.7)$$

They have also provided a general prescription for constructing models with a so-called valance bond crystal (VBC) ground state. Their idea is based on the fact that a spin- s representation can be obtained as a symmetric product of $2s$ spin- $\frac{1}{2}$ representations. AKLT states are constructed by forming singlets among these spin- $\frac{1}{2}$'s belonging to neighbouring sites. Then the 'parent hamiltonian' for which a given

state is the ground state can be obtained as a polynomial in the scalar product of spin operators.

For $s = 1$, the hamiltonian in (1.7) has the state shown in Fig. 1.6 as the exact ground state. This state has a finite gap to the first excitation. This is considered as a strong support for Haldane's conjecture that all integer spin HAFM chains are gapped.

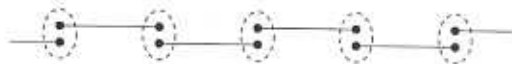


Figure 1.6: AKLT state for spin-1 chain. Dots represent spin- $\frac{1}{2}$'s; dashed ellipses indicate that the spins within are symmetrized and solid lines represent a singlet state

1.1.2 Dimerised spin chain and the θ term

θ -term changes sign under the parity transformation, $\hat{\mathbf{n}} \rightarrow -\hat{\mathbf{n}}$. For the spin chain, parity corresponds to translation by one unit. Thus θ has to be 0 or π for the uniform chain. This suggests that one should break translational invariance explicitly to make θ take arbitrary values. One simple way to do this is to introduce alternating bond strengths, known as *dimerisation* [12]. The dimerised spin chain has the hamiltonian,

$$H = J \sum_I (S_{I,1} \cdot S_{I,2} + \kappa S_{I,2} \cdot S_{I+1,1}) ; \kappa \equiv \frac{1 - \delta}{1 + \delta}$$

Haldane mapping for the above model gives,

$$g \sim \frac{(1 + \kappa)}{\sqrt{\kappa}} ; \quad c = \sqrt{\kappa} J s \quad \text{and} \quad \theta = 4\pi s \frac{\kappa}{(1 + \kappa)} .$$

θ varies from 0 in the limit of completely decoupled dimers to $2\pi s$ for the uniform chain.

One interesting consequence of θ depending on κ is that, at specific values of κ for which $\theta = \pi$, the system becomes gapless. This is true for both integer and half-integer spins. For $s = 1$ this corresponds to the intersection of the gapless

curve with the y -axis (see Fig 1.5). Unfortunately, numerically observed κ_{cr} does not match the value predicted by the NLSM mapping [3]. In fact, from the Haldane mapping, θ does not depend on γ whereas in the actual case it does.

For a spin- s dimerised chain, Haldane mapping predicts s gapless points for integer s and $s + \frac{1}{2}$ for half-integer s . This has an interesting physical picture in terms of AKLT states [13]. The gapless states are interpreted as a sea of valance bonds with a spin- $\frac{1}{2}$ chain floating on the top. Fig. 1.7 illustrates this for $s = \frac{3}{2}$. At each gapless point, one of the valance bonds between neighbouring dimers gets shifted to within the dimers.

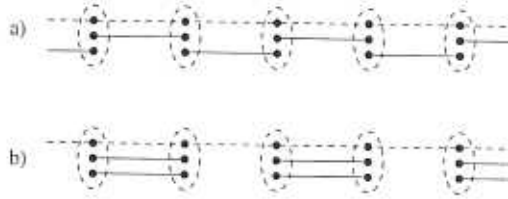


Figure 1.7: Approximate picture for the gapless points of $s = \frac{3}{2}$ dimerised chain. Dots represent spin- $\frac{1}{2}$'s; ellipses indicate that the spins within are symmetrized and solid lines represent a singlet state. Dashed line represents the 'ground state' of uniform spin- $\frac{1}{2}$ chain. a) is first gapless point and b) is the second one at a larger κ_{cr} .

1.1.3 Quantum Hall effect and the physics of θ term

The θ term has a very physical significance in the theory of quantum Hall effect (QHE). Levine *et al.* derived the Grassmann σ model in the replica limit as the two parameter scaling theory for a system of non-interacting electrons in two dimensions in the presence of a disorder potential [14, 15, 16]. This is the relevant theory for integer quantum Hall effect. The Grassmann σ model action is,

$$S = \int d^2x \quad \frac{1}{2} \quad \text{Tr} \left[\frac{\sigma_{xx}}{8} \partial_i Q \partial_i Q - \frac{\sigma_{xy}}{8} \epsilon^{ij} Q \partial_i Q \partial_j Q \right] \quad (1.8)$$

where $Q \in U(N_1 + N_2)/U(N_1) \times U(N_2)$, the Grassmannian manifold. σ_{xx} and σ_{xy} are respectively the longitudinal and Hall conductances. The physical theory

corresponds to the limit $N_1 \rightarrow 0$; $N_2 \rightarrow 0$. For $O(3)$ σ model, $N_1 = N_2 = 1$. The corresponding Grassmannian manifold is S^2 , with

$$Q = \hat{\mathbf{n}} \cdot \boldsymbol{\sigma} = U \sigma^3 U^\dagger ,$$

where $U \in SU(2)$ and σ^a 's are the Pauli matrices.

All Grassmann models in 2 dimensions are topologically equivalent in that, the map from S^2 to any Grassmannian manifold falls under the same homotopy group *i.e.* ,

$$\pi_2 \left(\frac{U(N_1 + N_2)}{U(N_1) \times U(N_2)} \right) = \mathbb{Z}, \text{ the set of integers.}$$

Thus the topological part of the action can be interpreted as the winding number or topological charge.

The physics of QHE tells us that, σ_{xy} is quantized to integer values, whereas σ_{xx} is zero. This means that with renormalization group, σ_{xx} should flow to zero and σ_{xy} to integers in the infra-red limit.

Chiral edge currents are known to exist in quantum Hall systems. Thus we need to allow free boundary conditions. This has an important consequence for the topological term. For fixed boundary condition, *i.e.*, when the edge is identified with a single point, the space has the topology of a sphere. Then the topological charge is an integer and the theory is periodic in σ_{xy} . But with free boundary condition, the topological charge will have a non-integer part and the theory is no longer periodic in σ_{xy} . Here we just mention that the action decouples into 'edge' and 'bulk' parts with all the non-periodicity going into the 'edge' part. At the attractive fixed points of RG ($\sigma_{xx} = 0$, $\sigma_{xy} = n$) the theory is purely edge and is critical.

Large N perturbative calculations done for the CP^{N-1} ($N_1 = N - 1$; $N_2 = 1$) model indicate that σ_{xx} flows to 0 at large length scales *i.e.*, the theory is asymptotically free [17]. Renormalization group flow derived from the 'dilute instanton gas' approximation at weak coupling brought out features like renormalization of σ_{xy} and masslessness at $\sigma_{xy} = 1/2$ [18] (see Fig. 1.8).

The above facts lead one to expect all Grassmann σ models to have the following common features.

- At larger length scales, σ_{xx} renormalizes to 0 and σ_{xy} to integer values.
- $\sigma_{xy} = \frac{1}{2}$ is massless.
- The bulk is gapped for all other values of σ_{xy} , but there are massless edge excitations.

1.1.4 Dimerised spin chain and strong coupling NLSM

From the Haldane mapping for the dimerised spin chain, it follows that the limit $\kappa \rightarrow 0$ corresponds to $g \rightarrow \infty$ and $\theta \rightarrow 0$. *i.e.*, weakly coupled dimers correspond to NLSM at strong coupling near $\theta = 0$. At weaker coupling between dimers, the correlation length gets smaller. The phase diagram for the $s = \frac{1}{2}$ model shows short range Néel order even for small values of κ (see Fig. 1.4). This ensures the validity of the continuum limit.

The RG flow in Fig. 1.8 is based on weak coupling instanton gas picture. In this thesis we have studied the dimerised spin chain with a view to understand $O(3)$ NLSM at strong coupling. To this end we have developed a real space renormalization group (RG) scheme for the dimerised spin chain from which we have obtained the anticipated RG flow. By analysing a semi-infinite chain, we are able to correctly describe the edge physics of the σ model.

1.2 Two dimensional systems

In two dimensions all unfrustrated systems have long range order. Even triangular lattice HAFM, which is frustrated, is ordered [21]. It requires stronger frustration to obtain a disordered ground state. Shastry-Sutherland (SSM) model is HAFM on the square lattice with an additional frustrating coupling which pairs all spins [22]. It is instructive to describe a ‘quadramerized’ version of SSM which has a rich phase diagram [23]. The hamiltonian is,

$$H = J \sum_{\langle i,j \rangle} \mathbf{S}_i \cdot \mathbf{S}_j + \beta J \sum_{\langle k,l \rangle'} \mathbf{S}_k \cdot \mathbf{S}_l + \alpha J \sum_{[m,n]} \mathbf{S}_m \cdot \mathbf{S}_n \quad (1.9)$$

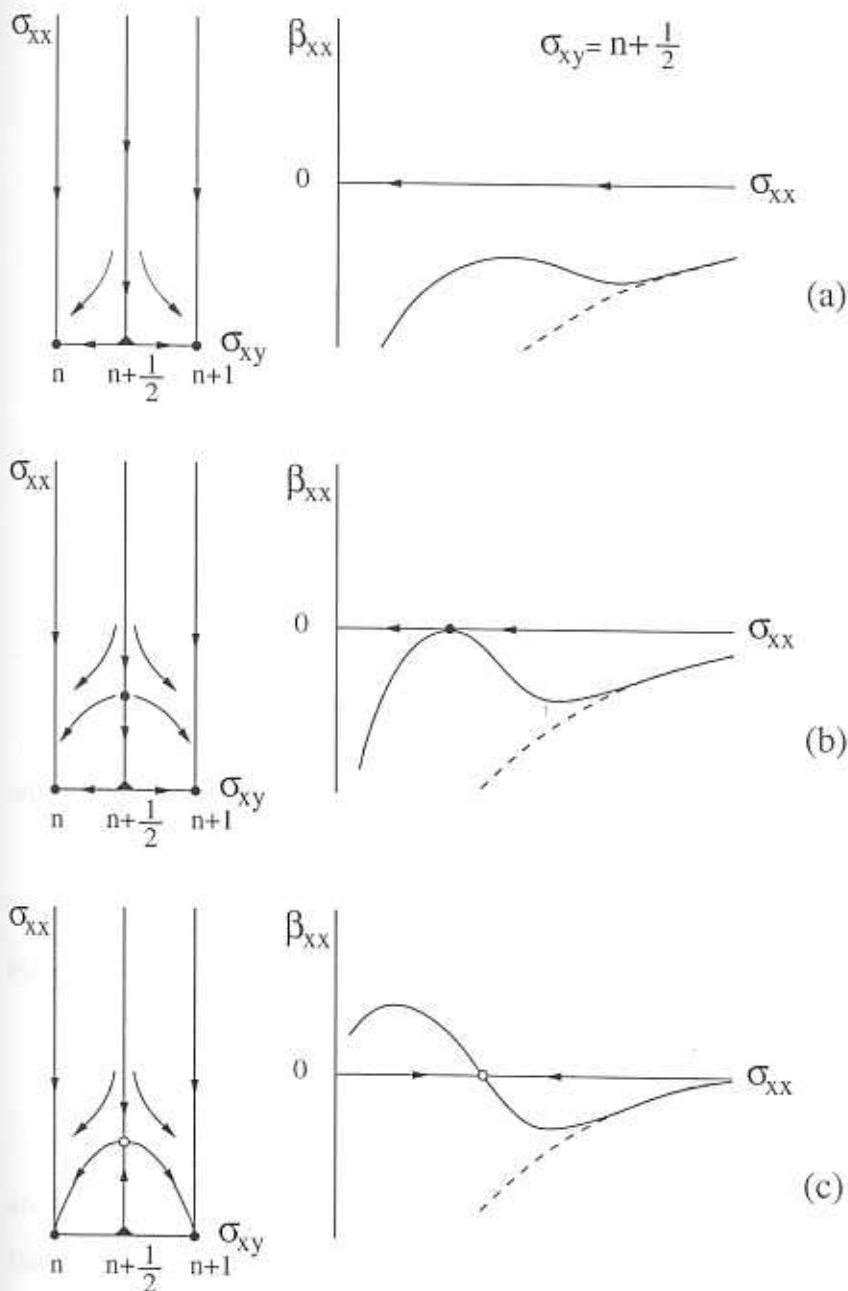


Figure 1.8: The renormalization group flow diagram for different values of N_1 and N_2 . The unstable fixed points may be located at (a) $\sigma_{xx} = 0$ as found in the large N expansion of the CP^{N-1} model; (c) at a finite value of σ_{xx} which is typical for the theory in the limit of small $N_1, N_2 \geq 0$; (b) at a finite value σ_{xx}^* but with *marginally irrelevant* ($\sigma_{xx} > \sigma_{xx}^*$) and *marginally relevant* ($\sigma_{xx} < \sigma_{xx}^*$) directions respectively, rather than plainly *irrelevant* as in (c). This behavior is expected for $N_1 = N_2 = 1$ ($O(3)$) and lies at the interface of cases (a) and (c).

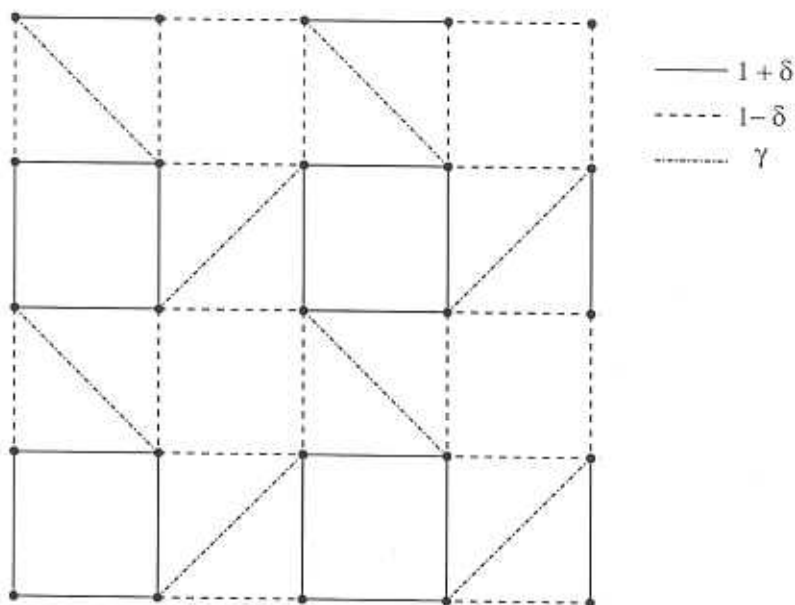


Figure 1.9: Quadramerized Shastry-Sutherland model.

where the different bonds are shown in Fig. 1.9

The classical phase diagram for this model (see Fig. 1.10) is exactly equivalent to that of the one-dimensional $J_1 - J_2 - \delta$ model in Fig. 1.2. For the classical ground state, the two models are connected by the transformation,

$$\delta = \frac{1 - \beta}{1 + \beta} ; \quad \gamma = \frac{\alpha}{1 + \beta} .$$

A qualitative phase diagram for $s = \frac{1}{2}$ quantum model based mostly on numerical analysis is shown in Fig. 1.11. For strong frustration, *i.e.*, large α , dimer-singlet is the ground state. As was discussed in the case of $1 - d$ systems, this is a highly disordered state with zero correlations between spins residing in different dimers. If $\alpha \geq 2$ it can be rigorously shown to be the exact ground state. $\alpha = 0$; $\beta = 1$ is the nearest neighbour square lattice, which has long range Néel order. As the frustration is turned on, the system goes into a disordered plaquette-singlet phase, through a second order transition [24]. It is interesting to note that, on the line $\beta = 1$, the plaquette-phase spontaneously breaks the translational invariance of the hamiltonian. Also the classical spiral phase is completely wiped out from the phase diagram, but the evidence for this is not conclusive [25, 26]. At a stronger frustration,

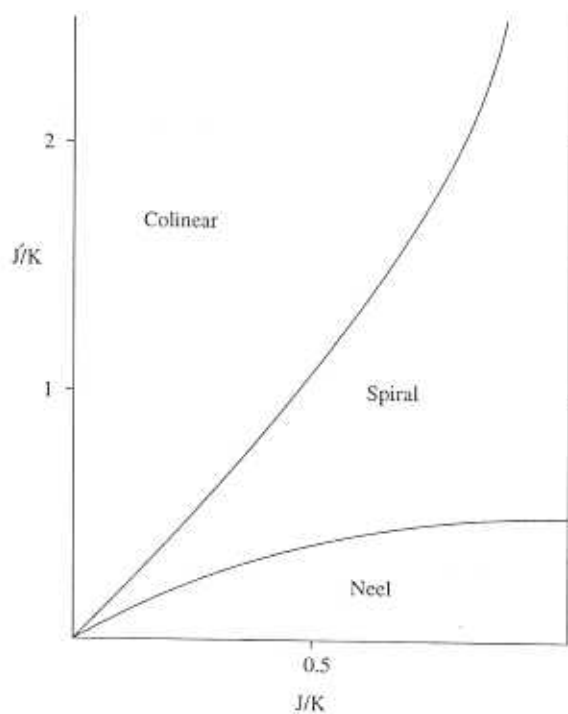


Figure 1.10: Classical phase diagram for the quadrimerized Shastry-Sutherland model.

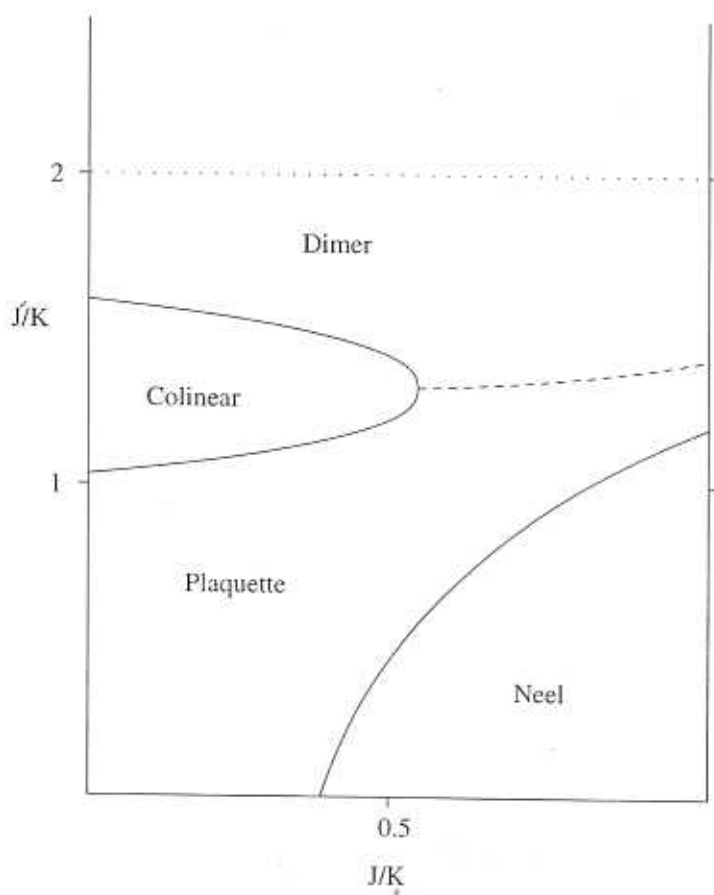


Figure 1.11: Phase diagram for the $s = \frac{1}{2}$ quadrimerized Shastry-Sutherland model. Solid and dashed curves represent second and first order transitions respectively. Above the dotted line, dimer-singlet is rigorously the exact ground state.

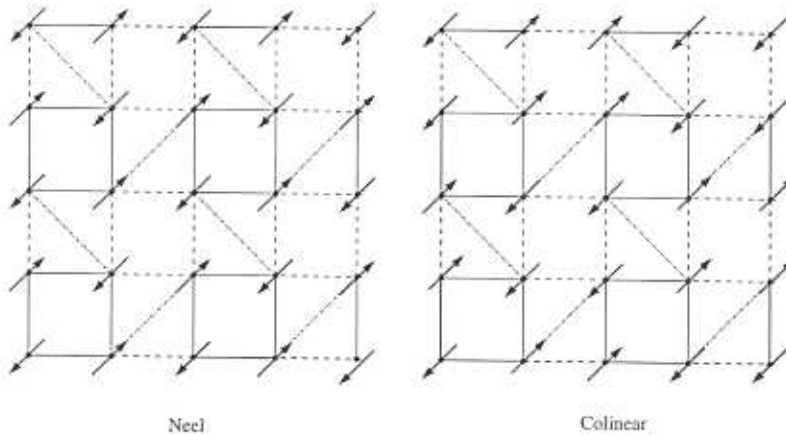


Figure 1.12: Ordering pattern for the Néel and collinear phases

the system goes into the dimer-singlet phase through a first order transition.

Another interesting limit of the model is at $\beta = 0$. As α is increased from 0 to ∞ , the model goes from decoupled ‘plaquettes’ to decoupled ‘dimers’. At $\alpha = 1$, the model is topologically equivalent to one-fifth depleted square lattice. For small α , the ground state is a plaquette ordered singlet. At a critical α , the system first goes into a ‘collinear’ ordered phase. This corresponds to the ‘Néel’ phase of the one-fifth depleted square lattice (see Fig. 1.12). At a higher α the system again becomes disordered, but now it goes into the dimer-singlet.

Shastry-Sutherland model can be looked upon as the two-dimensional analogue of Majumdar-Ghosh model, as both are frustrated systems with exact dimer-singlet ground states. Initially SSM was of theoretical interest because it was perhaps the first two dimensional model with an exact ground state. Recently it was experimentally realized in the compound $SrCu_2(BO_3)_2$ [27, 28].

1.2.1 $SrCu_2(BO_3)_2$ and the Shastry-Sutherland model

The compound $SrCu_2(BO_3)_2$ has a layered structure and the low temperature magnetic properties can be described by a two-dimensional model. Cu^{2+} ions carry a spin $s = \frac{1}{2}$ and the structure of the two-dimensional lattice formed by them is shown in Fig. 1.13a. This is topologically equivalent to Shastry-Sutherland lattice (see Fig.

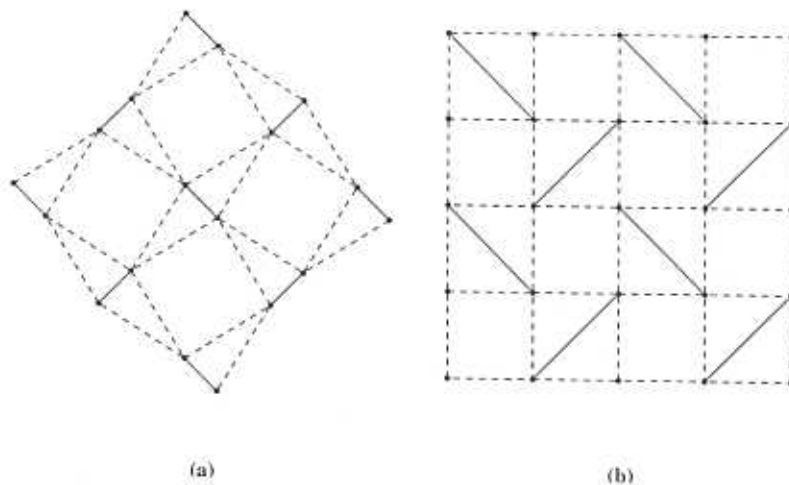


Figure 1.13: (a) Lattice structure of Cu^{2+} ions in $SrCu_2(BO_3)_2$ and (b) the Shastry-Sutherland lattice

1.13b).

$SrCu_2(BO_3)_2$ shows the following features:

1. The magnetic susceptibility has a maximum at around $20K$ and drops rapidly to zero with decreasing temperature. This shows that the ground state is disordered and has spin gap.
2. Low energy neutron scattering experiments shows an almost flat dispersion. This is due to highly localized triplet excitations.
3. At high magnetic fields, magnetisation plateaus have been observed at fractions $1/8$, $1/4$, and $1/3$.

All these features have been understood within the frame-work of SSM.

In this thesis, we have constructed a generalized SSM in arbitrary dimensions. Since mean-field theory becomes exact as $d \rightarrow \infty$, we have been able to do a $1/d$ expansion to probe the model away from $d = \infty$. This provides an extra tool to study the physical two-dimensional model. The general model at $d = 3$ has a physically feasible lattice structure.

1.3 Magnetisation plateaus

Another interesting phenomena shown by low-dimensional spin systems is their response to an external magnetic field. For many one-dimensional models, the magnetisation is not a smooth function of the field, but undergoes discrete jumps and develops plateaus at specific fractions of the full magnetisation. This has also been observed experimentally [29] - [32]. The magnetisation per site, m , is quantized according to the condition [33],

$$n(s - m) = \text{integer}, \quad (1.10)$$

where s is the spin and n , the periodicity of the ground state. At the plateaus, the ground state may or may not break the translational invariance.

$\text{SrCu}_2(\text{BO}_3)_2$ is one of the first two-dimensional systems in which magnetisation plateaus were observed. The plateaus can be understood by treating localized triplets in a sea of singlets as hard-core bosons [34, 35]. In this picture the magnetic field is analogous to the chemical potential and thus decides the density of the triplets. There is a competition between the kinetic and interaction energies of the triplets and at certain densities, it might be energetically favourable for the triplets to crystallize. This can lead to formation of plateaus.

Magnetisation plateaus due to the above mechanism can be demonstrated exactly for some models [36, 37, 38]. The common thread that connect these models is that the ground state at zero field consists of product of dimer-singlets and, more importantly, the total spin on each dimer is a conserved quantity.

In this thesis, we have studied the arbitrary dimensional generalized Shastry-Sutherland model in the presence of an external magnetic field. Ground state can be exactly solved in the large d limit and we have obtained a $1/2$ -plateau.

We have generalized $s = \frac{1}{2}$ models for which plateaus can be solved exactly, to arbitrary values of spin. We have also explored the possibility of two different mechanisms for the plateau formation in different parameter regimes.

1.4 An outline of subsequent chapters

From second to fifth chapter we study the dimerised spin chain and its connections with $O(3)$ σ model. In chapter 6 we derive Grassmann σ models from $SU(N)$ spin chains. In chapters 7 and 8 we study models with exact ground states before we draw conclusions in the final chapter. The following is the detailed break-up of each chapter:

Chapter 2 discusses the Haldane mapping for $SU(2)$ spin chains. We first do the path integral representation for a single spin in a magnetic field in the coherent state basis. Next we do the same for a two-spin system and a rotor and the two are compared. We derive NLSM for a semi-infinite dimerised spin chain as well as for a generalised ladder. The chapter closes with a discussion on the validity of the Haldane mapping.

Chapter 3 describes NLSM at 'bare' strong coupling. We derive the effective edge theory which is exactly equivalent to a single spin system. Correlation functions are calculated from the generating functional for a spin in a magnetic field. We then discuss the correspondence between the edge theory and the dimerised spin chain.

Chapter 4 describes the Renormalization group scheme. We define the RG step of integrating out alternate dimers. Fixed points are found neglecting time derivatives. Then we retain time derivatives and obtain a system of 'fermionic rotor' chain. RG and NLSM derivation are repeated for the general model.

Chapter 5 introduces effective spin- $\frac{1}{2}$ models for higher spin chains. We project a spin- s dimer to the singlet-triplet subspace using a Schwinger boson representation. The effective model obtained has a ladder structure. We do the RG for a general ladder. The effective model for the spin-1 system is used to determine its gapless point.

Chapter 6 gives the derivation of Grassmann σ model for dimerised $SU(N)$ spin

chains. We introduce Grassmann coherent states in a fermionic representation. Using the standard procedure NLSM parameters are derived.

Chapter 7 gives a construction of generalised Shastry-Sutherland model in arbitrary dimensions. We first give a geometric prescription to construct generalised Majumdar-Ghosh models using which the d -dimensional model is constructed. We discuss the physical feasibility of the 3-dimensional model. Using a large- d mean-field expansion we study the Néel-dimer transition and bring out the difference between odd and even dimensions. Ground state energy is corrected to leading order in $1/d$ and this expression is used to estimate the transition point for the physical 2-d case.

Chapter 3 starts with the mean-field solution of generalized SSM the presence of a magnetic field in the large d limit. We then discuss spin- s models with exact magnetisation plateaus. In certain parameter regime we exactly solve the ground state of 'Gelfand ladder' in the presence of a magnetic field for arbitrary s . Beyond the exact point, we argue for a different mechanism for the magnetisation process. The results are extended to a general model.

Chapter 9 summarizes and discusses the results. We outline the possible routes that can be taken in the future.

Appendix A gives the calculation of the solid angle term in the action for a dimer system.

Appendix B describes the calculation of the free energy of a dimer to all orders in κ . We also obtain the effective hamiltonian to all orders, neglecting time derivatives. This is then used to calculate the critical value of κ .

Chapter 2

Haldane mapping for dimerised $SU(2)$ spin chains

In this chapter we review Haldane's mapping by deriving it for a semi-infinite dimerised spin chain (DSC). In the process we take care of the subtlety of the edge while taking the continuum limit. We also do the mapping for a generalised ladder consisting of weakly coupled dimers.

We first do the path integral formalism for a single spin coupled to a magnetic field. Then we do the same for a dimer and discuss the conditions under which a dimer can be approximated by a rotor. This is one of the key approximations in the derivation of NLSM. In the next step we derive NLSM for DSC and the generalised ladder. Finally we discuss the circumstances in which we can expect Haldane mapping to be valid.

We shall follow Fradkin [39] and Affleck [12] for the derivation of the σ model. But there is a difference in our view-point from the theirs. They treat the system as slowly varying in the Néel order parameter, whereas we treat it as a coupled dimer system.

2.1 Path integral for a single spin in a magnetic field

The basic observables of the system are the components of the spin vector \mathbf{S} . They obey the $SU(2)$ algebra,

$$[S^a, S^b] = i\epsilon^{abc} S^c \quad (2.1)$$

The Hilbert space is a spin- s irreducible representation of $SU(2)$,

$$\mathbf{S} \cdot \mathbf{S} |\psi\rangle = s(s+1) |\psi\rangle \quad (2.2)$$

The hamiltonian is given by,

$$H = \mathbf{B}_0 \cdot \mathbf{S} \quad (2.3)$$

Without loss of generality, we can choose the z axis to be along \mathbf{B}_0 . The ground state is then,

$$H| -s\rangle = -sB_0| -s\rangle \quad (2.4)$$

where,

$$S^3|m\rangle = m|m\rangle \quad (2.5)$$

$$m = -s, -s+1, \dots, s$$

2.1.1 The coherent state basis

Consider the set of states [40],

$$|g\rangle \equiv D^\dagger(g)| -s\rangle, \quad (2.6)$$

where $g \in G = SU(2)$ and $D(g)$ is the spin- s representation matrix of g . Let $H \subset G$ denote the $U(1)$ group of rotations about the z axis. We then have,

$$\begin{aligned} D^\dagger(h)| -s\rangle &= e^{-i\Omega}| -s\rangle \\ \Rightarrow |hg\rangle &= e^{-i\Omega}|g\rangle. \end{aligned} \quad (2.7)$$

Hence $|g\rangle$ and $|hg\rangle$ differ only by a phase and represent the same physical state.

The distinct physical states are therefore in one-to-one correspondence with the

coset space $G/H = SU(2)/U(1) = S^2$. We represent the unit vectors $\mathbf{n} \in S^2$ by 2×2 hermitian matrices,

$$Q \equiv \mathbf{n} \cdot \boldsymbol{\sigma}, \quad (2.8)$$

where σ^a 's are the Pauli spin matrices. We then have,

$$\begin{aligned} |Q\rangle &= D^\dagger(g) | -s \rangle, \\ Q &= -g^\dagger \sigma^3 g. \end{aligned} \quad (2.9)$$

The set of coherent states defined above satisfy the following three properties,

1. Resolution of Identity:

$$\int dQ |Q\rangle \langle Q| = \frac{1}{2s+1} I, \quad (2.10)$$

where dQ denotes the normalised measure on the sphere. In polar coordinates,

$$dQ \equiv \frac{1}{4\pi} \sin \theta \, d\theta \, d\phi. \quad (2.11)$$

2. Expectation Value:

$$\langle Q | S^a | Q \rangle = s \frac{1}{2} \text{tr} \sigma^3 Q. \quad (2.12)$$

3. Overlap:

$$\langle Q + \delta Q | Q \rangle = e^{i2s(L^3 + O(\delta Q)^2)}, \quad (2.13)$$

where $L^a \equiv \frac{i}{2} \text{tr}(\sigma^a \delta g g^\dagger)$.

2.1.2 The generating functional

Define the generating functional by looking at the system in a (Euclidean) time dependent magnetic field, $\mathbf{B}(\tau)$, where $\mathbf{B}(0) = \mathbf{B}(\beta) = \mathbf{B}_0$.

$$Z[\mathbf{B}(\tau)] \equiv \text{tr} \mathcal{T}(e^{-\int_0^\beta d\tau \mathbf{B}(\tau) \cdot \mathbf{S}}) \quad (2.14)$$

$Z[\mathbf{B}(\tau)]$ generates the time ordered N point spin-spin correlation functions,

$$\begin{aligned} \frac{1}{Z[\mathbf{B}(\tau)]} \prod_{i=1}^N \frac{\delta^N}{\delta B^{a_i}(\tau_i)} Z[\mathbf{B}(\tau)] |_{\mathbf{B}=\mathbf{B}_0} &= \text{tr}(e^{-\beta H} \mathcal{T}(\prod_i S^{a_i}(\tau_i))) \quad (2.15) \\ &\equiv G_N(\{\tau_i, a_i\}) \end{aligned}$$

where,

$$S^a(\tau) \equiv e^{\beta H} S^a e^{-\beta H} \quad (2.16)$$

2.1.3 The path integral representation

We now derive a path integral representation for the generating functional, $Z[\mathbf{B}(\tau)]$. We divide the interval $0 - \beta$ into N intervals of $\Delta\tau = \beta/N$. We then use the resolution of unity in Eq. (2.10) after each interval to get,

$$Z[\mathbf{B}(\tau)] = \int \prod_{n=0}^{N-1} dQ_n \prod_{m=0}^{N-1} \langle Q_{m+1} | e^{(-\Delta\tau \frac{1}{2} \text{tr} B(m\Delta\tau) Q_m)} | Q_m \rangle \quad (2.17)$$

Where $B(\tau) \equiv B^a(\tau) \sigma^a$ and $Q_N \equiv Q_0$. We can now use Eq. (2.12) and Eq. (2.13) to get,

$$Z[\mathbf{B}(\tau)] = \int \prod_{n=0}^{N-1} dQ_n \prod_{m=0}^{N-1} e^{(\sum_{m=0}^{N-1} \Delta\tau (i2sL^3(m\Delta\tau) - \frac{1}{2} \text{tr} B(m\Delta\tau) Q(m\Delta\tau)))} \quad (2.18)$$

Where we have denoted $Q(m\Delta\tau) \equiv Q_m$. We can now take the limit $N \rightarrow \infty$ to get the path integral,

$$Z[\mathbf{B}(\tau)] = \int \mathcal{D}[Q(\tau)] e^{\int_0^\beta d\tau (i2sL^3(\tau) - \frac{1}{2} \text{tr} B(\tau) Q(\tau))} \quad (2.19)$$

Where $Q(0) = Q(\beta)$. Note that the coefficient of the phase of the functional integrand is an integer ($2s$). This is forced by the requirement of single valuedness of the integrand.

We can write the generating functional in terms of the unit vector defined in Eq. (2.8). We then have,

$$Z[\mathbf{B}(\tau)] = \int \mathcal{D}[\hat{\mathbf{n}}(\tau)] e^{is \int_0^\beta d\tau \int_0^1 ds \hat{\mathbf{n}} \cdot \partial_\tau \hat{\mathbf{n}} \times \partial_s \hat{\mathbf{n}} - \int_0^\beta d\tau \mathbf{B}(\tau) \cdot \hat{\mathbf{n}}(\tau)} \quad (2.20)$$

2.2 The dimer system

Consider a system of two spins, \mathbf{S}_1 and \mathbf{S}_2 . Let H be the Hamiltonian of the system given by,

$$H = \frac{1}{2} (\mathbf{S}_1 + \mathbf{S}_2)^2 \quad (2.21)$$

The Euclidean path integral in the coherent state basis is,

$$Z \equiv e^{-S_{dimer}},$$

where,

$$S_{dimer} = -is \int_0^\beta d\tau \int_0^1 ds \sum_{\alpha=1}^2 \hat{\mathbf{n}}_\alpha \cdot \partial_\tau \hat{\mathbf{n}}_\alpha \times \partial_s \hat{\mathbf{n}}_\alpha + \frac{s^2}{2} \int_0^\beta d\tau (\mathbf{n}_1 + \mathbf{n}_2)^2 \quad (2.22)$$

Define,

$$\mathbf{m} = \frac{(\hat{\mathbf{n}}_1 - \hat{\mathbf{n}}_2)}{2}, \quad (2.23)$$

$$\mathbf{l} = \frac{(\hat{\mathbf{n}}_1 + \hat{\mathbf{n}}_2)}{2}. \quad (2.24)$$

The constraints $\hat{\mathbf{n}}_\alpha \cdot \hat{\mathbf{n}}_\alpha = 1$ translate to $\mathbf{l} \cdot \mathbf{m} = 0$ and $l^2 + m^2 = 1$. Then we have,

$$\hat{\mathbf{n}}_1 = \sqrt{1-l^2} \hat{\mathbf{m}} + \mathbf{l} \quad (2.25)$$

$$\hat{\mathbf{n}}_2 = -\sqrt{1-l^2} \hat{\mathbf{m}} + \mathbf{l}, \quad (2.26)$$

with $|\mathbf{l}|^2 \leq 1$. The action in terms of \mathbf{m} and \mathbf{l} becomes,

$$S_{dimer} = \int_0^\beta d\tau (-2is \mathbf{l} \cdot \hat{\mathbf{m}} \times \partial_\tau \hat{\mathbf{m}} + 2s^2 l^2). \quad (2.27)$$

We refer to Appendix A for the calculation of the solid angle term. Note that the above expression is *exact* and *not an* $O(l^2)$ *expansion*. But it should be mentioned that the integral is globally well-defined only when $\hat{\mathbf{m}} \neq 0$.

We now write down the Hamiltonian and the path integral representation for a rotor and make a comparison with the dimer.

2.2.1 The rotor

The rotor Hamiltonian is,

$$H_{rotor} = \frac{1}{2} \mathbf{L}^2, \quad (2.28)$$

where L^a 's are the angular momentum generators. The action in the path integral representation has the form,

$$S_{rotor} = \int d\tau \frac{1}{2} \partial_\tau \hat{\mathbf{n}} \cdot \partial_\tau \hat{\mathbf{n}}. \quad (2.29)$$

We could obtain the above action by integrating out l from the action for dimer given in Eq.(2.22), except that now the range of l has to be 0 to ∞ unlike for the dimer where, $l \leq 1$. This is the essential difference between the two cases and can be understood as follows.

The Hilbert space of the rotor consists of one representation of each spin- j , $j = 0, 1, 2, \dots, \infty$, the spectrum being $E_j = \frac{1}{2}j(j+1)$. The spin- s dimer has an identical Hilbert space and spectrum, except that it is truncated at $j = 2s$. Thus the approximation becomes exact as $s \rightarrow \infty$.

In the next section we consider a semi-infinite chain consisting of coupled dimers and do the Haldane mapping.

2.3 Haldane mapping for semi-infinite dimerised spin chain

The spins are denoted as $S_{I,\alpha}$ where I is the index for the dimer and α takes values 1 and 2. Within the dimer the bonds are of strength J and the (weak) bonds between dimers are κJ (see Fig. 2.1a). The Hamiltonian is given by,

$$H = J \left[\sum_{I=0}^{\infty} S_{I,1} \cdot S_{I,2} + \kappa \sum_{I=0}^{\infty} S_{I,2} \cdot S_{I+1,1} \right]. \quad (2.30)$$

Notice that for large values of κ the roles of 'dimers' and 'weak bonds' get interchanged. In this case the Hamiltonian can appropriately be written in a *dual representation*

$$\tilde{H} = \tilde{J} \left[S_E \cdot S_{0,1} + \tilde{\kappa} \sum_{I=0}^{\infty} S_{I,1} \cdot S_{I,2} + \sum_{I=0}^{\infty} S_{I,2} \cdot S_{I+1,1} \right]. \quad (2.31)$$

Here, $\tilde{\kappa} = \kappa^{-1}$ and $\tilde{J} = \tilde{\kappa}^{-1}J = \kappa J$. Notice that as $\tilde{\kappa} \rightarrow 0$ the system not only consists of weakly coupled dimers but also has a dangling spin S_E located at the edge (see Fig 2.1b).

The Hamiltonians H and \tilde{H} indicate that apart from edge effects the spin system

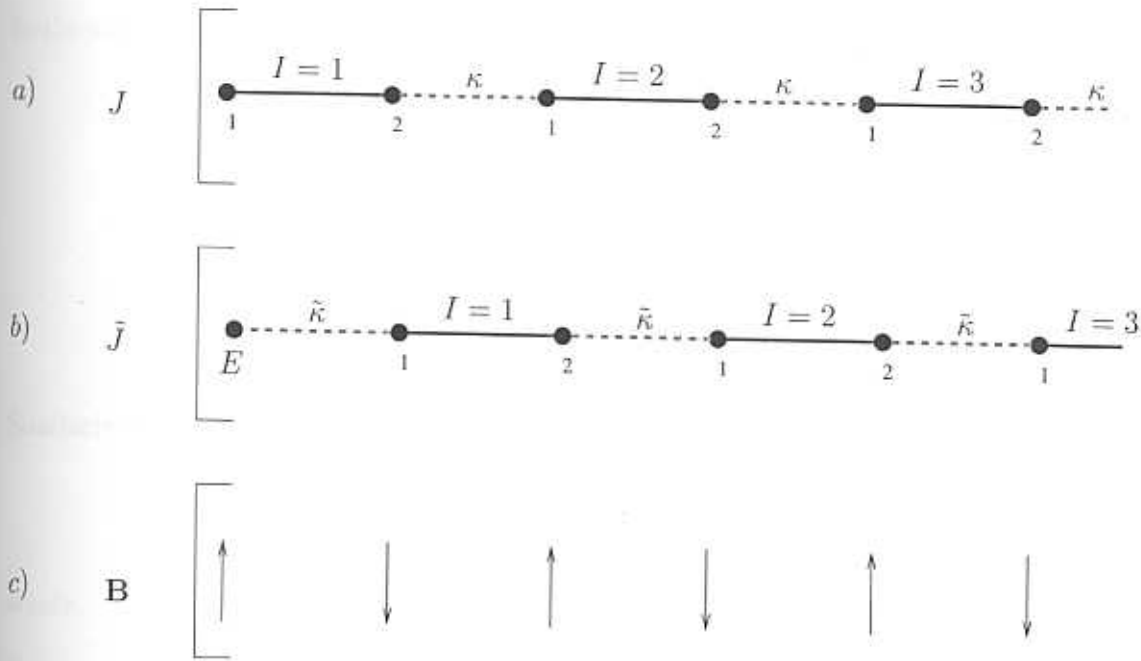


Figure 2.1: Semi-infinite dimerised spin chain with no edge spin (a) and with the edge spin in the dual representation (b). (c) shows the orientation of the staggered magnetic field.

has a *dual symmetry*

$$\begin{aligned}\kappa &\rightarrow \kappa^{-1} \\ J &\rightarrow \kappa J.\end{aligned}\tag{2.32}$$

This symmetry has a different meaning dependent on the value S of the spin. In what follows we shall separately derive the effective action of the spin system in the completely equivalent representations given by H and \tilde{H} respectively.

To proceed it is helpful to introduce a staggered magnetic field \mathbf{B} in H

$$H \rightarrow H + \sum_{I=0}^{\infty} \mathbf{B} \cdot (\mathbf{S}_{I,1} - \mathbf{S}_{I,2}).\tag{2.33}$$

This term favours an anti-ferromagnetic spin arrangement of the semi-infinite chain (see Fig 2.1c). Notice that the same anti-ferromagnetic order is induced by adding the following terms to \tilde{H}

$$\tilde{H} \rightarrow \tilde{H} + \mathbf{B}_0 \cdot \mathbf{S}_E - \sum_{I=0}^{\infty} \mathbf{B} \cdot (\mathbf{S}_{I,1} - \mathbf{S}_{I,2}).\tag{2.34}$$

In the coherent state path integral representation we obtain the action as,

$$\begin{aligned}
S = & \quad is \sum_{I=0}^{\infty} \quad \Omega[\hat{\mathbf{n}}_{I,1}] + \Omega[\hat{\mathbf{n}}_{I,2}] \\
& + s^2 J \int dt \sum_{I=0}^{\infty} \quad \frac{1}{2}(\hat{\mathbf{n}}_{I,1} + \hat{\mathbf{n}}_{I,2})^2 + \kappa \hat{\mathbf{n}}_{I,2} \cdot \hat{\mathbf{n}}_{I+1,1} \\
& + s \int dt \sum_{I=0}^{\infty} \quad \mathbf{B} \cdot (\hat{\mathbf{n}}_{I,1} - \hat{\mathbf{n}}_{I,2}).
\end{aligned} \tag{2.35}$$

Similarly we obtain in the dual representation,

$$\tilde{S} = \tilde{S}_{edge} + \tilde{S}_{bulk}, \tag{2.36}$$

where,

$$\tilde{S}_{edge} = is\Omega[\hat{\mathbf{n}}_E] + s^2 \tilde{J} \int dt \tilde{\kappa} \hat{\mathbf{n}}_E \cdot \hat{\mathbf{n}}_{0,1} + s \int dt \mathbf{B}_0 \cdot \hat{\mathbf{n}}_E \tag{2.37}$$

$$\begin{aligned}
\tilde{S}_{bulk} = & \quad is \sum_{I=0}^{\infty} \quad \Omega[\hat{\mathbf{n}}_{I,1}] + \Omega[\hat{\mathbf{n}}_{I,2}] \\
& + s^2 \tilde{J} \int dt \sum_{I=0}^{\infty} \quad \frac{1}{2}(\hat{\mathbf{n}}_{I,1} + \hat{\mathbf{n}}_{I,2})^2 + \tilde{\kappa} \hat{\mathbf{n}}_{I,2} \cdot \hat{\mathbf{n}}_{I+1,1} \\
& - s \int dt \sum_{I=0}^{\infty} \quad \mathbf{B} \cdot (\hat{\mathbf{n}}_{I,1} - \hat{\mathbf{n}}_{I,2}).
\end{aligned} \tag{2.38}$$

Here,

$$\Omega[\hat{\mathbf{n}}] = \int ds dt \hat{\mathbf{n}} \cdot \partial_t \mathbf{n} \times \partial_s \hat{\mathbf{n}} \tag{2.39}$$

2.3.1 Change of variables

As in the case of the single dimer we now make the change of variables from $\hat{\mathbf{n}}_1$ and $\hat{\mathbf{n}}_2$ to \mathbf{m} and \mathbf{l} defined in Eqs. (2.25) and (2.26). Here the variable \mathbf{m} describes the quantum fluctuations of the *antiferromagnetic* ordering whereas the \mathbf{l} is associated with a *ferromagnetic* ordering of the spin chain. Since one expects the former to control the physics of the problem, the idea next is to eliminate the \mathbf{l} in a standard manner and formulate an effective action in terms of the field variable \mathbf{m} alone.

Using Eqs. (2.25) and (2.26) we can rewrite the different terms in the Action.

$$(\hat{\mathbf{n}}_{I,1} + \hat{\mathbf{n}}_{I,2})^2 = 4l_I^2, \quad (2.40)$$

$$\sum \hat{\mathbf{n}}_{I,2} \cdot \hat{\mathbf{n}}_{I+1,1} = \sum \left(\mathbf{l}_I \cdot \mathbf{l}_I + \mathbf{l}_I \cdot \mathbf{l}_{I+1} + \frac{1}{2}(\hat{\mathbf{m}}_{I+1} - \hat{\mathbf{m}}_I)^2 + \mathbf{l}_I \cdot (\hat{\mathbf{m}}_{I+1} - \hat{\mathbf{m}}_{I-1}) \right), \quad (2.41)$$

$$\hat{\mathbf{n}}_{I1} - \hat{\mathbf{n}}_{I2} = 2 \left(1 - \frac{l_I^2}{2} \right) \hat{\mathbf{m}}_I. \quad (2.42)$$

The solid angle term becomes (see Appendix A),

$$\Omega[\hat{\mathbf{n}}_{I1}] + \Omega[\hat{\mathbf{n}}_{I2}] = 2 \int dt \mathbf{l}_I \cdot \hat{\mathbf{m}}_I \times \partial_t \hat{\mathbf{m}}_I. \quad (2.43)$$

The effective action, S_{eff} is obtained by substituting Eqs. (2.40 - 2.43) into Eq.(2.35), integrating over the Gaussian fluctuations in the \mathbf{l} fields (which amounts to a systematic expansion of the theory in powers of $1/s$) and after taking the continuum limit. The result is,

$$S_{eff} = \int_0^\infty dx \int_0^\beta dt \mathcal{L}, \quad (2.44)$$

where,

$$\mathcal{L} = \int dt dx \left[\frac{is\kappa}{(1+\kappa)} \hat{\mathbf{m}} \cdot \partial_t \hat{\mathbf{m}} \times \partial_x \hat{\mathbf{m}} + \frac{\alpha J s^2 a}{2(1+\kappa)} \partial_x \hat{\mathbf{m}} \cdot \partial_x \hat{\mathbf{m}} + \frac{1}{2(1+\kappa)Ja} \partial_t \hat{\mathbf{m}} \cdot \partial_t \hat{\mathbf{m}} - \frac{s}{a} \mathbf{B} \cdot \hat{\mathbf{m}} \right]. \quad (2.45)$$

Here, $a/2$ is the lattice spacing. It is important to remark that the theory is defined with *free boundary conditions* on the vector field variables $\hat{\mathbf{m}}$. Notice that the presence of the staggered magnetic field (\mathbf{B}) term eliminates all the arbitrariness of the problem, indicating that S_{eff} is the appropriate quantum theory for anti-ferromagnetic ordering.

Next we compare the results with those obtained in the dual representation. In this case we obtain extra pieces associated with the edge vector field $\hat{\mathbf{n}}_E$. The answer can be written as,

$$\tilde{S}_{eff} = \int_0^\beta dt \tilde{L}_0 + \int_0^\infty dx \int_0^\beta dt \tilde{\mathcal{L}}, \quad (2.46)$$

where,

$$\begin{aligned}\tilde{L}_0 = & -is\Omega[\hat{\mathbf{n}}_E] \\ & + \frac{\tilde{\kappa}^2 \tilde{J}s^2(1 - (\hat{\mathbf{n}}_E \cdot \hat{\mathbf{m}}_0)^2) - 4\tilde{\kappa}\hat{\mathbf{n}}_E \cdot \hat{\mathbf{m}}_0 \times \partial_t \hat{\mathbf{m}}_0}{2(4 + 3\tilde{\kappa}) + 2\tilde{\kappa}\hat{\mathbf{n}}_E \cdot \hat{\mathbf{m}}_0} \\ & - 2s\mathbf{B}_0 \cdot \hat{\mathbf{n}}_E\end{aligned}\quad (2.47)$$

$$\begin{aligned}\tilde{\mathcal{L}} = & - \frac{is\tilde{\kappa}}{(1 + \tilde{\kappa})} \hat{\mathbf{m}} \cdot \partial_t \hat{\mathbf{m}} \times \partial_x \hat{\mathbf{m}} \\ & + \frac{\tilde{\kappa}\tilde{J}s^2a}{2(1 + \tilde{\kappa})} \partial_x \hat{\mathbf{m}} \cdot \partial_x \hat{\mathbf{m}} + \frac{1}{2(1 + \tilde{\kappa})\tilde{J}a} \partial_t \hat{\mathbf{m}} \cdot \partial_t \hat{\mathbf{m}} \\ & - \frac{s}{a} \mathbf{B} \cdot \hat{\mathbf{m}}.\end{aligned}\quad (2.48)$$

2.3.2 Nonlinear sigma model

Notice that Eq. (2.47) still contains two independent field variables, $\hat{\mathbf{n}}_E$ and $\hat{\mathbf{m}}_0$ respectively. This obviously has to be reduced further before a comparison between the effective actions S_{eff} and \tilde{S}_{eff} can be made. Here, $\hat{\mathbf{n}}_E$ is the original vector field at the edge as it appeared in the dual representation. On the other hand, $\hat{\mathbf{m}}_0$ is defined as the slowly varying vector field $\hat{\mathbf{m}}$ evaluated at the edge, i.e. $\hat{\mathbf{m}}_0 = \hat{\mathbf{m}}(x = 0, t)$.

On the basis of the classical equations of motion, however, it is readily established that the appropriate result for \tilde{S}_{eff} is obtained if one identifies the vectors $\hat{\mathbf{n}}_E$ and $\hat{\mathbf{m}}$ not only at the edge but also at each and every point in space-time, i.e.

$$\hat{\mathbf{n}}_E(x, t) = \hat{\mathbf{m}}(x, t). \quad (2.49)$$

Under these circumstances Eq. (2.47) reduces to

$$\tilde{L}_0 = -is\Omega[\hat{\mathbf{m}}_0] - 2s\mathbf{B}_0 \cdot \hat{\mathbf{m}}_0, \quad (2.50)$$

or, equivalently,

$$\int_0^\beta dt \tilde{L}_0 = is \int_0^\beta \int_0^\infty dx \hat{\mathbf{m}} \cdot \partial_t \hat{\mathbf{m}} \times \partial_x \hat{\mathbf{m}} - 2s \int_0^\beta dt \mathbf{B}_0 \cdot \hat{\mathbf{m}}_0. \quad (2.51)$$

We are now in a position to compare the theory S_{eff} and the dual theory \tilde{S}_{eff} and show that they are the same. More specifically, we obtain the lagrangian for the

standard $O(3)$ nonlinear sigma model,

$$\begin{aligned}\mathcal{L}_{NLSM} = & \frac{1}{2g} \left[c \partial_x \hat{\mathbf{m}} \cdot \partial_x \hat{\mathbf{m}} + \frac{1}{c} \partial_t \hat{\mathbf{m}} \cdot \partial_t \hat{\mathbf{m}} \right] - \frac{s}{a} \mathbf{B} \cdot \hat{\mathbf{m}} \\ & + i \frac{\theta}{4\pi} \hat{\mathbf{m}} \cdot \partial_t \hat{\mathbf{m}} \times \partial_x \hat{\mathbf{m}}.\end{aligned}\quad (2.52)$$

The spin-wave velocity c , the coupling constant g and the instanton angle θ are expressed as follows,

$$\begin{aligned}c &= as \sqrt{\kappa} J = as \sqrt{\tilde{\kappa}} \tilde{J}, \\ g &= s^{-1} \frac{(1+\kappa)}{\sqrt{\kappa}} = s^{-1} \frac{(1+\tilde{\kappa})}{\sqrt{\tilde{\kappa}}}, \\ \theta &= 4\pi s \frac{\kappa}{1+\kappa} = 4\pi s \left[1 - \frac{\tilde{\kappa}}{1+\tilde{\kappa}} \right].\end{aligned}\quad (2.53)$$

Here g and θ depend only on one parameter - κ , the dimerisation strength. Thus for a fixed spin s , DSC will map onto a curve in the $1/g - \theta$ plane, the parameter space of NLSM. With this in mind we now proceed to do the Haldane mapping for a generalised ladder. This also consists of weakly coupled dimers but with extra couplings. We can then associate every point in the $1/g - \theta$ plane with a corresponding spin model.

2.4 Nonlinear σ model for a generalised ladder

The Hamiltonian for the system is,

$$H = \sum_I \frac{1}{2} (S_{I1} + S_{I2})^2 + \kappa_{\alpha\beta} S_{I\alpha} \cdot S_{I+1\beta}, \quad (2.54)$$

where, I is the dimer index and α labels the two sites within the dimer. $\kappa_{\alpha\beta}$ couples $S_{I\alpha}$ and $S_{I+1\beta}$, (see Fig. 2.2). As before we can write the path integral in the coherent state basis. The action is,

$$\begin{aligned}S = & is \sum_I \Omega[\hat{\mathbf{n}}_{I,1}] + \Omega[\hat{\mathbf{n}}_{I,2}] \\ & + s^2 J \int dt \sum_I \frac{1}{2} (\hat{\mathbf{n}}_{I,1} + \hat{\mathbf{n}}_{I,2})^2 + \kappa_{\alpha\beta} \hat{\mathbf{n}}_{I,2} \cdot \hat{\mathbf{n}}_{I+1,1},\end{aligned}\quad (2.55)$$

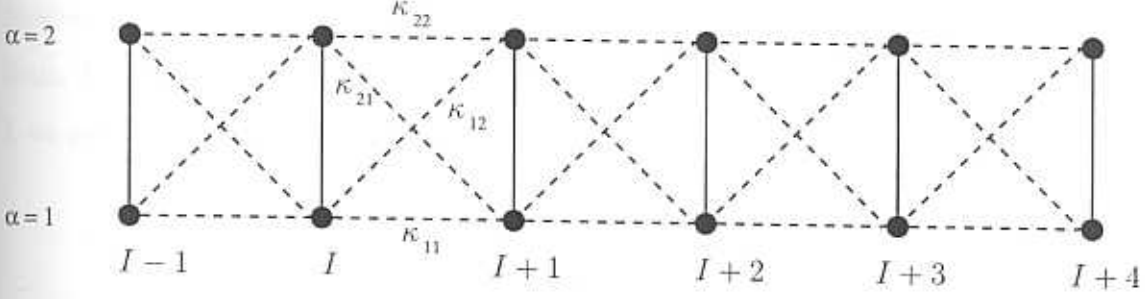


Figure 2.2: A Generalised ladder consisting of weakly coupled dimers

where $\Omega[\hat{\mathbf{n}}]$ is defined in Eq. (2.39). Now we make the change of variables from $\hat{\mathbf{n}}_1$ and $\hat{\mathbf{n}}_2$ to \mathbf{m} and \mathbf{l} as defined in Eq. (2.23). Only the inter dimer term in the Action is different from the previous case and in terms of the new variables it becomes,

$$\begin{aligned}
 \kappa_{\alpha\beta} \mathbf{n}_{I\alpha} \cdot \mathbf{n}_{I+1\beta} &= \kappa_{\alpha\beta} \left(\frac{\mathbf{l}_I}{2} - (-1)^\alpha \mathbf{m}_I \right) \cdot \left(\frac{\mathbf{l}_{I+1}}{2} - (-1)^\beta \mathbf{m}_{I+1} \right) \\
 &= \frac{1}{4} \left(\sum_{\alpha\beta} \kappa_{\alpha\beta} \right) \mathbf{l}_I \cdot \mathbf{l}_{I+1} - \frac{1}{2} \left(\sum_{\alpha\beta} (-1)^\beta \kappa_{\alpha\beta} \right) \mathbf{l}_I \cdot \mathbf{m}_{I+1} \\
 &\quad - \frac{1}{2} \left(\sum_{\alpha\beta} (-1)^\alpha \kappa_{\alpha\beta} \right) \mathbf{l}_{I+1} \cdot \mathbf{m}_I \\
 &\quad + \frac{1}{2} \left(\sum_{\alpha\beta} (-1)^{\alpha+\beta} \kappa_{\alpha\beta} \right) \mathbf{m}_I \cdot \mathbf{m}_{I+1}.
 \end{aligned} \tag{2.56}$$

Define,

$$\begin{aligned}
 \kappa_0 &\equiv - \sum_{\alpha\beta} (-1)^{\alpha+\beta} \kappa_{\alpha\beta} = (\kappa_{12} + \kappa_{21} - \kappa_{11} - \kappa_{22}), \\
 \kappa_1 &\equiv \sum_{\alpha\beta} (-1)^\alpha \kappa_{\alpha\beta} = (\kappa_{21} + \kappa_{22} - \kappa_{12} - \kappa_{11}), \\
 \kappa_2 &\equiv - \sum_{\alpha\beta} (-1)^\beta \kappa_{\alpha\beta} = (\kappa_{12} + \kappa_{22} - \kappa_{21} - \kappa_{11}), \\
 \kappa_3 &\equiv - \sum_{\alpha\beta} \kappa_{\alpha\beta} = (\kappa_{11} + \kappa_{12} + \kappa_{21} + \kappa_{22}).
 \end{aligned}$$

Then,

$$\begin{aligned}
 \sum_I J s^2 \kappa_{\alpha\beta} \mathbf{n}_{I\alpha} \cdot \mathbf{n}_{I\alpha} &= J s^2 \sum_I \left(\frac{\kappa_3}{4} \mathbf{l}_I \cdot \mathbf{l}_{I+1} - \frac{\mathbf{l}_I}{2} \cdot (\kappa_2 \mathbf{m}_{I+1} + \kappa_1 \mathbf{m}_{I-1}) \right. \\
 &\quad \left. - \kappa_0 \mathbf{m}_I \cdot \mathbf{m}_{I+1} \right).
 \end{aligned} \tag{2.57}$$

Now we substitute Eqs. (2.40), (2.43) and (2.57) in (2.55) and take the continuum limit. Keeping only up to quadratic order in \mathbf{l} and derivatives and integrating out \mathbf{l} , we get the effective action,

$$S_{eff} = \int d\tau dx \left[\frac{1}{2Ja \left(1 + \frac{\kappa_0 + \kappa_3}{2}\right)} \partial_\tau \mathbf{m} \cdot \partial_\tau \mathbf{m} + \frac{Jas^2 \kappa_0}{2} \partial_x \mathbf{m} \cdot \partial_x \mathbf{m} + \frac{is(\kappa_2 - \kappa_1)}{2 \left(1 + \frac{\kappa_0 + \kappa_3}{2}\right)} \mathbf{m} \cdot \partial_\tau \mathbf{m} \times \partial_x \mathbf{m} \right]. \quad (2.58)$$

Comparing with the standard NLSM action in Eq.(2.52) we get,

$$g = \frac{1}{s} \sqrt{\frac{1 + \frac{\kappa_0 + \kappa_3}{2}}{\kappa_0}}, \quad (2.59)$$

$$c = Jas \sqrt{\kappa_0 \left(1 + \frac{\kappa_0 + \kappa_3}{2}\right)}, \quad (2.60)$$

$$\theta = \frac{4\pi s(\kappa_2 - \kappa_1)}{2 \left(1 + \frac{\kappa_0 + \kappa_3}{2}\right)}, \quad (2.61)$$

where,

$$\begin{aligned} \kappa_0 &= \kappa_{21} + \kappa_{12} - \kappa_{11} - \kappa_{22}, \\ \frac{\kappa_0 + \kappa_3}{2} &= \kappa_{21} + \kappa_{12}, \\ \frac{\kappa_2 - \kappa_1}{2} &= \kappa_{12} - \kappa_{21}. \end{aligned}$$

In the strong coupling limit, $g \rightarrow \infty$ and hence $\kappa_0 \rightarrow 0$. We now show that this condition is satisfied by a $s = 1/2$ generalized Majumdar-Ghosh (see Chapter 2) ladder which has a dimerised singlet as the exact ground state. We also prove that, modulo one condition, converse of the above is true. *i.e.*, $\kappa_0 = 0$ implies that the system comes under the class of generalised Majumdar-Ghosh models (GMGM).

Proof :

First we show that a generalised Majumdar-Ghosh ladder maps to NLSM at strong coupling.

The generalised Majumdar-Ghosh ladder that we consider consists of coupled dimers and has the Hamiltonian,

$$H = \sum_I h_I, \quad (2.62)$$

where h_I can be diagrammatically represented as in Fig 2.3.

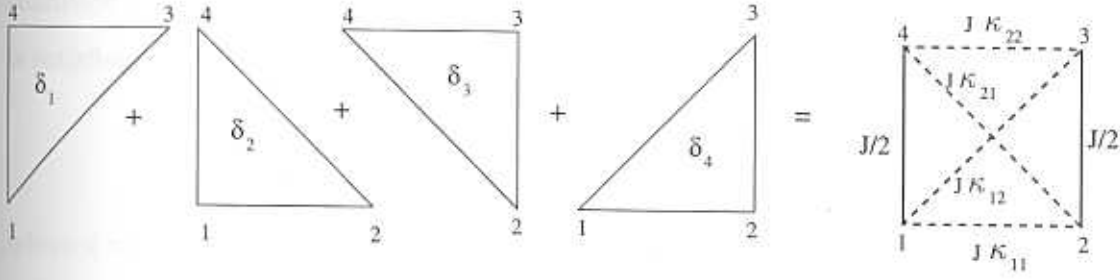


Figure 2.3: One unit of the generalised Majumdar-Ghosh ladder.

Here each triangle corresponds to the term, $\delta_i(\mathbf{S}_{i1} \cdot \mathbf{S}_{i2} + \mathbf{S}_{i2} \cdot \mathbf{S}_{i3} + \mathbf{S}_{i3} \cdot \mathbf{S}_{i1})$, where \mathbf{S}_{i1} , \mathbf{S}_{i2} and \mathbf{S}_{i3} are the three spins forming the triangle and δ_i is the coupling strength. Comparing L.H.S and R.H.S, we get the following set of equations,

$$\delta_2 + \delta_3 = J\kappa_{11}, \quad (2.63)$$

$$\delta_1 + \delta_4 = J\kappa_{22}, \quad (2.64)$$

$$\delta_1 + \delta_3 = J\kappa_{12}, \quad (2.65)$$

$$\delta_2 + \delta_4 = J\kappa_{21}, \quad (2.66)$$

$$\delta_1 + \delta_2 + \delta_3 + \delta_4 = J \quad (2.67)$$

It then immediately follows that $\kappa_0 \equiv \kappa_{11} + \kappa_{22} - \kappa_{12} - \kappa_{21} = 0$.

To prove the converse we need to show that $\kappa_0 = 0$ implies that the above set of equations can be solved for δ_i 's. We can explicitly construct the solution for Eqs. (2.63) through (2.66) as follows.

Let $\delta_1 = J\gamma$, where γ is arbitrary. Then,

$$\delta_2 = J(\kappa_{11} - \kappa_{12} + \gamma) \quad (2.68)$$

$$\delta_3 = J(\kappa_{12} - \gamma) \quad (2.69)$$

$$\delta_4 = J(\kappa_{22} - \gamma) \quad (2.70)$$

forms a solution of Eqs. (2.63 - 2.66) if $\kappa_0 = 0$. Eq. (2.67) will then be satisfied only if,

$$\kappa_{11} + \kappa_{22} = 1 \quad (2.71)$$

Therefore we are getting an additional condition other than just the strong coupling condition for the Hamiltonian to be written as sum over triangles. When only $\kappa_0 = 0$ is satisfied, we will have an additional term in the Hamiltonian of the form,

$$H_d = cJ \sum_I \mathbf{S}_{I1} \cdot \mathbf{S}_{I2} \quad (2.72)$$

where $c = 1 - \kappa_{11} + \kappa_{22}$. When $c \geq 0$ the dimer singlet remains the exact ground state.

Thus we have the interesting result that, for strong enough dimerisation (*i.e.* when $\kappa_{11} + \kappa_{22} = \kappa_{12} + \kappa_{21} \leq 1$),

"Strong coupling limit of NLSM \iff Generalised Majumdar-Ghosh model".

2.5 Validity of Haldane mapping

The following two assumptions went into the derivation of Haldane mapping.

1. **Small l** : In keeping terms only up to quadratic order in l , $l \equiv |l|$ is assumed small. Also while integrating out l we took the range of $|l|$ to be 0 to ∞ whereas in fact $|l| \leq 1$.
2. **Large correlation length** : While going from the lattice model to the continuum model, it is assumed that the correlation length $\xi \gg a$, the lattice parameter.

Let us see when we can expect these assumptions to be valid.

Dropping $O(l^3)$ terms amounts to dropping $O(1/(\sqrt{s})^3)$ terms. We know from Section ?? that the contribution to the action from within the dimer is exactly quadratic in l . So all the $O(l^3)$ terms come from the inter-dimer terms. Thus dropping $O(l^3)$ terms should be a good approximation at small κ even for small s .

Extending the upper limit of integration for $|l|$ to ∞ is equivalent to replacing the dimer with a rotor. This, as we have seen in Section ??, is a good approximation for large s and at lower energies.

For the continuum limit to be valid ξ should be $\gg a$. At stronger coupling (*i.e.* larger values of g) ξ gets smaller and at some point this assumption is bound to break down. For the dimerised chain, the coupling constant g given in Eq.(2.53) is,

$$g = \frac{(1 + \kappa)}{s\sqrt{\kappa}} \quad (2.73)$$

Smaller spin and stronger dimerisation (small κ) implies stronger coupling for NLSM. Thus we expect the continuum limit to be valid for large s and weak dimerisation ($\kappa \approx 1$). From the above discussion we can make the following conclusions.

- Both the approximations get better at large s .
- The rotor approximation is good at strong dimerisation whereas the continuum limit is good at weak dimerisation.

In this thesis we are interested in NLSM at strong coupling, which corresponds to strongly dimerised spin chains. In this regime NLSM will describe the low energy physics if the continuum limit is valid. The following are a few indications to believe that this may be the case.

- In the previous section we saw that generalised Majumdar-Ghosh ladders with dimer singlets as the exact ground state satisfies the strong coupling limit condition for NLSM. This fits in with the picture of isolated dimers corresponding to the strong coupling limit of NLSM.
- For the dimerised spin chain with an edge, we shall see that the strong coupling edge theory of NLSM exactly corresponds to decoupled dimers with a dangling edge spin. This will be elaborated upon in the next chapter.

Chapter 3

Strong coupling NLSM and the edge spin

In this chapter we analyse the sigma model in the strong coupling limit (*i.e.* when $g \rightarrow \infty$) and at quantized values of θ ($= 2\pi n$). As a first step we decompose the field into bulk and edge components and integrate out the bulk component to get an effective theory for the edge. Next we examine the theory in the above limit and see that the action depends only on the value of the field at the edge. The edge theory thus obtained is exactly equivalent to a single-spin system. We calculate the two point correlation function and show that the theory is critical. Finally we look at the correspondence with the dimerised spin chain (DSC) in this limit.

3.1 The edge theory

In terms of the Q field, $O(3)$ NLSM has the following action.

$$\begin{aligned} S[Q] = & \frac{1}{4g} \int dx dt \operatorname{tr} \left(c \operatorname{tr} \partial_x Q \partial_x Q + \frac{1}{c} \operatorname{tr} \partial_t Q \partial_t Q \right) \\ & + \frac{\theta}{16\pi} \int dx dt \operatorname{tr} \epsilon_{ij} Q \partial_i Q \partial_j Q \\ & - \frac{sB}{a} \int dx dt \operatorname{tr} \tau^3 Q. \end{aligned} \tag{3.1}$$

For a system with an edge, we have to specify the boundary conditions satisfied by the Q fields. As always, this has to be decided by the physics of the system

under consideration. It was shown in [19] that free boundary conditions implied the existence of chiral edge currents. Deriving motivation from quantum Hall Physics, where such states are relevant, we thus use free boundary conditions.

The most important consequence of the free boundary conditions is that the topological charge is not quantized. In general we have,

$$\begin{aligned} q[Q] &\equiv \frac{1}{8\pi} \int d^2x \operatorname{tr} \epsilon_{ij} Q \partial_i Q \partial_j Q \\ &= n[Q] + \delta q[Q] \end{aligned} \quad (3.2)$$

where $n[Q]$ is the integer part and $\delta q[Q]$ is the fractional part of the topological charge $q[Q]$. We now separate the “edge” and the “bulk” modes as follows. We put,

$$Q = t^{-1} Q_0 t \quad (3.3)$$

where, Q_0 satisfies,

$$Q_0|_{\text{edge}} = \tau^3 \quad q[Q_0] = n[Q] \quad (3.4)$$

Thus Q_0 contains information about the winding in the bulk and t specifies the edge modes which cause the fluctuations of the topological charge about its quantised values.

The effective action for the edge modes is obtained by integrating over Q_0 ,

$$e^{-S_{eff}[t]} = \int_{Q_0} e^{-S[t^{-1}Q_0t]} \quad (3.5)$$

By general symmetry considerations, the effective action has to be of the form,

$$\begin{aligned} S_{eff}[t] &= \int dx dt \frac{1}{4g'} \operatorname{tr} \left(c \operatorname{tr} \partial_x Q \partial_x Q + \frac{1}{c} \operatorname{tr} \partial_t Q \partial_t Q \right) \\ &+ \frac{\theta'}{16\pi} \int dx dt \operatorname{tr} \epsilon_{ij} Q \partial_i Q \partial_j Q \\ &- \frac{sB'}{a} \int dx dt \operatorname{tr} \tau^3 Q. \end{aligned} \quad (3.6)$$

where we have defined $\tilde{Q} \equiv t^{-1} \tau^3 t$. g' , θ' and B' are the renormalized parameters.

We now examine the theory in the strong coupling limit of the ‘bare’ parameters, $g=0$ and $\theta=2\pi m$. Then the action becomes simply,

$$S[Q] = \frac{m}{8} \int d^2x \operatorname{tr} \epsilon_{ij} Q \partial_i Q \partial_j Q, \quad (3.7)$$

which can be written as,

$$S[Q] = 2\pi i m q[Q_0] + \frac{m}{2} \oint d\vec{x} \cdot \text{tr}(\tau^3 t \nabla t^{-1}). \quad (3.8)$$

The significance of the quantization of $\theta = 2\pi m$ is now clear. When $g = 0$, the action sees only the integer valued topological charge $q[Q_0]$ of the bulk configuration. For the quantized values of θ , the partition function and correlation functions becomes independent of Q_0 . Hence a quantized θ implies that the system is completely insensitive to the bulk configuration and depends only on the edge part which are the fluctuations of the θ term about its integer values.

The effective action is then trivially seen to be

$$S[t] = \frac{m}{2} \oint d\vec{x} \cdot \text{tr}(\tau^3 t \nabla t^{-1}) \quad (3.9)$$

It has been shown [19] that the theory in (3.9) was exactly equivalent to a system of chiral fermions on the edge. The Q field correlation functions at non-coincident points were exactly computable using the theory of non-interacting fermion by the replacement,

$$Q_{\alpha\beta}^{pp'}(x) \rightarrow \bar{\psi}_{\alpha i}^p(x) \psi_{\beta i}^{p'}(x) \quad (3.10)$$

Where $\psi_{\alpha i}^p(x)$ are the fermion operators and the action is,

$$S_{RF} = \int_{-\infty}^{\infty} dx \bar{\psi}_{\alpha i p} (-i\omega\tau^3 - i v_d \partial_x)_{pp'} \psi_{\alpha i p'} \quad (3.11)$$

Using the standard notation, $: O : \equiv O - \langle O \rangle$, the only non-vanishing two point function is,

$$\langle : Q_{\alpha_1 \beta_1}^{-+}(x_1) : : Q_{\alpha_2 \beta_2}^{+-}(x_2) : \rangle = m \delta_{\alpha_1 \beta_2} \delta_{\alpha_2 \beta_1} \theta(x_1 - x_2) e^{-2\omega(x_1 - x_2)} \quad (3.12)$$

At $\omega = 0$, there is no length scale involved and hence the edge theory is critical.

3.2 Edge spin

The edge-action in (3.7), which is the fractional part of the θ term, is the solid angle of the curve traced out on the sphere by \hat{n} as it goes around the edge. In terms of the unit vector-field defined by $Q = \hat{n} \cdot \vec{\tau}$, the edge-action can be written as,

$$S[Q] = is \int dx dy \hat{n} \cdot \partial_x \hat{n} \times \partial_y \hat{n} + 2\pi \rho_{edge} \omega n^3 \quad (3.13)$$

with $s = \frac{m}{2}$. This is exactly the action obtained for the problem of a spin- s system derived in Section 2.1. The euclidean time of the spin system is identified with the coordinate that parametrizes the edge, say x . The other coordinate, y , that goes into the bulk plays the role of the fictitious dimension that it is necessary to introduce in the spin problem in order to write down a globally well defined action. We now calculate the correlation functions for the spin system using an operator formalism.

The Hamiltonian is,

$$H = B_0 \cdot S. \quad (3.14)$$

The generating functional (defined in Section ??),

$$Z[B(x)] \equiv tr \mathcal{T}(e^{-\int_0^\beta dx B(x) \cdot S}) \quad (3.15)$$

generates the time ordered N point spin-spin correlation functions,

$$\begin{aligned} \frac{1}{Z[B(x)]} \prod_{i=1}^N \frac{\delta^N}{\delta B^{a_i}(x_i)} Z[B(x)]|_{B=B_0} &= tr \left(e^{-\beta H} \mathcal{T} \left(\prod_i^N S^{a_i}(x_i) \right) \right) \\ &\equiv G_N(\{x_i, a_i\}) \end{aligned} \quad (3.16)$$

where,

$$S^a(x) \equiv e^{\beta H} S^a e^{-\beta H}, \quad (3.17)$$

Some of the correlations functions of $Q(x)$ can be computed easily using equation(3.16).

The partition function (zero point function) is,

$$\begin{aligned} Z &= \sum_{m=-s}^s e^{-m\beta B_0} \\ &= \frac{\sinh((s + \frac{1}{2})\beta B_0)}{\sinh(\frac{\beta B_0}{2})} \end{aligned} \quad (3.18)$$

The one point function is also easy to compute,

$$\begin{aligned} \langle Q(x_1) \rangle_\beta &= \frac{1}{Z} \sigma^a tr(e^{-\beta H} \frac{1}{s} S^a) \\ &= -\sigma^3 \frac{1}{s B_0} \frac{\partial}{\partial \beta} \ln Z \\ &= -\sigma^3 \left(\left(1 + \frac{1}{2s}\right) \coth \left(\left(s + \frac{1}{2}\right) \beta B_0 \right) - \frac{1}{2s} \coth \left(\frac{\beta B_0}{2} \right) \right) \end{aligned} \quad (3.19)$$

In the limit $\beta \rightarrow \infty$, the result simplifies to,

$$\lim_{\beta \rightarrow \infty} \langle Q \rangle_\beta = \sigma^3 \quad (3.20)$$

In the $\beta \rightarrow \infty$ limit, the 2 point function $\langle Q_{-+}(x_1)Q_{+-}(x_2) \rangle_\beta$ can be calculated as follows.. We have,

$$\langle Q_{-+}(x_1)Q_{+-}(x_2) \rangle_\beta = \frac{1}{Zs^2} \text{tr}(e^{-\beta H} \mathcal{T}(S^-(x_1)S^+(x_2))) \quad (3.21)$$

Using equation(3.17) and equation(3.14), we get,

$$S^-(x_1) = e^{B_0 x_1} S^- \quad (3.22)$$

$$S^+(x_2) = e^{-B_0 x_2} S^+ \quad (3.23)$$

We then have,

$$\begin{aligned} \lim_{\beta \rightarrow \infty} \langle Q_{-+}(x_1)Q_{+-}(x_2) \rangle_\beta &= \frac{1}{s^2} e^{-B_0|x_1-x_2|} (\Theta(x_1-x_2) \langle -s|S^-S^+|-s \rangle \\ &\quad + \Theta(x_2-x_1) \langle -s|S^+S^-|-s \rangle) \\ &= \Theta(x_1-x_2) e^{-B_0(x_1-x_2)} \end{aligned} \quad (3.24)$$

Thus we have shown that the critical edge action and correlation functions obtained in the bare strong coupling limit is exactly the same as that of a single spin- $\frac{m}{2}$ system.

3.3 Correspondence between NLSM edge theory and DSC

In this section we examine the correspondence between the semi-infinite dimerised spin chain in the strong dimerisation limit and the strong coupling limit of NLSM.

The Hamiltonian for the spin system as defined in Section 2.3 is,

$$H_{DSC} = \sum_{I=0}^{\infty} J (\mathbf{S}_{2I} \cdot \mathbf{S}_{2I+1} \kappa \mathbf{S}_{2I1} \cdot \mathbf{S}_{2I+2}) \quad (3.25)$$

The results in the previous section implies that the bare strong coupling limit of the NLSM is exactly equivalent to the low energy physics of spin- $\frac{m}{2}$ dimerised

spin chain (DSC), in the strong dimerisation limit. We first consider the case of semi-infinite DSC's and will discuss the case of finite chains later. The hamiltonian is,

$$H_{DSC} = \sum_{I=0}^{\infty} J (\mathbf{S}_{2I} \cdot \mathbf{S}_{2I+1} \kappa \mathbf{S}_{2I+1} \cdot \mathbf{S}_{2I+2}) \quad (3.26)$$

At $\kappa = 0$, the model consists of decoupled dimers and is trivially solved. All dimers being in the singlet state constitutes the ground state. Any one of the dimers being in the triplet state constitute the lowest energy excitations. Thus the system has a gap $= J$ and there are no excitations at energy scales small compared to J .

At $\kappa = \infty$ also, the model decouples. The hamiltonian can be written in a *dual* representation where the roles of the 'dimers' and 'weak' bonds get interchanged,

$$\tilde{H}_{DSC} = \sum_{i=0}^{\infty} \tilde{J} (\tilde{\kappa} \mathbf{S}_{2i} \cdot \mathbf{S}_{2i+1} + \mathbf{S}_{2i+1} \cdot \mathbf{S}_{2i+2}) \quad (3.27)$$

where we have defined $\tilde{\kappa} \equiv \frac{1}{\kappa}$, $\tilde{J} \equiv \kappa J$. Thus $\kappa = \infty \Leftrightarrow \tilde{\kappa} = 0$. The system now decouples into a set of dimers and a free spin at the edge. The dynamics at energy scales small compared to J will therefore be that of the free spin at the edge.

Thus, consistent with the Haldane mapping, the low energy physics of the DSC at $\kappa = 0$ and $\kappa = \infty$ is the same as that of the NLSM at $g = \infty$, $\theta = 0$ and $g = \text{infy}$, $\theta = 2\pi m$ respectively. In the former case both models have no low energy dynamics and in the latter case both have low energy dynamics confined to edge with identical correlation functions.

After having established the correspondence between DSC and NLSM at the 'bare' strong coupling and quantized θ , we now go one step ahead and extend it away from this limit. This chapter and the previous one have now set the stage for the real space renormalization group analysis that we do for DSC in the next chapter.

Chapter 4

Real space RG for $s = 1/2$ dimerised spin chain.

In the previous two chapters we derived $O(3)$ NLSM as the effective low energy theory for the semi-infinite dimerised spin chain (DSC) and found that the low energy dynamics of the latter in the strong dimerisation limit is exactly reproduced by the corresponding strong coupling limit of NLSM. Now we push this correspondence away from the above limit, *i.e.*, when the dimers are weakly coupled. In this chapter we do a real-space renormalisation group analysis for DSC to throw light on NLSM at strong coupling.

The RG scheme is formulated using a combination of hamiltonian and path integral techniques. It involves integrating out spins residing on alternate dimers to obtain a systematic perturbative expansion in the weak inter-dimer coupling and in time derivatives. We compute the RG equations to lowest non-trivial order in both the coupling and derivatives and then discuss the solutions. The RG flow suggests that we start with a more general model for which DSC is a special case. We repeat the RG for the general model and finally do the mapping to NLSM.

4.1 The decimation scheme

The dimerised spin chain was defined in Section ?? . The hamiltonian is,

$$H = J \sum_I \left(\frac{1}{2} (\mathbf{S}_{I1} + \mathbf{S}_{I2})^2 + \kappa \mathbf{S}_{I2} \cdot \mathbf{S}_{I+1,1} \right). \quad (4.1)$$

Using the spin coherent states we can derive the path integral representation for the partition function,

$$Z = \text{Tre}^{-\beta H} = \int \prod_{I\alpha} \mathcal{D}[\hat{\mathbf{n}}_{I\alpha}] e^{-S[\{\hat{\mathbf{n}}_{I\alpha}\}]}. \quad (4.2)$$

The action is,

$$S = \sum_{I\alpha} -is\Omega[\hat{\mathbf{n}}_{I\alpha}] + Js^2 \int_0^\beta d\tau \sum_I \left(\frac{1}{2} (\hat{\mathbf{n}}_{I1} + \hat{\mathbf{n}}_{I2})^2 + \kappa \hat{\mathbf{n}}_{I2} \cdot \hat{\mathbf{n}}_{I+1,1} \right), \quad (4.3)$$

where $\Omega[\hat{\mathbf{n}}]$ is the solid angle subtended by the curve that $\hat{\mathbf{n}}(\tau)$ traces out on the unit sphere. It is given by,

$$\Omega[\hat{\mathbf{n}}] = \int d\tau ds \hat{\mathbf{n}} \cdot \partial_\tau \hat{\mathbf{n}} \times \partial_s \hat{\mathbf{n}}. \quad (4.4)$$

This can also be written as,

$$\Omega[\hat{\mathbf{n}}] = \int d\tau \mathbf{A}_{mon}(\hat{\mathbf{n}}) \cdot \partial_\tau \hat{\mathbf{n}}, \quad (4.5)$$

where \mathbf{A}_{mon} is the vector potential of a magnetic monopole of unit strength placed at the center on the sphere described by $\hat{\mathbf{n}}$.

4.1.1 The first RG step

We integrate out the odd dimers in the path integral in Eq.(4.2) to obtain an effective action for the even dimers,

$$S^{eff} = \sum_{I\alpha} -is\Omega[\hat{\mathbf{n}}_{2I,\alpha}] + Js^2 \int_0^\beta d\tau \sum_I \frac{1}{2} (\hat{\mathbf{n}}_{2I,1} + \hat{\mathbf{n}}_{2I,2})^2 + S_{int}^{eff},$$

where S_{int}^{eff} is given by,

$$\begin{aligned}
\exp(-S_{int}^{eff}) &= \int \prod_{I\alpha} \mathcal{D}[\hat{\mathbf{n}}_{2I+1\alpha}] \exp \left(is \sum_{I\alpha} \Omega[\hat{\mathbf{n}}_{2I+1\alpha}] \right. \\
&\quad - Js^2 \int_0^\beta d\tau \sum_I \frac{1}{2} (\hat{\mathbf{n}}_{2I+1,1} + \hat{\mathbf{n}}_{2I+1,2})^2 \\
&\quad \left. - Js^2 \int_0^\beta d\tau \sum_I \kappa (\hat{\mathbf{n}}_{2I,2} \cdot \hat{\mathbf{n}}_{2I+1,1} + \hat{\mathbf{n}}_{2I+1,2} \cdot \hat{\mathbf{n}}_{2I+2,1}) \right) \\
&= \prod_I \int \mathcal{D}[\hat{\mathbf{n}}_1] \mathcal{D}[\hat{\mathbf{n}}_2] \exp \left(is \sum_\alpha \Omega[\hat{\mathbf{n}}_\alpha] \right. \\
&\quad \left. - Js^2 \int_0^\beta d\tau \frac{1}{2} (\hat{\mathbf{n}}_1 + \hat{\mathbf{n}}_2)^2 + \kappa (\hat{\mathbf{n}}_2 \cdot \hat{\mathbf{n}}_{2I+2,1} + \hat{\mathbf{n}}_1 \cdot \hat{\mathbf{n}}_{2I,2}) \right). \quad (4.7)
\end{aligned}$$

Therefore, computing S_{int}^{eff} involves computing the partition function of a two-spin system in the presence of time dependent external fields. This two-spin problem can be expressed in the hamiltonian formalism as,

$$e^{-F[\mathbf{m}_1, \mathbf{m}_2]} = \text{Tr} \left(T e^{-\int_0^\beta d\tau (h_0 + \kappa h_{int})} \right), \quad (4.8)$$

where,

$$h_0 = \frac{J}{2} (\mathbf{S}_1 + \mathbf{S}_2)^2 \quad (4.9)$$

$$h_{int} = \mathbf{S}_1 \cdot \mathbf{m}_2(\tau) + \mathbf{S}_2 \cdot \mathbf{m}_1(\tau), \quad (4.10)$$

and we have defined,

$$\mathbf{m}_1 \equiv s \hat{\mathbf{n}}_{I-1,1} \quad (4.11)$$

$$\mathbf{m}_2 \equiv s \hat{\mathbf{n}}_{I+1,2} \quad (4.12)$$

From now, we will concentrate on the $s = 1/2$ case.

4.1.2 $s = \frac{1}{2}$ dimer system

We will be computing F as a perturbative series in κ . We first develop some useful formalism for the $\kappa = 0$ problem.

The hamiltonian h_0 is trivially diagonalised. We label the eigenstates by the total spin quantum number, and its z component. Define,

$$\mathbf{S} \equiv \mathbf{S}_1 + \mathbf{S}_2. \quad (4.13)$$

Then we have,

$$\mathbf{S} \cdot \mathbf{S} |L, M\rangle = L(L+1) |L, M\rangle \quad (4.14)$$

$$S^z |L, M\rangle = M |L, M\rangle. \quad (4.15)$$

The only possible values for L are 0 and 1. The singlet is the ground state with energy 0. The three triplet states are degenerate with energy J . From now, we will set $J = 1$, *i.e.*, all energies will be in units of J .

We now construct operators that act on the singlet state and produce a triplet state and vice-versa. First define,

$$\mathbf{n} \equiv \frac{\mathbf{S}_1 - \mathbf{S}_2}{2} \quad (4.16)$$

$$\chi^a \equiv \epsilon^{abc} S_2^b S_1^c \quad (4.17)$$

These operators satisfy the relations,

$$[h_0, n^a] = -i\chi^a \quad (4.18)$$

$$[h_0, \chi^a] = in^a \quad (4.19)$$

Now define,

$$A^a \equiv \chi^a - in^a \quad (4.20)$$

$$A^{a\dagger} \equiv \chi^a + in^a. \quad (4.21)$$

Then we have,

$$[h_0, A^a] = -A^a \quad (4.22)$$

$$[h_0, A^{a\dagger}] = A^{a\dagger}. \quad (4.23)$$

The (euclidean) time evolution of these operators is very simple.

$$A^a(\tau) = e^{-\tau} A^a(0) \quad (4.24)$$

$$A^{a\dagger}(\tau) = e^{\tau} A^{a\dagger}(0). \quad (4.25)$$

These operators also satisfy the relation

$$A^a A^{b\dagger} = \delta_{ab} \left(\frac{1}{4} - \mathbf{S}_1 \cdot \mathbf{S}_2 \right). \quad (4.26)$$

Using equations (4.24-4.26), The correlation functions of $A^a, A^{a\dagger}$ can easily be computed. We have,

$$\langle 0 | T \left(A^a(\tau_1) A^{b\dagger}(\tau_2) \right) | 0 \rangle = e^{-(\tau_1 - \tau_2)} \Theta(\tau_1 - \tau_2) + e^{(\tau_1 - \tau_2)} \Theta(\tau_2 - \tau_1) \quad (4.27)$$

$$= e^{-|\tau_1 - \tau_2|}. \quad (4.28)$$

4.1.3 The free energy for the dimer

The free energy $F[\mathbf{m}_1, \mathbf{m}_2]$, defined in Eq. (4.8) can be expanded in a cumulant expansion in powers of κ . We refer to Appendix B for the calculation to all orders. Now we concentrate on the lowest order term, which is $O(\kappa^2)$. To this order, F is given by,

$$F = -\frac{\kappa^2}{2!} \int_{-\infty}^{\infty} d\tau_1 d\tau_2 \langle 0 | T(h_{int}(\tau_1) h_{int}(\tau_2)) | 0 \rangle \quad (4.29)$$

The 2-spin hamiltonian can be written in terms of the operators defined in Eqs. (4.13) and (4.16) as,

$$h_0 = \frac{1}{2} \mathbf{S} \cdot \mathbf{S} \quad (4.30)$$

$$h_{int} = \mathbf{S} \cdot \mathbf{M} - \mathbf{n} \cdot \mathbf{m} \quad (4.31)$$

where,

$$\mathbf{M} \equiv \frac{\mathbf{m}_1 + \mathbf{m}_2}{2}, \quad (4.32)$$

$$\mathbf{m} \equiv \mathbf{m}_1 - \mathbf{m}_2. \quad (4.33)$$

Since $S^a | 0 \rangle = 0$, Eq. (4.29) can be written as,

$$F = -\kappa^2 \int_{-\infty}^{\infty} d\tau_1 \int_{-\infty}^{\tau_1} d\tau_2 \langle 0 | n^a(\tau_1) n^b(\tau_2) | 0 \rangle m^a(\tau_1) m^b(\tau_2) \quad (4.34)$$

Using Eqs. (4.16), (4.17), (4.20), (4.21) and (4.27) we compute this to be,

$$F = -\frac{\kappa^2}{4} \int_{-\infty}^{\infty} d\tau_1 \int_{-\infty}^{\tau_1} d\tau_2 e^{-(\tau_1 - \tau_2)} m^a(\tau_1) m^a(\tau_2) \quad (4.35)$$

$$= -\frac{\kappa^2}{4} \int_{-\infty}^{\infty} d\tau \int_0^{\infty} dt e^{-t} m^a(\tau + t/2) m^a(\tau - t/2) \quad (4.36)$$

For fields slowly varying over a time scale of ~ 1 , we can expand $m^a(\tau \pm t)$ about τ and develop a local derivative expansion for F .

4.1.4 Fixed points neglecting the time derivatives

For the moment we neglect the derivatives and get,

$$F = -\frac{\kappa^2}{8} \int_{-\infty}^{\infty} d\tau \mathbf{m}_1 \cdot \mathbf{m}_2 \quad (4.37)$$

Using Eqs. (4.6),(4.7),(4.11),(4.12) and (4.37) and relabeling the sites $2I \rightarrow I$, we get the effective hamiltonian,

$$H_{eff} = \sum_I (S_{I1} \cdot S_{I2} + \kappa' S_{I2} \cdot S_{I+11}) \quad (4.38)$$

This is exactly of the initial form in Eq. (4.1), with the renormalised coupling $\kappa' = \kappa^2/2$. We therefore have the recursion relation for the coupling constant

$$\kappa^{n+1} = \frac{(\kappa^n)^2}{2} \quad (4.39)$$

The solution to this recurrence relation is,

$$\kappa^n = 2 \left(\frac{\kappa^0}{2} \right)^L, \quad L \equiv 2^n \quad (4.40)$$

Thus, there are two fixed points,

$$\kappa^* = 0 \quad \text{and} \quad \kappa^* = 2 \quad (4.41)$$

and the coupling constant flows from $\kappa^* = 2$ to $\kappa^* = 0$. Note that the hamiltonian in Eq. (4.1) with coupling $\kappa = 1$ is the uniform $s = 1/2$ Heisenberg model and is known to be gapless. This implies that we should get $\kappa = 1$, corresponding to $\theta = \pi$, as a fixed point of the RG equations. Thus $\kappa^* = 2$ is well off the mark. In fact, if the time derivatives are neglected, κ^* can be calculated taking all orders into account (see Appendix B). Then we obtain $\kappa^* = 0.61$, which is still not very good.

Independent of the uniform chain being gapless, $\kappa = 1$ has to be a fixed point if the RG flow is closed within the one parameter space involving only κ (we have assumed this by neglecting the time derivatives). This is because $\kappa = 1$ is dual

symmetric, *i.e.*, invariant under $\kappa \rightarrow 1/\kappa$ and RG flow must preserve this symmetry. Thus it has become clear that neglecting time derivative terms is not a good approximation and we need to retain them.

4.1.5 The derivative expansion and the effective action

We proceed by expanding $m^a(\tau \pm t)$ about τ . To second order in derivatives we have,

$$F = -\frac{\kappa^2}{4} \int_{-\infty}^{\infty} d\tau \left[m^a(\tau) m^a(\tau) + \frac{1}{2} \left(\partial_\tau m^a(\tau) m^a(\tau) - m^a(\tau) \partial_\tau m^a(\tau) \right) - \partial_\tau m^a(\tau) \partial_\tau m^a(\tau) \right] \quad (4.42)$$

Rewriting in terms of \mathbf{m}_1 and \mathbf{m}_2 ,

$$F[\mathbf{m}_1, \mathbf{m}_2] = \frac{\kappa^2}{2} \int_{-\infty}^{\infty} d\tau \left(-\frac{1}{4} \sum_{\alpha} \mathbf{m}_{\alpha} \cdot (1 + \partial_\tau^2) \mathbf{m}_{\alpha} + \frac{1}{2} \mathbf{m}_1 \cdot (1 + \partial_\tau^2) \mathbf{m}_2 \right) \quad (4.43)$$

We define,

$$\hat{\mathbf{n}}'_{I\alpha} = \hat{\mathbf{n}}_{2I\alpha}. \quad (4.44)$$

We now have the result for S_{int}^{eff} defined in Eq. (4.7),

$$S_{int}^{eff} = \sum_I F[\hat{\mathbf{n}}'_{I1}/2, \hat{\mathbf{n}}'_{I+12}/2] \quad (4.45)$$

$$= \int_{-\infty}^{\infty} d\tau \sum_I \left(\frac{\kappa'}{8} \sum_{\alpha} (\partial_\tau \hat{\mathbf{n}}'_{I\alpha})^2 + \frac{\kappa'}{4} \hat{\mathbf{n}}'_{I2} \cdot (1 + \partial_\tau^2) \hat{\mathbf{n}}'_{I+1,1} \right). \quad (4.46)$$

In the above expression we have defined the renormalised coupling constant,

$$\kappa' \equiv \frac{\kappa^2}{2} \quad (4.47)$$

The effective action is then given by,

$$S^{eff} = \int_{-\infty}^{\infty} d\tau \sum_{I\alpha} \left(\frac{\kappa'}{8} (\partial_\tau \hat{\mathbf{n}}_{I\alpha})^2 - \frac{1}{2} \mathbf{A}_{mon}(\hat{\mathbf{n}}_{I\alpha}) \cdot \partial_\tau \hat{\mathbf{n}}_{I\alpha} + \frac{1}{8} (\hat{\mathbf{n}}_{I1} + \hat{\mathbf{n}}_{I2})^2 + \frac{\kappa'}{4} \hat{\mathbf{n}}_{I2} \cdot (1 + \partial_\tau^2) \hat{\mathbf{n}}_{I+1,1} \right). \quad (4.48)$$

In the last step we have dropped the superfix ' ' from the fields.

The system described by the action above is no longer a spin chain. It now corresponds to a system of charged particles confined to the surface of a sphere with a unit monopole at the center. If we neglect the derivative terms coupling neighbouring sites, the Hilbert space at each site has one representation of all half odd integer angular momenta, $J = 1/2, 3/2, 5/2, \dots$. Namely, at every site we have a fermionic rotor. Thus under renormalisation, the spin chain goes over to a fermionic rotor chain (FRC). This can be understood qualitatively as follows. The degree of freedom at each site in the effective action corresponds to the motion of the original spin at that site and a block of even number of spins that have been integrated out. Thus we can expect many excitations with higher (half odd integer) angular momenta.

4.2 RG for the fermionic rotor chain

We therefore begin with a general fermionic rotor chain described by the action,

$$S = \int_{-\infty}^{\infty} d\tau \left[\sum_{I\alpha} \left(\frac{\kappa_3 s'^2}{2} \partial_\tau \mathbf{n}_{I\alpha} \cdot \partial_\tau \mathbf{n}_{I\alpha} - \frac{i}{2} \mathbf{A}(\mathbf{n}_{I\alpha}) \cdot \partial_\tau \mathbf{n}_{I\alpha} \right) + \sum_I s'^2 \left(\mathbf{n}_{I1} \cdot \mathbf{n}_{I2} + \mathbf{n}_{I2} \cdot (\kappa_1 + \kappa_2 \partial_\tau^2) \mathbf{n}_{I+1,1} \right) \right] \quad (4.49)$$

We have introduced three coupling constants, κ_1 , κ_2 and κ_3 . $s' \equiv 3/2$ for reasons that will become clear later. This type of a model, for a uniform chain, has been previously considered by Read and Shankar [41].

The action for the dimer problem is,

$$S = \int_{-\infty}^{\infty} d\tau \left[\sum_{\alpha} \left(\frac{\kappa_3 s'^2}{2} \partial_\tau \mathbf{n}_{\alpha} \cdot \partial_\tau \mathbf{n}_{\alpha} - \frac{i}{2} \mathbf{A}(\mathbf{n}_{\alpha}) \cdot \partial_\tau \mathbf{n}_{\alpha} \right) + s'^2 \mathbf{n}_1 \cdot \mathbf{n}_2 + s'^2 \sum_{\alpha} \mathbf{n}_{\alpha} \cdot \mathbf{m}_{\alpha} \right] \quad (4.50)$$

where,

$$\mathbf{m}_1 = (\kappa_1 + \kappa_2 \partial_\tau^2) \mathbf{n}_{I-1,2} \quad (4.51)$$

$$\mathbf{m}_2 = (\kappa_1 + \kappa_2 \partial_\tau^2) \mathbf{n}_{I+1,1} \quad (4.52)$$

The hamiltonian corresponding to the action in Eq.(4.50) is then,

$$h_d = h_0 + h_{int} \quad (4.53)$$

$$h_0 = \frac{1}{2\kappa_3 s'^2} \sum_{\alpha} \left(\mathbf{J}_{\alpha} \cdot \mathbf{J}_{\alpha} - \frac{1}{4} \right) \quad (4.54)$$

$$h_{int} = s'^2 \mathbf{n}_1 \cdot \mathbf{n}_2 + s'^2 \sum_{\alpha} \mathbf{n}_{\alpha} \cdot \mathbf{m}_{\alpha} \quad (4.55)$$

\mathbf{J}_{α} are the angular momentum operators. The spectrum of h_0 is,

$$\begin{aligned} h_0 |(j_1, m_1), (j_2, m_2)\rangle &= E_{j_1 j_2} |(j_1, m_1), (j_2, m_2)\rangle \\ E_{j_1 j_2} &= \frac{1}{2\kappa_3 s'^2} \sum_{\alpha} \left(j_{\alpha}(j_{\alpha} + 1) - \frac{1}{4} \right) \end{aligned} \quad (4.56)$$

with $j_{\alpha} = 1/2, 3/2, \dots$ and $m_{\alpha} = -j_{\alpha}, \dots, j_{\alpha}$. The ground states are the four $j_1 = j_2 = \frac{1}{2}$ states. When $\kappa \ll 1$, the gap between the $(1/2, 1/2)$ states and the excited states is very large. In this limit, to a very good approximation, we can project the model into the $(j_1, j_2) = (1/2, 1/2)$ subspace. The matrix elements of $\hat{\mathbf{n}}$ between the $j = 1/2$ states can be explicitly computed using the monopole harmonics ?? and we have,

$$\langle \frac{1}{2}, \sigma_1 | n^a | \frac{1}{2}, \sigma_2 \rangle = \frac{2}{3} S^a = \frac{1}{s'} S^a \quad (4.57)$$

Thus to leading order in κ_3 , we recover the two-spin system as the effective hamiltonian,

$$h_{eff} = \mathbf{S}_1 \cdot \mathbf{S}_2 + \sum_{\alpha} \mathbf{S}_{\alpha} \cdot \mathbf{m}_{\alpha}$$

The previous results can now be used to integrate out the dimer system and get the recursion relations to second order in the κ 's. They are,

$$\kappa_1^{(n+1)} = \frac{(\kappa_1^{(n)})^2}{2} \quad (4.59)$$

$$\kappa_2^{(n+1)} = \frac{(\kappa_1^{(n)})^2}{2} + \kappa_1^n \kappa_2^n \quad (4.60)$$

$$\kappa_3^{(n+1)} = \kappa_3^n + \frac{(\kappa_1^{(n)})^2}{2} + \kappa_1^n \kappa_2^n \quad (4.61)$$

4.2.1 The strong coupling fixed points

The recursion relations in equations (5.53), (4.60) and (4.61) can be solved explicitly with the initial conditions,

$$\kappa_1^{(0)} = \kappa_{10}, \kappa_2^{(0)} = \kappa_{20}, \kappa_3^{(0)} = \kappa_{30} \quad (4.62)$$

The solution is,

$$\kappa_1^{(n)} = 2 \left(\frac{\kappa_{10}}{2} \right)^L \quad (4.63)$$

$$\kappa_2^{(n)} = (aL - 1) \kappa_1^{(n)} \quad (4.64)$$

$$\kappa_3^{(n)} = \kappa_{30} + \sum_{m=0}^{n-1} \kappa_2^{(m)}, \quad (4.65)$$

where $L \equiv 2^n$ as before and $a = (1 + \kappa_{10}/\kappa_{20})$. Note that the flow does not depend on κ_{20} or κ_{30} except for an overall additive constant to κ_3 .

A fixed point of these recursion relations is,

$$\kappa_1 = 0, \quad \kappa_2 = 0, \quad \kappa_3 = \kappa_3^*(\kappa_{10}, \kappa_{20}, \kappa_{30}) \quad (4.66)$$

This corresponds to decoupled dimers. For any $\kappa_{10} < 2$, the couplings flow to the above fixed point. The larger the value of κ_{10} , the larger is κ_3^* . At $\kappa_{10} = 2$, κ_1 does not change but κ_2 and consequently κ_3 diverge. Thus the intermediate coupling fixed point, $\kappa_1^* = 2$ obtained earlier now corresponds to the fixed point $(\kappa_1^* = 2, \kappa_2^* = \infty, \kappa_3^* = \infty)$. However, the recursion relations have been derived in the approximation that $\kappa_3 \ll 1$. So they are valid if $\kappa_3^* \ll 1$. Figs. (4.1-4.3) show the flow of the couplings for different values of κ_{10} with $\kappa_{20} = \kappa_{30} = 0$. It can be seen that the above condition is indeed true for $\kappa_0 \approx 0.5$ or less. Thus the higher angular momentum states and hence the derivative terms can be neglected in this regime. However, as we approach the non-zero fixed point, the higher angular momentum states are important and have to be taken into account. Thus we need to go to higher orders in the perturbation theory of the dimer hamiltonian in Eq. (4.53) in order to analyse the intermediate coupling fixed point.

In the next section we derive the NLSM for the general model to establish the correspondence between the RG flow for the above and that for NLSM.

4.3 NLSM for the fermionic rotor chain

In equation(4.49) we scale the time by,

$$\tau \rightarrow \sqrt{\kappa_3} \tau \quad (4.67)$$

The action can then be written as,

$$\begin{aligned} S = & -\frac{i}{2} \int_{-\infty}^{\infty} d\tau \mathbf{A}(\mathbf{n}_{I\alpha}) \cdot \partial_\tau \mathbf{n}_{I\alpha} + \sqrt{\kappa_3} \int_{-\infty}^{\infty} d\tau \left[\sum_{I\alpha} \frac{s'^2}{2} \partial_\tau \mathbf{n}_{I\alpha} \cdot \partial_\tau \mathbf{n}_{I\alpha} \right. \\ & \left. + \sum_I s'^2 \mathbf{n}_{I1} \cdot \mathbf{n}_{I2} + \sum_I s'^2 \mathbf{n}_{I2} \cdot \left(\kappa_1 + \frac{\kappa_2}{\kappa_3} \partial_\tau^2 \right) \mathbf{n}_{(I+1)1} \right] \end{aligned} \quad (4.68)$$

Motivated by the fact that κ_2 never grew very large, we can drop the last term in equation(4.68) and get,

$$\begin{aligned} S = & -\frac{i}{2} \int_{-\infty}^{\infty} d\tau \mathbf{A}(\mathbf{n}_{I\alpha}) \cdot \partial_\tau \mathbf{n}_{I\alpha} + \sqrt{\kappa_3} \int_{-\infty}^{\infty} d\tau \left[\sum_{I\alpha} \frac{s'^2}{2} \partial_\tau \mathbf{n}_{I\alpha} \cdot \partial_\tau \mathbf{n}_{I\alpha} \right. \\ & \left. + \sum_I s'^2 (\mathbf{n}_{I1} \cdot \mathbf{n}_{I2} + \kappa_1 \mathbf{n}_{I2} \cdot \mathbf{n}_{(I+1)1}) \right] \end{aligned} \quad (4.69)$$

Thus we see that $\sqrt{\kappa_3}$ scales out of the real part of the action. The path integral may then performed in the saddle point approximation in the large κ_3 limit. We proceed exactly as in Section 2.3 and obtain the NLSM parameters.

$$g = 2(1 + \kappa_1) \left(\frac{2}{\kappa_1(81\kappa_1\kappa_3 + 81\kappa_3 + 2)} \right)^{\frac{1}{2}} \quad (4.70)$$

$$c = 9 \left(\frac{\kappa_1\kappa_2}{\kappa_1(81\kappa_1\kappa_3 + 81\kappa_3 + 2)} \right)^{\frac{1}{2}} \quad (4.71)$$

$$\theta = 2\pi \frac{\kappa_1}{1 + \kappa_1} \quad (4.72)$$

The above derivation of NLSM is valid for large κ_3 . But we are interested in the regime where κ_3 is small. This requires a more careful treatment than what we did above. We shall assume that the mapping will still hold, though the parameter values may be different.

4.4 Discussion

To summarise the results of this chapter, we started with the real space RG for DSC and found that the system flows to a more general fermionic rotor chain (FRC). After that we extended the RG scheme to FRC and finally did its Haldane mapping to get the NLSM parameters. Now we are in a position to translate the RG flow of κ_1 , κ_2 and κ_3 that we obtained in Section 4.2 for FRC to the flow for NLSM in the $1/g - \theta$ plane. This is shown in Figs. (4.4-4.6), corresponding to different values of κ_{10} . Thus we obtain the anticipated renormalisation of θ . With successive steps of RG, θ and g approach 0 and ∞ respectively.

Now let us consider the case of the semi-infinite chain. When the dimerisation is such that there is an unpaired spin at the edge, the fixed point would correspond to not only decoupled dimers but also a dangling spin at the edge. Strictly speaking, it is no longer a spin degree of freedom since $\kappa_3^* \neq 0$. But, for small values of κ_3^* , as we saw in Section 4.2, we can restrict ourselves to the $s = 1/2$ subspace. Thus we still have an effective spin degree of freedom at the edge. This fixed point corresponds to NLSM at $g = \infty$ and $\theta = 2\pi$, which we know is gapped in the bulk, but has a critical edge which is exactly equivalent to a single spin. Through the real space RG, we have shown that a dangling edge spin is dynamically generated.

Thus the semi-infinite DSC demonstrates the following two generic features expected of all $U(N+M)/U(N) \times U(M)$ Grassmann σ models, in the context of the $O(3)$ ($N = M = 1$) model.

- Renormalisation of θ to integer multiples of 2π .
- Massless edge excitations.

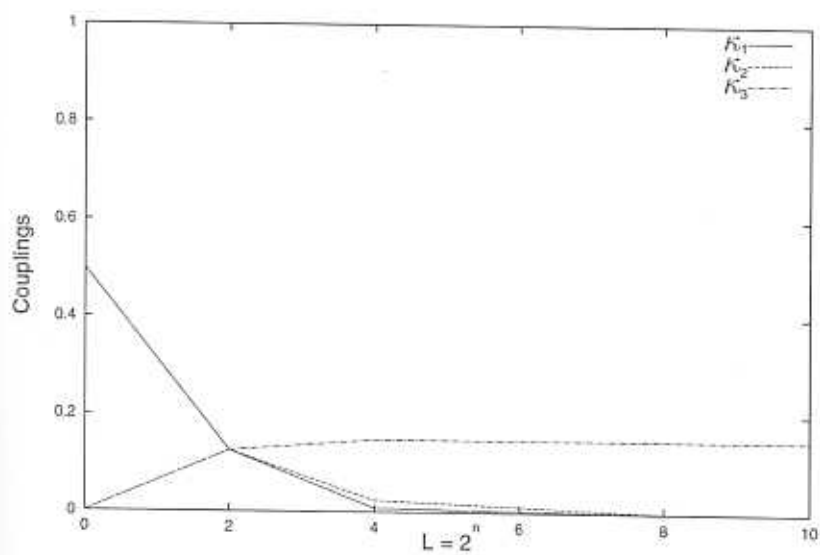


Figure 4.1: RG flows for κ_1 , κ_2 and κ_3 at $\kappa_{10} = 0.5$, $\kappa_{20} = \kappa_{30} = 0$. n is the number of RG steps.

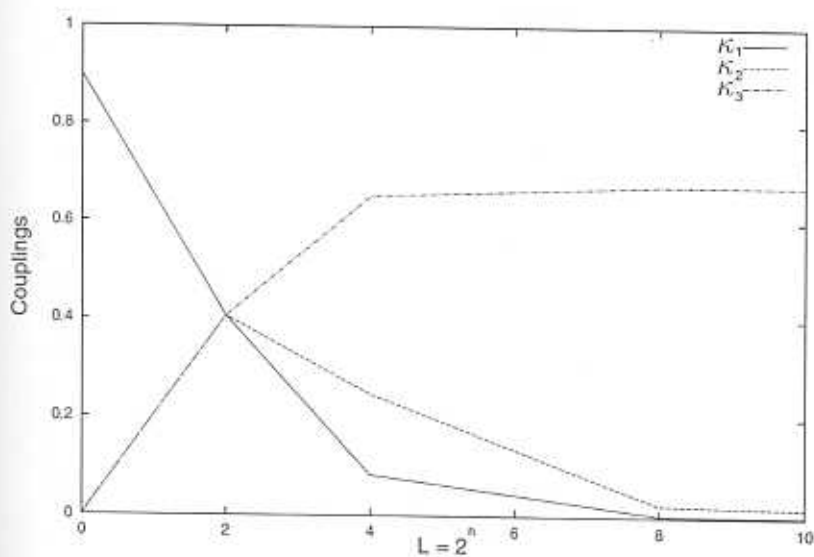


Figure 4.2: Flow for $\kappa_{10} = 0.9$, $\kappa_{20} = \kappa_{30} = 0$.

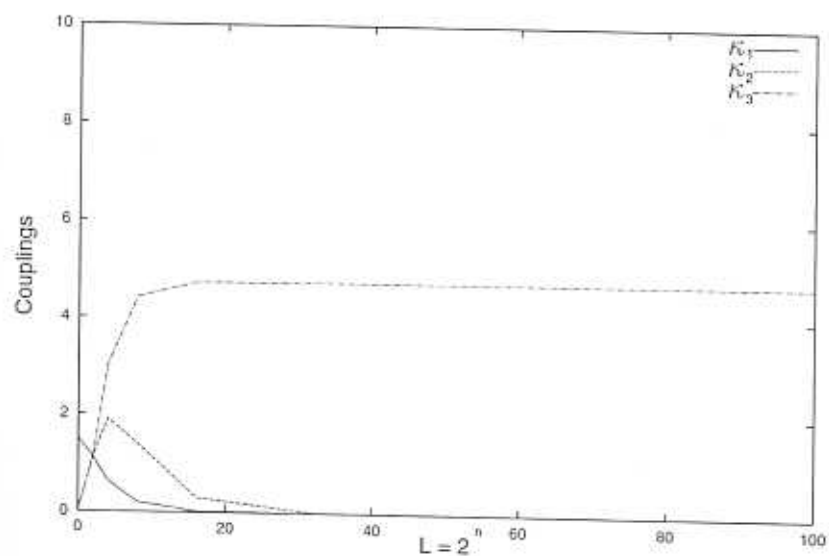


Figure 4.3: Flow for $\kappa_{10} = 1.5$, $\kappa_{20} = 0 = \kappa_{30}$.

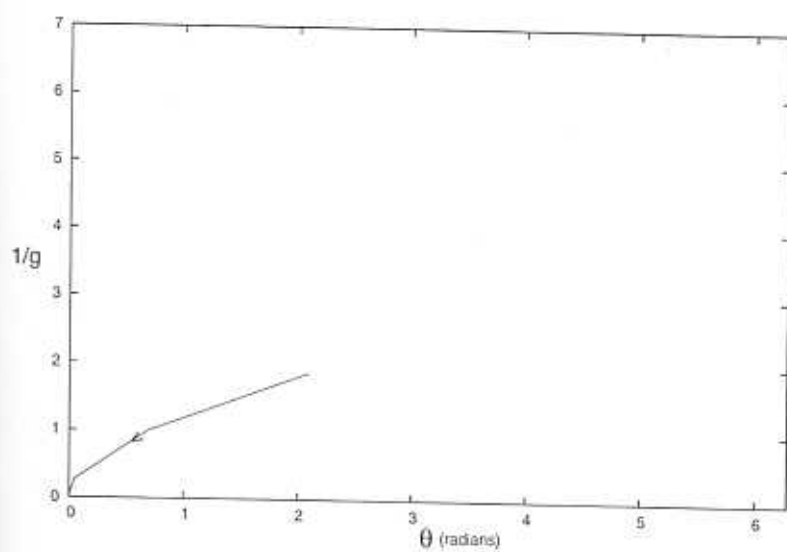


Figure 4.4: RG flow on $1/g - \theta$ plane corresponding to $\kappa_{10} = 0.5$.

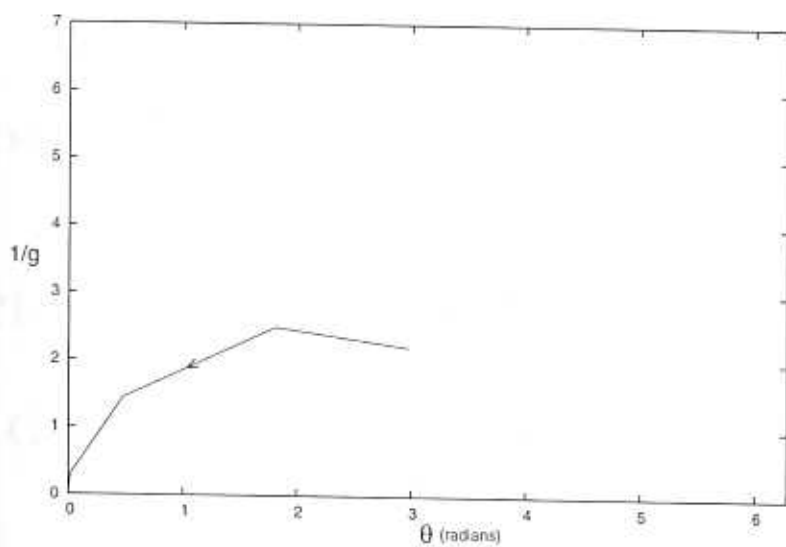


Figure 4.5: RG flow on $1/g - \theta$ plane corresponding to $\kappa_{10} = 0.9$.

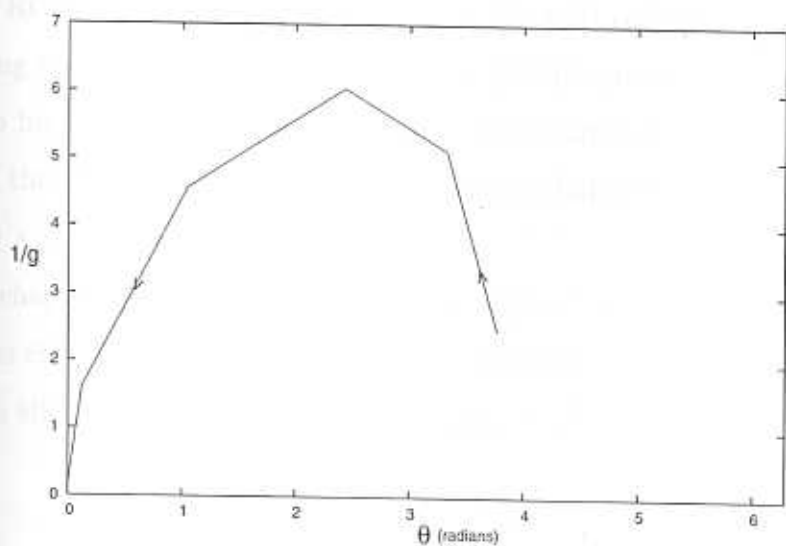


Figure 4.6: RG flow on $1/g - \theta$ plane corresponding to $\kappa_{10} = 1.5$.

Chapter 5

Effective $s = \frac{1}{2}$ models for higher spin dimerised chains

In the previous chapter we used $s = 1/2$ dimerised spin chain to obtain the RG flow for NLSM in certain parameter regime. The RG procedure we developed is valid at strong dimerisation and thus we are able to access NLSM at strong coupling near $\theta = 0$ and 2π . Strong coupling regime near $\theta = 2\pi m$ would correspond to a spin- $\frac{m}{2}$ dimerised chain with an unpaired spin at the edge. Thus it would seem that we need to do RG for the spin- $\frac{m}{2}$ model to access the said region. This in turn would mean solving the spin- $\frac{m}{2}$ dimer problem which gets progressively more complicated as we go to higher spins. But there is a way to get around this difficulty. We will see that, in the strong dimerisation limit the spin- s chain can be approximated with an effective $s = \frac{1}{2}$ model.

In this chapter, we first derive the effective spin- $\frac{1}{2}$ model. The RG analysis of the previous chapter is then extended to the effective model. In the $s = 1$ case, we also use the effective model to estimate the gapless point.

5.1 Spin- s dimerised chain

The hamiltonian for the spin- s dimerised chain is,

$$H = \sum_I \left[\frac{1}{2} (\mathbf{S}_{I1} + \mathbf{S}_{I2})^2 + \kappa \mathbf{S}_{I2} \cdot \mathbf{S}_{I+11} \right], \quad (5.1)$$

with $\mathbf{S}_{I\alpha} \cdot \mathbf{S}_{J\beta} = s(s+1)$. I as usual labels the dimer and α distinguishes the sites within a dimer. We are interested in the strongly dimerised limit, *i.e.* $\kappa \ll 1$. Then eigenstates of H at $\kappa = 0$ (decoupled dimers) form a convenient basis to work with. The spectrum of each dimer consists of one integer spin L representation for $L = 0, 1, 2, \dots, 2s$. Thus,

$$\mathbf{S}_I \cdot \mathbf{S}_I |L_I M_I\rangle = L_I(L_I + 1) |L_I M_I\rangle \quad (5.2)$$

where, $L_I = 1, 2, \dots, 2s$ and $M_I = -L_I, (-L_I+1), \dots, (L_I-1), L_I$. Then,

$$|\{L_I, M_I\}\rangle = \prod_I \otimes |L_I M_I\rangle \quad (5.3)$$

forms a basis for the Hilbert space of the chain.

5.2 The effective spin- $\frac{1}{2}$ model

From Eq. (5.2) we see that the singlet is the ground state, the triplet has gap equal to 1, the $L = 2$ has a gap of 3 and the higher angular momentum states have larger gaps. So for $\kappa \ll 1$, the low energy excitations should be dominantly composed of the triplets. This motivates us to project out the $L_I \geq 2$ states and take the low energy subspace to be composed of the singlets and triplets alone. Thus the subspace is spanned by the basis defined in Eq. (5.3) with the constraint that $L_I \leq 1$.

We now have a collection of dimers in the singlet-triplet subspace. Therefore, each dimer can be modelled as an effective system of two $s = \frac{1}{2}$ spins, *i.e.* effective

spin- $\frac{1}{2}$ dimers. The mapping being explicitly given by,

$$\begin{aligned} |\uparrow\uparrow\rangle &= |1, 1\rangle, \\ |\uparrow\downarrow\rangle &= \frac{1}{\sqrt{2}} (|1, 0\rangle + |0, 0\rangle), \\ |\downarrow\uparrow\rangle &= \frac{1}{\sqrt{2}} (|1, 0\rangle - |0, 0\rangle), \\ |\downarrow\downarrow\rangle &= |1, -1\rangle. \end{aligned}$$

This mapping can be used to derive the effective hamiltonian in terms of the effective spin- $\frac{1}{2}$ operators which we will denote by $\tilde{S}_{I\alpha}$. It is clear that the total spin operator of the spin- s dimer will project to the total spin operator of the effective spin- $\frac{1}{2}$ dimer.

$$P(S_{I1} + S_{I2})P = \tilde{S}_{I1} + \tilde{S}_{I2} \quad (5.4)$$

where the projection operator has been denoted by P . Since the hamiltonian in Eq. (5.1) has only nearest neighbour dimer-dimer interactions, so will the effective hamiltonian. The most general spin- $\frac{1}{2}$ dimer-dimer interaction is of the form,

$$\tilde{\kappa}_{\alpha\beta} \tilde{S}_{1\alpha} \cdot \tilde{S}_{2\beta} \quad (5.5)$$

The effective model will therefore be a spin- $\frac{1}{2}$ chain with a hamiltonian of the form,

$$H_{eff} = \sum_I \left(\frac{1}{2} (\tilde{S}_{I1} + \tilde{S}_{I2})^2 + \tilde{\kappa}_{\alpha\beta} \tilde{S}_{I\alpha} \cdot \tilde{S}_{I+1\beta} \right) \quad (5.6)$$

5.2.1 Schwinger bosons

We will use the Schwinger boson representation for the two spins composing the dimer,

$$[z_{\alpha\sigma}, z_{\beta\sigma'}^\dagger] = \delta_{\alpha\beta} \delta_{\sigma\sigma'}; \quad \alpha, \beta = 1, 2 \text{ and } \sigma, \sigma' = \uparrow, \downarrow \quad (5.7)$$

The spin operators are,

$$S_\alpha^a = \frac{1}{2} z_{\alpha\sigma_1}^\dagger \tau_{\sigma_1\sigma_2}^a z_{\alpha\sigma_2} \quad (5.8)$$

It then follows that,

$$\mathbf{S}_\alpha \cdot \mathbf{S}_\alpha = \frac{\tilde{N}_\alpha}{2} \left(\frac{\tilde{N}_\alpha}{2} + 1 \right) \quad (5.9)$$

where,

$$\hat{N}_\alpha = z_\alpha^\dagger z_\alpha \quad (5.10)$$

Thus we have the constraint,

$$\hat{N}_\alpha |\psi\rangle = 2s |\psi\rangle \quad (5.11)$$

Valence bond operators

We define the valence bond creation operators,

$$V_\mu^\dagger = \frac{1}{\sqrt{2}} (\tau^\mu i \tau^2)_{\sigma_1 \sigma_2} z_{1\sigma_1}^\dagger z_{2\sigma_2}^\dagger \quad (5.12)$$

where τ^0 is the identity matrix and τ^μ , $\mu = 1, 2, 3$ are the Pauli spin matrices. It then follows that,

$$V_\mu = -\frac{1}{\sqrt{2}} (i \tau^2 i \tau^\mu)_{\sigma_2 \sigma_1} z_{1\sigma_1} z_{2\sigma_2} \quad (5.13)$$

It can also be checked that,

$$[S^a, V_0^\dagger] = 0 \quad (5.14)$$

$$[S^a, V_a^\dagger] = i \epsilon^{abc} V_c^\dagger \quad (5.15)$$

The singlet and triplet states are therefore given by,

$$|0, 0\rangle = \frac{1}{\sqrt{f_n}} (V_0^\dagger)^n |0\rangle \quad (5.16)$$

$$|1, a\rangle = \frac{1}{\sqrt{g_n}} V_a^\dagger (V_0^\dagger)^{n-1} |0\rangle \quad (5.17)$$

where $n = 2s$, f_n and g_n are normalisation constants and,

$$z_{\alpha\sigma} |0\rangle = 0 \quad (5.18)$$

Valence bond operator algebra

To compute the normalisation constants and the matrix elements of the spin operators between in the singlet-triplet subspace, it is useful to compute the algebra of the valence bond operators. A straightforward computation yields,

$$[V_\mu, V_\nu^\dagger] = \frac{1}{2} \left(z_1^\dagger (\tau^\nu \tau^\mu) z_1 + z_2^\dagger (\tau^2 (\tau^\nu)^T (\tau^\mu)^T \tau^2) z_2 + 2\delta^{\mu\nu} \right). \quad (5.19)$$

From the above it follows that,

$$[V_0, V_0^\dagger] = \frac{\hat{N} + 1}{2}, \quad (5.20)$$

$$[V_0, V_a^\dagger] = n^a, \quad (5.21)$$

$$[V_a, V_0^\dagger] = n^a, \quad (5.22)$$

$$[V_a, V_b^\dagger] = \delta_{ab} \left(\frac{\hat{N} + 1}{2} \right) + i\epsilon_{abc} S^c. \quad (5.23)$$

Where we have defined,

$$\hat{N} \equiv z_1^\dagger z_1 + z_2^\dagger z_2 \quad (5.24)$$

$$\mathbf{S} = \mathbf{S}_1 + \mathbf{S}_2 \quad (5.25)$$

$$\mathbf{n} = \mathbf{S}_1 - \mathbf{S}_2 \quad (5.26)$$

The commutation relations between \mathbf{S} , \mathbf{n} and the valence bond operators are given by,

$$[S^a, V_0^\dagger] = 0 \quad (5.27)$$

$$[S^a, V_a^\dagger] = i\epsilon^{abc} V_c^\dagger \quad (5.28)$$

$$[n^a, V_0^\dagger] = V_a^\dagger \quad (5.29)$$

$$[n^a, V_b^\dagger] = \delta_{ab} V_0^\dagger \quad (5.30)$$

Normalisation constants

We will now use the valence bond operator algebra to compute the normalisation constants f_n and g_n of the singlet and triplet states as defined in Eqs. (5.16) and (5.17).

$$\begin{aligned} f_n &= \langle 0 | V_0^n V_0^{\dagger n} | 0 \rangle \\ &= \langle 0 | V_0^{n-1} \left(\frac{\hat{N} + 2}{2} V_0^{\dagger n-1} + V_0^\dagger \frac{\hat{N} + 2}{2} V_0^{\dagger n-1} + \dots + V_0^{\dagger n-1} \frac{\hat{N} + 2}{2} \right) | 0 \rangle \\ &= \frac{1}{2} (n+1)n f_{n-1} = \frac{1}{2^n} (n+1)! n! \end{aligned}$$

g_n is given by,

$$g_n = \frac{1}{3} \langle 0 | V_0^{n-1} V_a V_a^\dagger V_0^{\dagger n-1} | 0 \rangle \quad (5.31)$$

Using the identity,

$$\frac{1}{2}\tau_{\sigma_2\sigma_1}^a\tau_{\sigma_3\sigma_4}^a + \frac{1}{2}\delta_{\sigma_1\sigma_2}\delta_{\sigma_3\sigma_4} = \delta_{\sigma_1\sigma_3}\delta_{\sigma_2\sigma_4} \quad (5.32)$$

we derive,

$$\begin{aligned} V_a V_a^\dagger &= (\hat{N}_1 + 2)(\hat{N}_2 + 2) - V_0 V_0^\dagger \\ &= \left(\frac{\hat{N} + 4}{2}\right)^2 - V_0 V_0^\dagger \end{aligned} \quad (5.33)$$

where we have used the fact that we will always be in the $N_1 = N_2 = N/2$ subspace. It then follows that,

$$\begin{aligned} g_n &= \frac{1}{3} \langle 0 | V_0^{n-1} \left(\left(\frac{\hat{N} + 4}{2} \right)^2 - V_0 V_0^\dagger \right) V_0^{\dagger n-1} | 0 \rangle \\ &= \frac{1}{3} ((n+1)^2 f_{n-1} - f_n) = \frac{1}{3} \frac{(n+2)}{n} f_n \end{aligned}$$

5.2.2 The effective model

We now compute the matrix elements of the operators $\mathbf{n} = \mathbf{S}_1 + \mathbf{S}_2$. Angular momentum conservation implies,

$$\langle 00 | \mathbf{n} | 00 \rangle = 0 \quad (5.34)$$

\mathbf{n} is odd under parity ($\mathbf{S}_1 \leftrightarrow \mathbf{S}_2$). Hence it changes the parity of the state that it acts on. This implies,

$$\langle 1a | \mathbf{n} | 1b \rangle = 0 \quad (5.35)$$

Using the operator algebra that we derived earlier in this section,

$$n^a |00\rangle = n \sqrt{\frac{n+2}{3n}} |1a\rangle \quad (5.36)$$

We therefore have,

$$\langle 1b | n^a | 00 \rangle = \delta_{ab} 2 \sqrt{\frac{s(s+1)}{3}} = \langle 00 | n^a | 1a \rangle \quad (5.37)$$

Comparing the expressions for spin- $\frac{1}{2}$ and spin- s , we get,

$$PS_1P = a(s)\tilde{S}_1 + b(s)\tilde{S}_2 \quad (5.38)$$

$$PS_2P = b(s)\tilde{S}_1 + a(s)\tilde{S}_2 \quad (5.39)$$

where,

$$a(s) = \frac{1}{2} + \sqrt{\frac{s(s+1)}{3}} \quad (5.40)$$

$$b(s) = \frac{1}{2} - \sqrt{\frac{s(s+1)}{3}} \quad (5.41)$$

The coupling constant matrix $\tilde{\kappa}$ for the effective hamiltonian as defined in Eq. (5.6) is given by,

$$\tilde{\kappa} = \kappa \begin{pmatrix} a(s)b(s) & b(s)^2 \\ a(s)^2 & a(s)b(s) \end{pmatrix} \quad (5.42)$$

The effective model that we have derived is a general ladder consisting of weakly coupled dimers. In Section 2.4 we derived the NLSM for this system. In the next section we extend the RG scheme that we developed for the dimerised chain in Chapter 4, to the case of the ladder.

5.3 Real space RG for the ladder

The hamiltonian we start with is,

$$H = \sum_I \frac{1}{2} (S_{I1} + S_{I2})^2 + \kappa_{\alpha\beta} S_{I\alpha} \cdot S_{I+1\beta}. \quad (5.43)$$

As in the case of DSC, we write the path integral and then isolate a dimer. The hamiltonian for the dimer is then,

$$h = h_0 + h_{int}.$$

Where,

$$h_0 = \frac{1}{2} (S_1 + S_2)^2 ; \quad h_{int} = \sum_{\alpha} S_{\alpha} \cdot m_{\alpha}$$

and $m_{\alpha} = s \sum_{\beta} (\kappa_{\alpha\beta} n_{I+1\beta} + \kappa_{\alpha\beta}^{\dagger} n_{I-1\beta})$ (5.44)

Now we can use the results from the previous chapter to integrate out the dimer. To leading order in derivatives and κ (see Eq. (4.36)), the interaction term in the effective action is,

$$S_{int}^{eff} = \frac{-1}{4} \int d\tau \mathbf{m}(\tau) \mathbf{m}(\tau).$$

Where $\mathbf{m} = \mathbf{m}_1 - \mathbf{m}_2$. In terms of \mathbf{m}_1 and \mathbf{m}_2 , S_{int}^{eff} can be written as,

$$S_{int}^{eff} = \frac{-1}{4} \int d\tau \mathbf{m}_\alpha^a(\tau) P_{\alpha\beta} \mathbf{m}_\beta^a(\tau) \quad (5.45)$$

where,

$$P \equiv \begin{pmatrix} 1 & -1 \\ -1 & 1 \end{pmatrix} \quad (5.46)$$

Substituting Eq. (5.44) in Eq. (5.45) we get,

$$S_{int}^{eff} = \frac{-s^2}{4} \int d\tau \left((\kappa^\dagger P \kappa)_{\alpha\beta} \mathbf{n}_{I+1\alpha} \cdot \mathbf{n}_{I+1\beta} + (\kappa P \kappa^\dagger)_{\alpha\beta} \mathbf{n}_{I-1\alpha} \cdot \mathbf{n}_{I-1\beta} + 2(\kappa P \kappa)_{\alpha\beta} \mathbf{n}_{I-1\alpha} \cdot \mathbf{n}_{I+1\beta} \right) \quad (5.47)$$

Then the effective interaction hamiltonian between two dimers is,

$$h_{eff}^{int} = \sum_I \left(\frac{-1}{4} ((\kappa^\dagger P \kappa) + (\kappa P \kappa^\dagger))_{\alpha\beta} \mathbf{S}_{I\alpha} \cdot \mathbf{S}_{I\beta} - \frac{1}{2} (\kappa P \kappa)_{\alpha\beta} \mathbf{S}_{I\alpha} \cdot \mathbf{S}_{I+1\beta} \right) \quad (5.48)$$

5.3.1 The recurrence relations and the strong coupling fixed point

Unlike the case of DSC, RG has now generated not just inter-dimer terms, but a term coupling the spins within a dimer as well. From Eq. (5.48) it follows that the effective hamiltonian obtained after integrating out alternate dimers is,

$$H_{eff} = \sum_I (1 + f) \mathbf{S}_{I1} \cdot \mathbf{S}_{I2} + \bar{\kappa}_{\alpha\beta} \mathbf{S}_{I\alpha} \cdot \mathbf{S}_{I+1\beta} \quad (5.49)$$

where,

$$f \equiv -\frac{1}{4} ((\kappa^\dagger P \kappa + \kappa P \kappa^\dagger)_{12} + (\kappa^\dagger P \kappa + \kappa P \kappa^\dagger)_{21}) \quad (5.50)$$

and

$$\tilde{\kappa} \equiv -\frac{1}{2}\kappa P\kappa \quad (5.51)$$

The factor $(1+f)$ in Eq. (5.49) can be absorbed by rescaling the time (temperature) so that the effective hamiltonian has the same form as the original one (Eq. (5.43))

$$H = \sum_I \frac{1}{2} (S_{I1} + S_{I2})^2 + \kappa'_{\alpha\beta} S_{I\alpha} S_{I+1\beta} \quad (5.52)$$

Thus under the R.G transformation κ goes to,

$$\kappa' = \frac{-1}{2(1+f)} \kappa P \kappa \quad (5.53)$$

It is convenient to analyse this equation in a basis where P is diagonal. This is achieved by the following transformation,

$$UPU^\dagger = \begin{pmatrix} 2 & 0 \\ 0 & 0 \end{pmatrix} \quad (5.54)$$

where,

$$U = \frac{1}{\sqrt{2}} \begin{pmatrix} 1 & -1 \\ 1 & 1 \end{pmatrix} \quad (5.55)$$

Under this transformation, κ becomes,

$$U\kappa U^\dagger = -\frac{1}{2} \begin{pmatrix} \kappa_0 & \kappa_1 \\ \kappa_2 & -\kappa_3 \end{pmatrix} \quad (5.56)$$

where,

$$\begin{aligned} \kappa_0 &\equiv -\sum_{\alpha\beta} (-1)^{\alpha+\beta} \kappa_{\alpha\beta} = (\kappa_{12} + \kappa_{21} - \kappa_{11} - \kappa_{22}) \\ \kappa_1 &\equiv \sum_{\alpha\beta} (-1)^\alpha \kappa_{\alpha\beta} = (\kappa_{21} + \kappa_{22} - \kappa_{12} - \kappa_{11}) \\ \kappa_2 &\equiv \sum_{\alpha\beta} (-1)^\beta \kappa_{\alpha\beta} = (\kappa_{12} + \kappa_{22} - \kappa_{21} - \kappa_{11}) \\ \kappa_3 &\equiv \sum_{\alpha\beta} \kappa_{\alpha\beta} = (\kappa_{11} + \kappa_{12} + \kappa_{21} + \kappa_{22}) \end{aligned} \quad (5.57)$$

f is then computed using Eq. (5.50) to be,

$$f = \frac{-\kappa_0(\kappa_1 + \kappa_2)}{2} \quad (5.58)$$

Using Eqs. (5.53) and (5.56) the recurrence relations for κ_0 , κ_1 , κ_2 and κ_3 are found to be,

$$\kappa'_0 = \frac{1}{2(1+f)}\kappa_0^2 \quad (5.59)$$

$$\kappa'_1 = \frac{1}{2(1+f)}\kappa_0\kappa_1 \quad (5.60)$$

$$\kappa'_2 = \frac{1}{2(1+f)}\kappa_0\kappa_2 \quad (5.61)$$

$$\kappa'_3 = -\frac{1}{2(1+f)}\kappa_1\kappa_2 \quad (5.62)$$

It can be easily seen that $\kappa_a = 0$ is a stable fixed point.

5.4 RG flow in the $1/g - \theta$ plane

Now we have at our disposal spin models, through which we can access NLSM at strong coupling near $\theta = 2\pi m$ for all values of m . The spin model corresponding to a particular m is the spin- $\frac{m}{2}$ dimerised chain. In the strong dimerisation limit (which corresponds to the regime we are interested in) these models can be well approximated by an effective $s = \frac{1}{2}$ ladder. The real space RG for the ladder shows that $(1/g = 0, \theta = 2\pi m)$ are stable fixed points. At these points we have an effective edge spin of magnitude $\frac{m}{2}$. The expected RG flow in the $1/g - \theta$ plane is shown in Fig. 5.1.

5.5 Effective model for $s = 1$ chain and the gapless points

Putting $s = 1$ in Eq. (5.42) we get the effective coupling constant matrix to be,

$$\tilde{\kappa} = \kappa \begin{pmatrix} -.42 & .1 \\ 1.73 & -.42 \end{pmatrix} \quad (5.63)$$

Substituting for κ_{ij} in Eqs. (2.59-2.61) we get the NLSM parameters for the

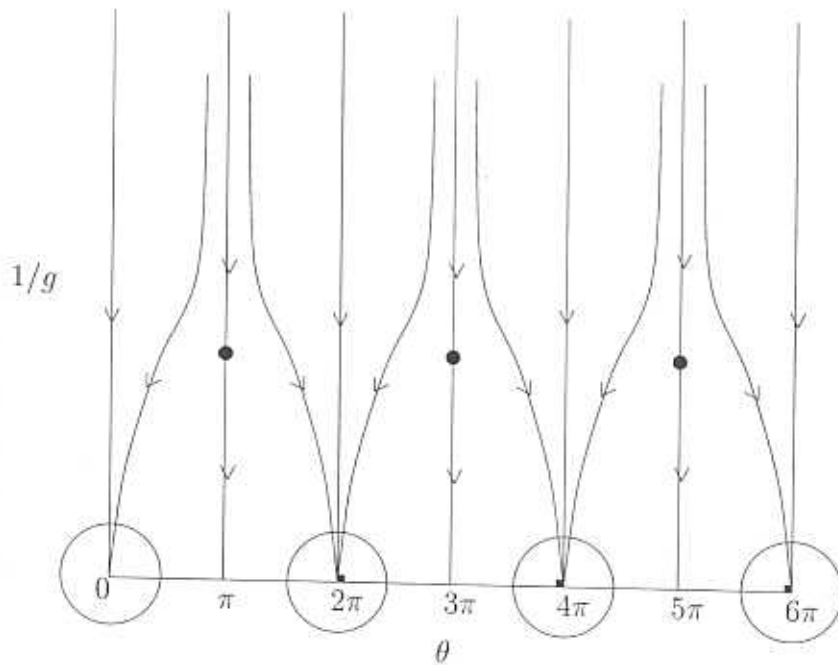


Figure 5.1: The solid circles are the critical points at $\theta = (2n+1)\pi$ corresponding to the half-integer spin uniform chains. The solid squares are the points with a critical edge. The real space RG for the spin models accesses the circled regions.

effective model as,

$$\tilde{g} = 2\sqrt{\frac{1+1.83\kappa}{2.67\kappa}} \quad (5.64)$$

$$\tilde{c} = \frac{1}{2}\sqrt{2.67\kappa(1+1.83\kappa)} \quad (5.65)$$

$$\tilde{\theta} = 2\pi\frac{1.63\kappa}{1+1.83\kappa} \quad (5.66)$$

We know that NLSM is gapless at $\theta = \pi$ [41]. θ for spin- s dimerised chain is given by,

$$\theta = 4\pi s \frac{\kappa}{1+\kappa} \quad (5.67)$$

For $s = 1$, by equating θ to π we obtain the gapless point at $\kappa_{cr} = 0.33$. Pati *et al.* [3] have done a DMRG study of the spin-1 dimerised chain and found $\kappa_{cr} = 0.6$. Thus the NLSM result is well off the mark.

Now we estimate the gapless point by equating θ for the effective model, given

in Eq. (5.66), to π .

$$\tilde{\theta} = \pi \Rightarrow \kappa_H = 0.7 \quad (5.68)$$

The effective model thus gives a better estimate of the gapless point. Right now it is not very clear why κ_{cr} estimated *via* the effective spin- $\frac{1}{2}$ model should be better than that estimated directly. Afterall, in both the cases ultimately we are using the same Haldane mapping.

Pati *et al.* also found that if a frustrating next nearest neighbour coupling is introduced, then the value of κ_{cr} increases slightly. Haldane mapping predicts κ_{cr} to be independent of the frustration parameter.

The frustrating couplings can also be incorporated into our model. We begin with,

$$\kappa = \begin{pmatrix} \gamma & 0 \\ \kappa & \gamma \end{pmatrix} \quad (5.69)$$

This leads to,

$$\begin{aligned} \tilde{\kappa} &= \begin{pmatrix} ab\kappa + (a^2 + b^2)\gamma & b^2\kappa + 2ab\gamma \\ a^2\kappa + 2ab\gamma & ab\kappa + (a^2 + b^2)\gamma \end{pmatrix} \\ &= \begin{pmatrix} -.42\kappa + 1.83\gamma & 0.1\kappa - .83\gamma \\ 1.73\kappa - .83\gamma & -.42\kappa + 1.83\gamma \end{pmatrix} \end{aligned} \quad (5.70)$$

$\tilde{\theta}$ can be computed to give,

$$\tilde{\theta} = 2\pi \frac{1.63\kappa}{1 + 1.83\kappa - 1.66\gamma} \quad (5.71)$$

This gives,

$$\kappa_{cr} = 0.7 - 1.16\gamma \quad (5.72)$$

Though κ_{cr} now depends on γ , the frustrating coupling, the dependence is not in agreement with the DMRG result where κ_{cr} increases with γ . Thus it is crucial to calculate the effective hamiltonian to a higher order for a better understanding of the gapless points.

Chapter 6

Grassmann σ models and $SU(N)$ spin chains

In Chapters 2 - 5 we studied dimerised $SU(2)$ spin chain and its connections with $O(3)$ NLSM. The latter is ' $N_1 = N_2 = 1$ ' case of the Grassmann σ model defined on the manifold $\frac{U(N_1+N_2)}{U(N_1) \times U(N_2)}$. It has the action,

$$S = \int dx dt \frac{1}{2} \text{Tr} \left[\frac{c}{2g} \partial_x Q \partial_x Q + \frac{1}{2gc} \partial_t Q \partial_t Q - \frac{i\theta}{4\pi} Q \partial_x Q \partial_t Q \right] \quad (6.1)$$

where $Q \in \frac{U(N_1+N_2)}{U(N_1) \times U(N_2)}$.

In the $O(3)$ case, we used $SU(2)$ dimerised spin chain to access the strong coupling regime of NLSM. In this chapter, analogous to the Haldane mapping for $SU(2)$ spin chains, we derive the Grassmann σ model as the effective long wave-length theory for dimerised $SU(N)$ spin chains. Thus the latter can be used to study NLSM at strong coupling.

We first introduce Grassmannian coherent states and write the path integral representation for the system in that basis. Then we do the standard change of variables and integrating out of fast fluctuations to finally obtain NLSM in the continuum limit.

6.1 Grassmannian coherent states

6.1.1 $U(N_1 + N_2)$ generators

Let λ_N^a , $a = 0, 1, \dots, (N^2 - 1)$ be the generators of $U(N)$ in the fundamental representation [42]. λ_N^0 is defined to be the identity matrix. We then have,

$$[\lambda_N^a, \lambda_N^b] = i f_N^{abc} \lambda_N^c \quad (6.2)$$

where $a = 1, 2, \dots, N^2 - 1$ and f_N^{abc} are the $SU(N)$ structure functions. We can always choose the basis where,

$$\begin{aligned} \text{tr}(\lambda^a) &= 0 \\ \text{tr}(\lambda^a \lambda^b) &= \delta_{ab} \end{aligned}$$

for $a = 1, 2, \dots, (N^2 - 1)$.

Let $N = N_1 + N_2$. Then for our purposes it is convenient to label the $U(N_1 + N_2)$ generators as follows. We first define $N_1^2 + N_2^2$ matrices with non-zero entries only in the top left $N_1 \times N_1$ and bottom right $N_2 \times N_2$ blocks respectively.

$$(\lambda^{\dagger a})_{\alpha p \alpha' p'} \equiv \delta_{p1} \delta_{p'1} (\lambda_{N_1}^a)_{\alpha\alpha'} \quad (6.3)$$

$$(\lambda^{\dagger a})_{\alpha p \alpha' p'} \equiv \delta_{p-1} \delta_{p'-1} (\lambda_{N_2}^a)_{\alpha\alpha'} \quad (6.4)$$

Of the remaining $2N_1 N_2$ generators, $N_1 N_2$ can be chosen to have non-zero entries only in the top right $N_2 \times N_1$ block and the other $N_1 N_2$ to have non-zero entries only in the bottom left $N_1 \times N_2$ block.

$$(\lambda^{+a})_{\alpha p \alpha' p'} \propto \delta_{p1} \delta_{p'-1} \quad (6.5)$$

$$\lambda^{-a} = (\lambda^{+a})^\dagger \quad (6.6)$$

$\lambda^a, \lambda^{\dagger a}, \lambda^{+a}$ and λ^{-a} form a basis for the $(N_1 + N_2)^2$ dimensional $U(N_1 + N_2)$ algebra in the fundamental representation. Hereinafter, λ 's without explicit subscripts will refer to $N_1 + N_2$ dimensional matrices.

Define,

$$\Lambda \equiv \lambda^{\dagger 0} - \lambda^{i0} \quad (6.7)$$

It can be checked that,

$$[\Lambda, \lambda^{\uparrow a}] = 0 \quad (6.8)$$

$$[\Lambda, \lambda^{\downarrow a}] = 0 \quad (6.9)$$

$$[\Lambda, \lambda^{+a}] = 2\lambda^{+a} \quad (6.10)$$

$$[\Lambda, \lambda^{-a}] = -2\lambda^{-a} \quad (6.11)$$

6.1.2 The replica fermion representation

The Hilbert space of $N_1 + N_2$ species of replica fermions is defined by,

$$\{\psi_{\alpha p}, \psi_{\alpha' p'}^{\dagger}\} = \delta_{\alpha\alpha'} \delta_{pp'} \quad (6.12)$$

$$\begin{aligned} \alpha &= 1, 2, \dots, N_1 & p &= 1 \\ &= 1, 2, \dots, N_2 & p &= -1 \end{aligned}$$

$$\psi_{\alpha p}|0\rangle = 0 \quad (6.13)$$

This Hilbert space carries a representation of $U(N_1 + N_2)$. The generators are given by,

$$J^{ar} = \psi_{\alpha p}^{\dagger} (\lambda^{ar})_{\alpha p \alpha' p'} \psi_{\alpha' p'} \quad (6.14)$$

where r runs over $\uparrow, \downarrow, +$ and $-$. These operators do not change the total number of replica fermions and therefore can be block diagonalised into subspaces defined by,

$$(J^{0\uparrow} + J^{0\downarrow})|\phi\rangle = n|\phi\rangle \quad (6.15)$$

Each n -replica fermion subspace forms an irreducible representation of the $U(N_1 + N_2)$ algebra, corresponding to the fully antisymmetric product of n fundamental representations [42].

We denote the $U(N_1 + N_2)$ matrices as,

$$T = e^{i\lambda^{ar}\theta^{ar}} \quad (6.16)$$

where θ^{ar} parametrise the group elements. The corresponding operator in the replica fermion space is denoted by $U(T)$,

$$U(T) = e^{iJ^{ar}\theta^{ar}} \quad (6.17)$$

6.1.3 Coherent states and the path integral

Consider the replica fermion system with the hamiltonian,

$$H = \omega (J^{0\uparrow} - J^{0\downarrow}) \quad (6.18)$$

The ground state of the system is then,

$$|GS\rangle \equiv \prod_{\alpha=1}^{N_2} \psi_{\alpha-1}^{\dagger} |0\rangle \quad (6.19)$$

Since the hamiltonian does not change the total number of replica fermions, under time evolution the system is restricted to the N_2 replica fermion subspace defined by the constraint,

$$(J^{0\uparrow} + J^{0\downarrow})|\phi\rangle = N_2|\phi\rangle \quad (6.20)$$

We have,

$$J^{a\uparrow}|GS\rangle = 0 \quad (6.21)$$

$$J^{a\downarrow}|GS\rangle = 0, \quad a \neq 0 \quad (6.22)$$

$$J^{0\downarrow}|GS\rangle = N_2|GS\rangle \quad (6.23)$$

Thus the little group of this state is $U(N_1) \times U(N_2)$. The coherent states can be constructed using the standard procedure [40]. The states are in one-to-one correspondence with points on the grassmanian manifold, $U(N_1 + N_2)/(U(N_1) \times U(N_2))$ labelled by,

$$Q = T^{-1}\Lambda T \quad (6.24)$$

They are given by,

$$|Q\rangle = U(T)|GS\rangle \quad (6.25)$$

Now we derive the standard properties of coherent states.

Resolution of identity

$$\int dQ |Q\rangle\langle Q| = \frac{N_1!N_2!}{(N_1 + N_2)!} \mathbf{I} \quad (6.26)$$

Proof: Let U be an operator in the N_2 particle sector representing an element of $U(N_1 + N_2)$. Then,

$$U \int dQ |Q\rangle\langle Q| = \int dQ' |Q'\rangle\langle Q'| U ; \forall U.$$

Where we have made the transformation $U|Q\rangle = |Q'\rangle$. By Schur's lemma, any operator that commutes with all the group elements in an irreducible representation is proportional to the identity operator. Thus,

$$\int dQ |Q\rangle\langle Q| = c \mathbf{I}.$$

Taking trace on both sides, we get,

$$1 = c \times \text{dimension of the } N_2 \text{ particle sector} = c \frac{(N_1 + N_2)!}{N_1!N_2!}$$

Thus,

$$c = \frac{N_1!N_2!}{(N_1 + N_2)!}$$

and we have the result.

Expectation values

$$\langle Q|J^a|Q\rangle = -\frac{1}{2} \text{Tr} (\lambda^a Q) \quad (6.27)$$

Proof: For neatness of notation, we revert back to single indices for the time being.

Then using Eqs. (6.14) and (6.25),

$$\langle Q|J^a|Q\rangle = \langle GS|U^\dagger \psi_i^\dagger \lambda_{ij}^a \psi_j U|GS\rangle = T_{ki}^{-1} T_{jl} \lambda_{ij}^a \langle GS|\psi_p^\dagger \psi_l|GS\rangle$$

In the last step we have used the following transformation properties of ψ_i and ψ_i^\dagger under rotation,

$$U^\dagger \psi_i U = T_{ij} \psi_j, \quad (6.28)$$

$$U^\dagger \psi_i^\dagger U = T_{ji}^{-1} \psi_j^\dagger. \quad (6.29)$$

Now,

$$\langle GS|\psi_p^\dagger \psi_l|GS\rangle = \frac{1}{2}(1 - \Lambda)_{kl} \quad (6.30)$$

Noting that $\text{Tr} \lambda^a = 0$ and using Eqs. (6.24) and (6.30) we have the final result,

$$\langle Q|J^a|Q\rangle = -\frac{1}{2} \text{Tr} (\lambda^a Q)$$

Overlap

$$\langle Q + \delta Q | Q \rangle = \exp \left(\frac{1}{2} \text{Tr}(T^{-1} \delta T \Lambda) \right) \quad (6.31)$$

Proof:

$$\langle Q + \delta Q | Q \rangle = \langle GS | (U^\dagger + \delta U^\dagger) U | GS \rangle \quad (6.32)$$

Parametrise T as follows,

$$T + \delta T = T e^{i\gamma} = T + T i\gamma,$$

where γ is an infinitesimal matrix. Then we have,

$$T^{-1} \delta T = i\gamma. \quad (6.33)$$

Correspondingly,

$$U + \delta U = U e^{i\hat{\gamma}},$$

where $\hat{\gamma} = \psi_i^\dagger \gamma_{ij} \psi_j$. Then,

$$\delta U^\dagger U = -i\hat{\gamma} = -\psi_i^\dagger (T^{-1} \delta T)_{ij} \psi_j \quad (6.34)$$

Substituting Eq. (6.34) in (6.32) and using Eqs. (6.28) (6.29) and (6.30) we get,

$$\langle Q + \delta Q | Q \rangle = 1 - \frac{1}{2} \text{Tr}(T^{-1} \delta T) (1 - \Lambda)$$

By a suitable choice of gauge, the first term in the above equation can be made 0.

Then we have,

$$\langle Q + \delta Q | Q \rangle = \exp \left(\frac{1}{2} \text{Tr}(T^{-1} \delta T \Lambda) \right) \quad (6.35)$$

6.1.4 Correlation functions

Using the above properties, we can construct the path integral representation for the generating function,

$$\begin{aligned} Z[B(\tau)] &\equiv \text{Tr} \mathcal{T} \left(e^{-\int \text{tr} B(\tau) J} \right) \\ &= \int \mathcal{D}[Q(\tau)] e^{\int_{-\infty}^{\infty} d\tau \left(\frac{1}{2} \text{Tr}(\Lambda T^{-1} \partial_\tau T) - \text{Tr} B(\tau) Q(\tau) \right)} \end{aligned} \quad (6.36)$$

where,

$$B(\pm\infty) = \Lambda.$$

It is convenient to compute the correlation functions in the operator formalism. The (euclidean) equations of motion are,

$$\partial_\tau J^{ar} = [J^{ar}, H] \quad (6.37)$$

Using equations (6.8-6.11),

$$\begin{aligned} \partial_\tau J^{a\uparrow}(\tau) &= 0 \\ \partial_\tau J^{a\downarrow}(\tau) &= 0 \\ \partial_\tau J^{a+}(\tau) &= -2J^{a+} \\ \partial_\tau J^{a-}(\tau) &= +2J^{a-} \end{aligned}$$

Which have the solutions,

$$\begin{aligned} J^{a\uparrow}(\tau) &= J^{a\uparrow}(0) \\ J^{a\downarrow}(\tau) &= J^{a\downarrow}(0) \\ J^{a+}(\tau) &= J^{a+}(0)e^{-2\omega\tau} \\ J^{a-}(\tau) &= J^{a-}(0)e^{+2\omega\tau} \end{aligned}$$

Using these solutions, all correlation functions clearly can be reduced to computing the trace of products of the $U(N_1+N_2)$ generators in the appropriate representation.

6.2 Haldane mapping for dimerised $SU(N)$ spin chain

In this section we derive the Grassmann σ model as the long wave length effective theory for the dimerised $SU(N)$ spin chain. The Hamiltonian for the system is,

$$H = \sum_I J_{I,1}^a J_{I,2}^a + \kappa J_{I,2}^a J_{(I+1),1}^a \quad (6.38)$$

where J^a 's are the $SU(N)$ generators.

In the Fock space of N_1 species of fermions with chirality +1 and N_2 species with -1, that we constructed in Section 6.1.2, each particle sector carries an irreducible representation of $SU(N)$, where $N = N_1 + N_2$. In the N_2 -particle sector, the coherent states are in one to one correspondence with the Grassmanian manifold, $\frac{U(N_1+N_2)}{U(N_1) \times U(N_2)}$. In this representation, we use the coherent state basis to write the euclidean path integral for the system. Following the standard procedure (see Chapter 2), we obtain the action,

$$S = \int dt \sum_I \frac{1}{4} \text{Tr} (Q_{I1} Q_{I2} + \kappa Q_{I2} Q_{I+1,1}) - \frac{1}{2} \sum_{I,\alpha} \text{Tr} T_{I\alpha}^{-1} \partial_t T_{I\alpha} \Lambda \quad (6.39)$$

where $Q \in \frac{U(N_1+N_2)}{U(N_1) \times U(N_2)}$.

6.2.1 Change of variables

Now, similar to the $SU(2)$ case, we split the field into a slowly varying part and the part that fluctuates about it.

Let $\{\lambda^a\}$ be the generators diagonal in the chirality index and $\{\delta^a\}$ the off-diagonal ones. Define,

$$Q_1 \equiv T e^{i\pi} \Lambda e^{-i\pi} T^{-1} \quad (6.40)$$

$$Q_2 \equiv -T e^{-i\pi} \Lambda e^{i\pi} T^{-1} \quad (6.41)$$

$$Q \equiv T \Lambda T^{-1} \quad (6.42)$$

where $\pi = \pi^a \delta^a$.

We now calculate the different terms in the action in terms of the new variables. The first term becomes,

$$\text{Tr} Q_1 Q_2 = 8 \text{Tr} \pi^2 \quad (6.43)$$

where we have made use of the result $\text{Tr} \pi \Lambda \pi \Lambda = -\text{Tr} \pi^2$. Before rewriting the inter-dimer term, we first take the continuum limit.

$$Q_{I2} Q_{I+1,1} = Q_{I2} Q_{I1} + a Q_{I2} \partial_x Q_{I1} + \frac{a^2}{2} Q_{I2} \partial_x^2 Q_{I1} + \dots \quad (6.44)$$

Using Eqs. (6.40-6.42),

$$\text{Tr} Q_2 \partial_x Q_1 \approx -\text{Tr} Q \partial_x Q + 4i \text{Tr} Q \partial_x Q \tilde{\pi} \quad (6.45)$$

where $\tilde{\pi} \equiv T\pi T^{-1}$. Using the relation $\text{Tr } Q\partial Q = 0$ we get,

$$\text{Tr } Q_2 \partial_x Q_1 \approx 4i \text{Tr } Q \partial_x Q \tilde{\pi} \quad (6.46)$$

$$\text{Tr } \partial_x Q_2 \partial_x Q_1 \approx -\text{Tr } \partial_x Q \partial_x Q \quad (6.47)$$

The kinetic term

Define, $\Omega_\alpha \equiv \text{Tr } (T_\alpha^{-1} \partial_t T_\alpha \Lambda)$. Then,

$$\begin{aligned} \Omega_1 &\approx \text{Tr } (1 - i\pi) T^{-1} (\partial_t T + i\partial_t T \pi + iT \partial_t \pi) \Lambda \\ &= \text{Tr } T^{-1} \partial_t T \Lambda + i \text{Tr } T^{-1} \partial_t T [\pi, \Lambda] \end{aligned} \quad (6.48)$$

In $\Omega_1 + \Omega_2$, only odd powers of π appear.

$$\Omega_1 + \Omega_2 = 2i \text{Tr} [\tilde{\pi}, Q] \partial_t T T^{-1} \quad (6.49)$$

6.2.2 Effective action

Using Eqs (6.43), (6.46), (6.47) and (6.49) in Eq.(6.39), we get,

$$S = \int dx dt \text{Tr} \left(2(1 + \kappa) \pi^2 + i\kappa Q \partial_x Q \tilde{\pi} + \frac{\kappa}{8} \partial_x Q \partial_x Q - i[\tilde{\pi}, Q] \partial_t T T^{-1} \right) \quad (6.50)$$

Define the rotated generators as,

$$\tilde{\lambda}^a \equiv T \lambda^a T^{-1} \quad (6.51)$$

$$\tilde{\delta}^a \equiv T \delta^a T^{-1} \quad (6.52)$$

Then,

$$\tilde{\pi} = \pi^a \tilde{\delta}^a \quad (6.53)$$

The action can then be written as,

$$S = \int dx dt \left(\frac{\kappa}{8} \text{Tr } \partial_x Q \partial_x Q + 2(1 + \kappa) \pi^a \pi^a + \pi^a P^a \right) \quad (6.54)$$

where,

$$P^a \equiv \text{Tr} \left(i\kappa Q \partial_x Q \tilde{\delta}^a - i[\tilde{\delta}^a, Q] \partial_t T T^{-1} \right) \quad (6.55)$$

Now,

$$\text{Tr } Q \partial Q \tilde{\lambda}^a = \text{Tr} (\Lambda T^{-1} \partial T \Lambda \lambda^a + \partial T^{-1} T \lambda^a) = 0 \quad (6.56)$$

since $[\Lambda, \lambda^a] = 0$. Similarly,

$$\text{Tr } \partial Q \tilde{\lambda}^a = 0 \quad (6.57)$$

Therefore,

$$Q \partial Q = \tilde{\delta}^a \text{Tr} (Q \partial Q \tilde{\delta}^a) \quad (6.58)$$

$$\partial Q = \tilde{\delta}^a \text{Tr} (\partial Q \tilde{\delta}^a) \quad (6.59)$$

From Eqs. (6.58) and (6.59),

$$\sum_a P^a P^a = \kappa^2 \text{Tr} \partial_x Q \partial_x Q - \text{Tr} \partial_t Q \partial_t Q + 2\kappa \text{Tr} Q \partial_x Q \partial_t Q \quad (6.60)$$

Finally integrating out $\{\pi^a\}$ and using Eq.(6.60) we get the effective action as,

$$S = \int dx dt \left(\frac{\kappa}{8(1+\kappa)} \text{Tr } \partial_x Q \partial_x Q + \frac{1}{8(1+\kappa)} \text{Tr } \partial_t Q \partial_t Q - \frac{\kappa}{4(1+\kappa)} \text{Tr } Q \partial_x Q \partial_t Q \right) \quad (6.61)$$

This is the action for the Grassmann σ model. We can see that the σ model parameters are independent of N_1 and N_2 .

Chapter 7

Generalised Shastry-Sutherland models

Shastry-Sutherland model (SSM) is defined on a square lattice and has the following hamiltonian,

$$H = J \sum_{\langle i,j \rangle} \mathbf{S}_i \cdot \mathbf{S}_j + J' \sum_{[k,l]} \mathbf{S}_k \cdot \mathbf{S}_l \quad (7.1)$$

where \langle, \rangle indicates nearest neighbours and $[,]$ indicates the dimer bonds as shown in Fig. 7.1.

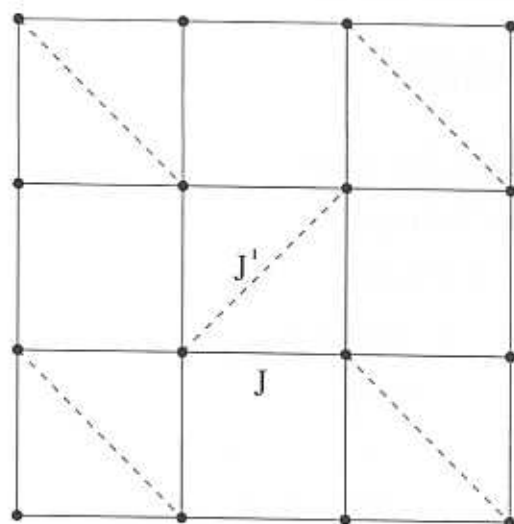


Figure 7.1: Shastry-Sutherland model.

In this chapter we give a generalisation of SSM to an arbitrary number of dimensions, d . The aim is to use the d -dimensional model to do a mean field theory which becomes exact as $d \rightarrow \infty$. Then one can do a systematic $1/d$ expansion about $d = \infty$.

We first give a geometric prescription to construct generalised Majumdar Ghosh models (GMGM). Using this we construct a model in 3 dimensions. The construction then readily generalises to d dimensions. We also discuss the experimental feasibility of the $3 - d$ model. Finally we do a mean field analysis, valid for large d , to study the Néel-Dimer transition.

7.1 Generalised Majumdar-Ghosh models

We define a class of models referred to as generalised Majumdar-Ghosh models (GMGM) as follows. Consider Hamiltonians of the form,

$$H = \sum_n J_n h_n \quad (7.2)$$

Where the sum is over all possible sets of three points formed by the sites of the lattice, J_n 's are arbitrary positive semidefinite couplings and h_n are given by,

$$h_n = \mathbf{S}(\mathbf{r}_i) \cdot \mathbf{S}(\mathbf{r}_j) + \mathbf{S}(\mathbf{r}_j) \cdot \mathbf{S}(\mathbf{r}_k) + \mathbf{S}(\mathbf{r}_k) \cdot \mathbf{S}(\mathbf{r}_i) \quad (7.3)$$

$\mathbf{S}(\mathbf{r}_i)$, $\mathbf{S}(\mathbf{r}_j)$ and $\mathbf{S}(\mathbf{r}_k)$ are the spins at sites \mathbf{r}_i , \mathbf{r}_j and \mathbf{r}_k respectively and n labels the set formed by them. A particular \mathbf{r}_i can be a part of more than one h_n .

It was noted in [22] that if, in the set corresponding to h_n , two of the spins are forming a singlet, then the state will be a ground state of h_n . It was also pointed out that h_n could be more general than given above. It could be spin anisotropic, the three terms could have different coefficients and the spin could be arbitrary. In suitable parameter ranges the dimer state will remain the ground state [22, 43].

A lattice is said to be dimer-covered when all the sites have been grouped into mutually exclusive pairs. Each pair is called a dimer. Suppose that it is possible to dimer-cover the lattice in such a way that the set of three sites corresponding

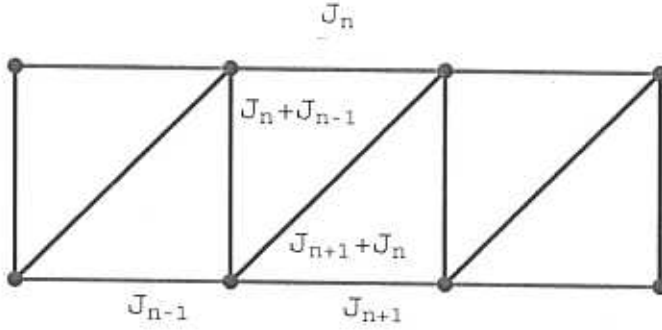


Figure 7.2: A generalised Majumdar-Ghosh Chain

to h_n contains one dimer, $\forall n$ with $J_n \neq 0$. Then the state consisting of singlets on all the dimers will be a simultaneous ground state of all h_n and hence that of H . The problem of constructing GMGMs thus reduces to the purely geometric one of assigning the non-zero couplings to the sets such that a dimer covering of the above type is possible. We will now give a class of solutions to this problem which naturally generalises the SSM to arbitrary dimensions. For simplicity, we will work with h_n as in Eq. (7.3) and with $s = 1/2$.

7.2 The generalised SSM

We will first construct the 3-d model and then generalise to arbitrary dimensions. We first set up the VBC and then build the Hamiltonian around it. We take a simple cubic lattice and choose the dimers to lie along the body diagonals. The body diagonals are assigned as follows. The sites are denoted by, $\mathbf{x} = \sum_{\mu=1}^3 x_{\mu} \hat{\mathbf{e}}_{\mu}$. x_{μ} 's take integer values and $\hat{\mathbf{e}}_{\mu}$ are three orthogonal unit vectors. The spin $\mathbf{S}(\mathbf{x})$ is paired to the spin $\mathbf{S}(\mathbf{y}(\mathbf{x}))$ where,

$$\mathbf{y}(\mathbf{x}) = \mathbf{x} + \mathbf{D}(\mathbf{x}) \quad (7.4)$$

$$\mathbf{D}(\mathbf{x}) = \sum_{\mu=1}^3 (-1)^{x_{\mu}+1} \hat{\mathbf{e}}_{\mu} \quad (7.5)$$

where we define $x_{3+1} \equiv x_1$. Two such body diagonals are shown in Fig. 7.3.

Note that $D(y) = -D(x)$ as it should be, since if $S(x)$ is paired with $S(y)$, then $S(y)$ should be paired with $S(x)$. All the four body diagonal directions occur in equal numbers and the VBC has cubic rotational symmetry. It is not parity invariant, the other parity choice being given by replacing $(-1)^{x_{\mu+1}}$ by $(-1)^{x_{\mu-1}}$ in Eq. (7.5).

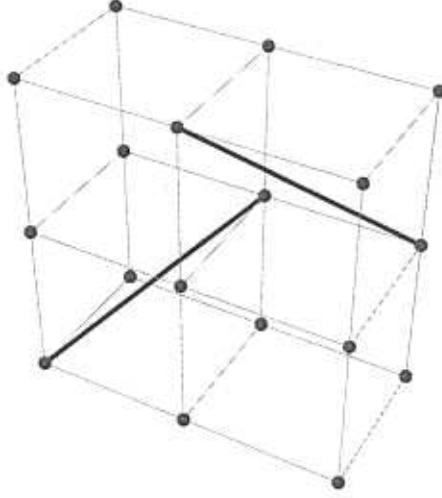


Figure 7.3: The 3-d lattice containing 18 sites, depicting the diagonals along which dimers are formed

We now choose the triangles with nonzero couplings as follows. Eq. (7.5) uniquely associates a body diagonal and hence a unit cube with every dimer, (x, y) . We give non-zero couplings to the six triangles formed by these two sites and each of the other six sites that belong to the cube as illustrated in Fig. 7.4. Thus every such triangle has one edge, one face diagonal and the body diagonal containing the dimer. This construction ensures that every triangle has one dimer (along the body diagonal) and hence is the exact ground state of Hamiltonians of the form given in Eq. (7.2). The Hamiltonian can be explicitly written as,

$$H = \sum_{\mathbf{x}} \sum_{\mu=1}^3 J(\mathbf{x}, \mu) h(\mathbf{x}, \mu) \quad (7.6)$$

where,

$$h(\mathbf{x}, \mu) = S(\mathbf{x}).S(\mathbf{z}(\mathbf{x}, \mu)) + S(\mathbf{z}(\mathbf{x}, \mu)).S(\mathbf{y}) + S(\mathbf{y}).S(\mathbf{x}) \quad (7.7)$$

$$\mathbf{z}(\mathbf{x}, \mu) = \mathbf{x} + (-1)^{x_{\mu+1}} \hat{\mathbf{e}}_{\mu} \quad (7.8)$$

$\mathbf{z}(\mathbf{x}, \mu)$ and \mathbf{x} form the 3 edges emanating from \mathbf{x} in the direction of the body diagonal $\mathbf{D}(\mathbf{x})$ and \mathbf{y} is given by Eq. (7.4). $J(\mathbf{x}, \mu)$ is the coupling associated with the triangle formed by \mathbf{x} , $\mathbf{y}(\mathbf{x})$ and $\mathbf{z}(\mathbf{x}, \mu)$.

Consider the simplest case when all the couplings are equal. i.e. $J(\mathbf{x}, \mu) = J$. The triangle corresponding to $h(\mathbf{x}, \mu)$ contributes a strength J to the edge it contains. Each edge is contained in exactly one triangle. Thus all edges have bond strengths J . Each triangle contributes a strength J to the face diagonal that it contains. Half the face diagonals are contained in exactly one triangle each and the other half are not contained in any triangle. Thus half the face diagonals have bond strength J and the others have no bonds. Fig. 7.4 illustrates the situation. Finally, each triangle contributes J to the body diagonal. Half the body diagonals are contained in six triangles each and hence have bond strengths $6J$ and the other half have no bonds. See Fig. 7.3.

The generalisation to higher dimensions, $d = 4, 5, \dots$ is straightforward. Simply replace 3 by d in all formulas from Eq. (7.4) to Eq. (7.8). All the 2^{d-1} body diagonal directions occur in equal numbers in the d dimensional VBC. The model is a simple hyper-cubic lattice with bonds of strength J along all the edges and along one of the face diagonals of each $(d-1)$ dimensional face. There are also bonds of strength $2dJ$ along one of the body diagonals of half the hyper-cubes. The construction ensures that the VBC is the exact ground state of the model.

It can be seen that the model reduces to SSM at $d = 2$, shown in Fig. 7.1. The diagonals are given by Eq. (7.4). The strength of the bonds along the diagonals is $4J$. $d = 2$ is a special case in that the $(d-1)$ dimensional face diagonals are also the edges. Thus the strength along the edges is $2J$, i.e., the strength of edge bonds are half that of the diagonal ones. Thus we have recovered the 2-d SSM.

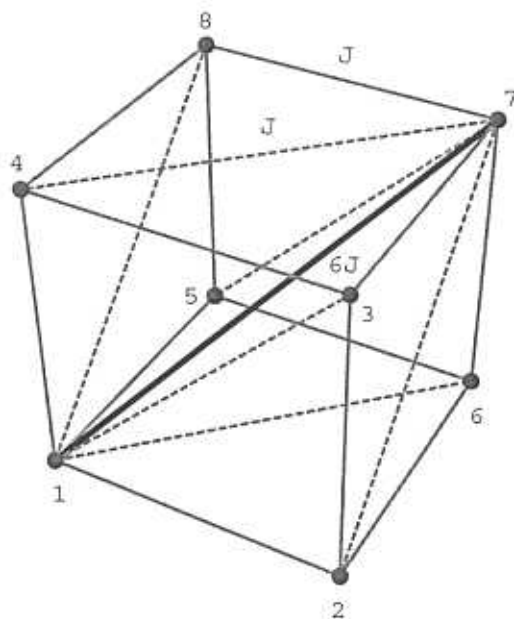


Figure 7.4: A cube containing diagonal bond. All the bonds are shown

7.3 Experimental feasibility of the 3 - d lattice

Now we come back to the $d = 3$ case. As it stands, it is not very physically realistic since the stronger bonds are between spins further apart. The same is true in the case of the 2-d model. However, the structure of magnetic ions in $SrCu_2(BO_3)_2$ can be obtained from the original theoretical lattice by moving the sites along the diagonals that have bonds. The squares containing the diagonals deform to rhombi and the body diagonal containing the dimer becomes shorter than the edges. As we will see, the procedure generalises to 3-d and we can obtain an analogous structure where the stronger bonds have shorter bond lengths.

We move all sites along the body diagonals with non-zero bond strengths. The new sites are then,

$$\mathbf{R}(\mathbf{x}) = \mathbf{x} + \frac{s}{2}\mathbf{D}(\mathbf{x}) \quad (7.9)$$

where s is a parameter and $\mathbf{D}(\mathbf{x})$ is given by Eq. (7.5). The cube shown in Fig. 7.4 deforms to the rhombohedron shown in Fig. 7.5. Before the deformation the sites formed a simple cubic lattice. The Hamiltonian was however only symmetric under

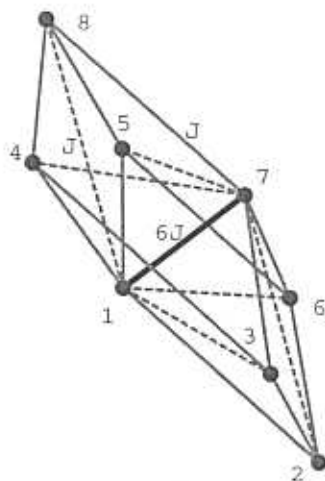


Figure 7.5: A deformed cube. Now the strongest bond is between nearest neighbour sites

translations by two units. After deformation, the lattice periodicity is also halved. It remains a cubic lattice but with 8 sites in a unit cell.

The lengths of the edges, face diagonals and body diagonals can be computed and are plotted as functions of s in Fig. 7.6. As we can see, for s more than around .7 or so, the edges and face diagonal with bonds become almost equal in length, are longer than the body diagonal with the bond and shorter than the other face diagonals and body diagonals. When $s=1$ the body diagonal becomes of zero length. The rhombohedron is then squashed into a hexagon lying in the plane orthogonal to the body diagonal.

We will now examine the models away from the exact ground state point at $d \rightarrow \infty$. We put the bond strengths along the body diagonals equal to $dJ_D/2$, along edges equal to $J_E/2$ and along the face diagonals to $J_F/2$. Actually, the VBC is an exact eigenstate when $J_E = J_F \equiv J'$ for all J_D [44]. It is proven to be the ground state when $J' \leq 0.5J_D$. However, the ground state is Néel ordered for $J_F = 0 = J_D$. So there will be a phase transition somewhere. The location and nature of the

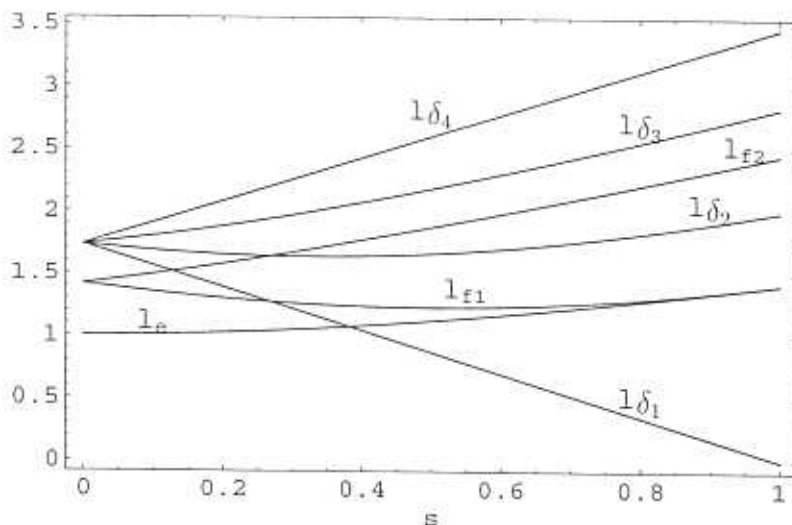


Figure 7.6: The various bond lengths as functions of s . l_e is the length of the edges, l_{f1} that of the face diagonals containing bond and l_{f2} corresponds to face diagonals without bond. l_{d1} is the length of the diagonals along which dimers are formed and l_{d2} , l_{d3} and l_{d4} correspond to body diagonals without bonds.

transition at $d = 2$ have been topics of much activity [28, 25, 24, 26, 23, 36].

7.4 Mean field theory for dimer-Nèel transition

Since the VBC is the exact ground state in some parameter range for all d , it is clear that mean field theory in terms of the spin variables fails even as $d \rightarrow \infty$. This is because one of the bond strengths grows as d and so the interactions cannot be approximated by an average field. However, if we take the dimers, i.e the two-spin systems on the body diagonals to be the basic units, then each dimer interacts with $\sim d$ of the dimers around it with bonds of strength ~ 1 . Thus the mean field theory in terms of the dimer variables is exact at $d \rightarrow \infty$ in this class of models. Perturbation theory around the mean field Hamiltonian then yields a systematic $1/d$ expansion for the fluctuations. We will now use this mean field theory to explore the physics at large d .

We label the spins as $\mathbf{S}_{I\alpha}$, where I labels the positions of the centers of the

dimers and $\alpha = 1, 2$ label the two spins that form the dimer. The Hamiltonian can be written as,

$$H = \sum_I \frac{dJ_D}{4} (S_{I1} + S_{I2})^2 + \frac{1}{2} \sum_{I\alpha, J\beta} J_{I\alpha, J\beta} S_{I\alpha} \cdot S_{J\beta} \quad (7.10)$$

Where $J_{I\alpha, J\beta}$ denote the edge and face diagonal bonds. The mean field Hamiltonian is,

$$H_{MF} = \sum_I \frac{dJ_D}{4} (S_{I1} + S_{I2})^2 + \sum_{I\alpha, J\beta} J_{I\alpha, J\beta} \mathbf{b}_{I\alpha} \cdot \mathbf{S}_{J\beta} - \frac{1}{2} \sum_{I\alpha, J\beta} J_{I\alpha, J\beta} \mathbf{b}_{I\alpha} \cdot \mathbf{b}_{J\beta} \quad (7.11)$$

The self consistency Eqs. are then,

$$\mathbf{b}_{I\alpha} = \langle \mathbf{S}_{I\alpha} \rangle \quad (7.12)$$

In different parameter regimes, the VBC as well as a variety of other phases are possible. The $1/d$ expansion, which is valid in all the phases can be used to analyse the phase diagram. Here we study the Néel-VBC transition at large d . There is a qualitative difference between odd and even dimensions and we treat them separately.

In even dimensions, the dimer lattice is bipartite and both the sites of a dimer have the same parity. The parity of a dimer is defined to be same as that of its sites. The Néel-state is described by the ansatz, $\mathbf{b}_{I\alpha} = P_I b \hat{z}$, where P_I is +1 on one sub-lattice and -1 on the other. Then the mean field Hamiltonian is,

$$H_{MF}^{even} = \sum_I \left(\frac{dJ_D}{4} (S_{I1} + S_{I2})^2 + P_I 2dJ' b (S_{I1}^z + S_{I2}^z) + 2db^2 J' \right) \quad (7.13)$$

Where $J' \equiv (J_E + J_F)/2$. For all values of $\alpha \equiv J'/J_D$, all the dimers forming singlets, *i.e.*, VBC, is a mean-field solution with $b = 0$. The state has energy 0. When $\alpha > 1/2$, the Néel state is a solution with $b = 1/2$ and has energy,

$$E^{Neel} = \frac{NdJ_D}{4} (1 - \alpha) \quad (7.14)$$

where N is the number of sites. However, this solution has lower energy than the VBC only when $\alpha > 1$. Thus we get a first order transition at $\alpha = 1$ at $d = \infty$.

Now we compute the leading order correction to the ground state energy in the Néel phase by treating $(H - H_{MF})$ as a perturbation. We get,

$$E = \frac{NJ_D}{4} \left(d(1 - \alpha) - \frac{\alpha}{4} \left(\frac{2\alpha}{4\alpha - 1} + \frac{1}{2} \right) \right) \quad (7.15)$$

At $d = 2$, the transition now occurs at $\alpha \approx 0.8$. More sophisticated calculations at $d = 2$ [26, 28] put this number at 0.69. There are indications that the transition may be second order [36] or that there may be an intermediate phase [25, 24, 26, 23].

In odd dimensions the two sites of a dimer are not of the same parity. By convention, we assign $\alpha = 1$ for the odd site and $\alpha = 2$ for the even site. Then the Néel ansatz is $\mathbf{b}_{I\alpha} = (-1)^\alpha b \hat{z}$. The mean field Hamiltonian is then given by,

$$H_{MF}^{odd} = \sum_I \left(\frac{dJ_D}{4} (\mathbf{S}_{I1} + \mathbf{S}_{I2})^2 + 2db\Delta J (S_{I1}^z - S_{I2}^z) + 2db^2\Delta J \right) \quad (7.16)$$

Where $\Delta J \equiv (J_E - J_F)/2$. In the ground state the dimer wave function is given by,

$$|\Psi\rangle = \cos(\theta/2) |0, 0\rangle + \sin(\theta/2) |1, 0\rangle \quad (7.17)$$

Where in $|l, m\rangle$, l is the total spin and m the z component and

$$\sin \theta = 2\Delta J |\mathbf{b}| / (\sqrt{J_D^2 + (8\Delta J |\mathbf{b}|)^2}) \quad (7.18)$$

The self consistency equation (7.12) reduces to,

$$\frac{4\Delta J}{\sqrt{J_D^2 + (8\Delta J |\mathbf{b}|)^2}} = 1 \quad (7.19)$$

Thus the transition occurs at $J_D = 4\Delta J$. The sub-lattice magnetisation, $|\mathbf{b}|$ goes continuously to zero at the transition as $\sim (1 - (J_D/4\Delta J))^{1/2}$. The interesting thing is that unlike in even dimensions, the transition point depends on the difference of J_E and J_F . So the VBC can occur at relatively low values of J_D .

The different physics in the even and odd dimensions arises from the fact that the two spins on a dimer belong to the same sub-lattice in former and on opposite ones in the latter. Consequently, the dimer wave-function in the VBC and in the Néel state have the same value of $S^z (= 0)$ in odd dimensions whereas in even dimension $S^z = 0$ in the VBC but $S^z = \pm 1$ (on odd and even sub-lattices) in the Néel state.

Since the S^z symmetry is unbroken in both the phases, the mean field Hamiltonian always conserves it. Thus in even dimensions the VBC state cannot smoothly transit to the Néel state and we get a first order transition whereas in odd dimensions it can and we get a second order transition.

A remark about the scaling of the diagonal bond is in order here. For the dimer mean-field theory to be valid in both the phases, the diagonal bond has to scale as d , so that d scales out of H_{MF} of Eqs. (7.13, 7.16). But numerically, the critical value of the diagonal bond could be small. For example, in odd dimensions the critical value of diagonal bond is proportional to $\Delta J \equiv (\frac{J_E - J_F}{2})$ and can be made arbitrarily small by suitable choice of J_E and J_F .

Chapter 8

Exact magnetisation plateaus for spin- s models

In this chapter we study the response of certain frustrated systems to an external magnetic field. We first do the mean-field analysis of the generalised SSM in d dimensions. After that we generalise the results of some exactly solvable spin- $\frac{1}{2}$ models to the case of higher spins, $s > \frac{1}{2}$. We then argue that, in the case of higher spins, there are two different mechanisms by which the system gets magnetized.

8.1 Magnetisation plateaus of generalized SSM

The mean field equations can be solved in the presence of an external magnetic field

B. The mean-field Hamiltonian in the presence of $\mathbf{B} = B\hat{\mathbf{z}}$ is given by,

$$\begin{aligned} H_{MF} = & \sum_I \frac{dJ_D}{4} (\mathbf{S}_{I1} + \mathbf{S}_{I2})^2 + \sum_{I\alpha, J\beta} J_{I\alpha, J\beta} \mathbf{b}_{I\alpha} \cdot \mathbf{S}_{J\beta} \\ & - B \sum_{I\alpha} S_{I\alpha}^z - \frac{1}{2} \sum_{I\alpha, J\beta} J_{I\alpha, J\beta} \mathbf{b}_{I\alpha} \cdot \mathbf{b}_{J\beta} \end{aligned} \quad (8.1)$$

We concentrate on the regime where the VBC is the ground state, in the absence of \mathbf{B} . A state in which one of the dimers is excited to a triplet with $S^z = 1$ and the rest are all in singlets is a self-consistent solution of the mean-field Hamiltonian of Eq. (8.1), with $\mathbf{b}_{I\alpha} = 0$ for those dimers in singlets and $\mathbf{b}_{I\alpha} = \frac{1}{2}\hat{\mathbf{z}}$ for the one in

triplet. The energy of this state is $dJ_D/2 - B$. Thus as we increase the strength of the magnetic field, when $B > dJ_D/2$, it is energetically favourable to excite as many dimers as possible into triplets pointing along \mathbf{B} , but no two of them being connected by a bond.

In even dimensions, using the fact that the lattice formed by the dimers is bipartite, we shall now show that the maximum fraction of dimers that can be excited without any two of them being connected by a bond is $1/2$.

Let us start with isolated dimers with no bonds connecting them. Now we add edge bonds such that every dimer is connected to one and only one other dimer. This can be done as follows. As mentioned before, both the sites of a dimer have the same parity. Each coordinate of the two sites will be differing by $+1$ or -1 . Choose an even dimer and pick out the site with odd x_1 -coordinate. Put the edge bond from this site in the positive x_1 -direction. This way every even dimer can be uniquely connected to one and only one odd dimer. Suppose these were the only bonds present. Then the configuration that maximizes the number of triplets without two of them being connected is where in every pair of connected dimers one is put in a singlet and the other in a triplet. Now the original model can be obtained by adding the remaining bonds. But in the presence of additional bonds also, each of the pairs that were initially connected can at the most have one triplet. Thus the maximum fraction of dimers that can be excited without any two of them being connected by a bond is $1/2$. This upper bound can be satisfied by putting triplets on one of the sub-lattices and singlets on the other. This state is a mean-field solution with $\mathbf{b}_{I\alpha} = 0$ for those dimers in singlets and $\mathbf{b}_{I\alpha} = \frac{1}{2}\hat{z}$ for those in triplets.

The state with the remaining singlets also being excited into triplets is also a mean-field solution and has energy $\frac{N}{2}(dJ_D/2 + dJ' - B)$ above the half-magnetized state. Thus when $B > dJ_D/2 + dJ'$ all the remaining dimers are excited into triplets and the system becomes fully magnetized.

When d is odd, the dimer lattice is not bipartite. We still assign parity to dimers as follows. In every dimer one site will be odd and the other even. The parity of the dimer is defined as the parity of the x_1 -coordinate of the even site. It can be

seen that out of the $4d$ dimers that are connected to a particular dimer only 4 are of the same parity. Since the critical B , at which it is energetically favourable to have isolated singlets, scales as d , this difference between odd and even dimensions is insignificant at large d .

For both the cases, there is a plateau at $1/2$ magnetisation for $dJ_D/2 < B < dJ_D/2 + dJ'$. At stronger fields, the system is fully magnetized. The $1/2$ plateau corresponds to all the dimers on even sites in the triplet and the ones on the odd sites in the singlet state. At $d = \infty$, the dimers have only nearest neighbour interactions. Previous work [28, 45, 34, 35, 36] indicates that the other fractions are due to longer range interactions induced by fluctuations. Thus it is reasonable that only the $1/2$ plateau occurs at $d = \infty$.

8.2 Gelfand ladder

In this section we analyse in detail, the prototype model which can be solved exactly in the presence of a magnetic field - the Gelfand ladder. This then readily generalises to the other models since the basic mechanism is the same.

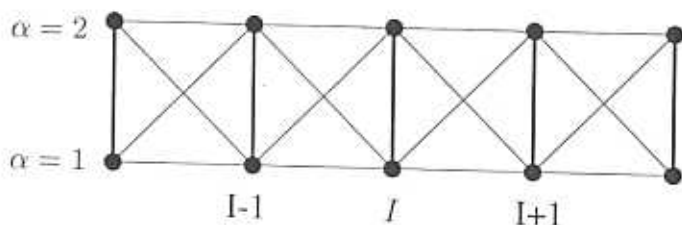


Figure 8.1: Gelfand ladder.

The hamiltonian for the system is (See Fig. 8.1),

$$H = \sum_I \left[\frac{1}{2} (\mathbf{S}_{I1} + \mathbf{S}_{I2})^2 + \kappa (\mathbf{S}_{I1} + \mathbf{S}_{I2}) \cdot (\mathbf{S}_{I+1,1} + \mathbf{S}_{I+1,2}) - B(S_{I1}^z + S_{I2}^z) \right] \quad (8.2)$$

where, $\mathbf{S}_{I\alpha}^2 = s(s+1)$. Define the total spin on a dimer as,

$$\mathbf{S}_{I+1,1} + \mathbf{S}_{I+1,2} \equiv \mathbf{J}_I, \quad (8.3)$$

Using Eq. (8.3) and after doing a shuffling of terms, the hamiltonian takes the form,

$$H = \sum_I \left[\left(\frac{1}{2} - \kappa \right) \mathbf{J}_I^2 + \frac{\kappa}{2} (\mathbf{J}_I + \mathbf{J}_{I+1})^2 - B J_I^z \right]. \quad (8.4)$$

Clearly the total spin on each dimer, \mathbf{J}_I^2 , is conserved. *i.e.*,

$$[\mathbf{J}_I^2, H] = 0.$$

Thus the energy eigen states can be labelled by the eigen values of \mathbf{J}_I^2 .

8.2.1 Ground state at $B = 0$

Let us first consider the case of zero magnetic field. Then it is easily seen that for $\kappa < \frac{1}{2}$, in the ground state each dimer is a singlet (this state from here on will be referred to as the 'dimer-singlet'). In this case, both the terms in the hamiltonian are positive definite and the dimer-singlet is the only state for which both have eigen value 0. Note that this is true for any value of s .

For $s = \frac{1}{2}$, the dimers can either be in a singlet or a triplet. The first term of H in Eq. (8.2) costs energy for the dimer to go into a triplet, but it can gain in interaction energy through the second term by Nèel ordering. So at large enough κ the system can form clusters of triplets. A dimer in such clusters will act like a single spin-1 and thus a cluster will be like a uniform string of spin-1. The ground state energy per spin for a finite uniform spin-1 chain decreases with the size of the chain and converges towards the value for the infinite chain [46]. Thus if any dimer goes into a triplet, then every dimer will follow suit. Comparing the dimer-singlet energy and the energy of the triplet state (numerically calculated for the uniform spin-1 chain) Gelfand estimated the transition to take place at $\kappa^* = 0.714$.

It is reasonable to expect a similar scenario for higher spin cases. For the spin s case, ground state will be the singlet for $\kappa < \kappa^*$ and for $\kappa > \kappa^*$ the dimers go into spin $2s$ multiplet and form the corresponding uniform chain ground state.

8.2.2 Magnetisation plateaus

Now we look at the system in the presence of magnetic field. It is convenient to write the hamiltonian as follows,

$$H = \sum_I h_I, \quad (8.5)$$

$$h_I = \frac{1}{2} \left(\frac{1}{2} - \kappa \right) (\mathbf{J}_I^2 + \mathbf{J}_{I+1}^2) + \frac{\kappa}{2} (\mathbf{J}_I + \mathbf{J}_{I+1})^2 - \frac{B}{2} (J_I^z + J_{I+1}^z). \quad (8.6)$$

Ground state for $\kappa < \frac{1}{2}$

When $\kappa \leq \frac{1}{2}$, the ground state can be solved exactly. In this case it is enough to solve the two dimer problem. Since the ground state for the two dimer problem turns out to be a product of dimer states, we can simply string the states together to obtain the ground state of the full hamiltonian.

We first solve the two dimer hamiltonian,

$$h = \frac{1}{2} \left(\frac{1}{2} - \kappa \right) (\mathbf{J}_1^2 + \mathbf{J}_2^2) + \frac{\kappa}{2} (\mathbf{J}_1 + \mathbf{J}_2)^2 - \frac{B}{2} (J_1^z + J_2^z). \quad (8.7)$$

Let $j(j+1)$, m , $j_1(j_1+1)$ and $j_2(j_2+1)$ denote the eigen values of $(\mathbf{J}_1 + \mathbf{J}_2)^2$, $(J_1^z + J_2^z)$, \mathbf{J}_1^2 and \mathbf{J}_2^2 respectively. Note that all these four operators mutually commute and can therefore be diagonalised simultaneously. The eigen values of h will then be,

$$E = \frac{1}{2} \left(\frac{1}{2} - \kappa \right) (j_1(j_1+1) + j_2(j_2+1)) + \frac{\kappa}{2} j(j+1) - \frac{B}{2} m. \quad (8.8)$$

For a given j , the minimum energy state will be such that

$$j_1 + j_2 = j. \quad (8.9)$$

Further, the first term in E , which is $\propto [j_1(j_1+1) + j_2(j_2+1)]$, is minimized by the following choice,

$$j_1 = \frac{j}{2} \quad ; \quad j_2 = \frac{j}{2}, \quad \text{if } j \text{ is even,} \quad (8.10)$$

$$j_1 = \frac{j}{2} - \frac{1}{2} \quad ; \quad j_2 = \frac{j}{2} + \frac{1}{2}, \quad \text{if } j \text{ is odd} \quad (8.11)$$

The last term in E is minimized by the choice,

$$m = j. \quad (8.12)$$

In the basis labelled by the eigen values of \mathbf{J}_1^2 , J_1^z , \mathbf{J}_2^2 and J_2^z , $\{ |j_1, m_1\rangle \otimes |j_2, m_2\rangle \}$, the minimum energy state is then,

$$|j_1, j_1\rangle \otimes |j_2, j_2\rangle, \quad (8.13)$$

where j_1 and j_2 are given by Eqs. (8.10) and (8.11). Substituting Eqs. (8.9 - 8.12) in Eq. (8.8), we get the minimum energy for a given j .

$$E_0^{\text{even}} = \frac{(1-2\kappa)}{8} j(j+2) + \frac{\kappa}{2} j(j+1) - \frac{B}{2} j, \text{ for even } j, \quad (8.14)$$

$$E_0^{\text{odd}} = \frac{(1-2\kappa)}{8} (j+1)^2 + \frac{\kappa}{2} j(j+1) - \frac{B}{2} j, \text{ for odd } j. \quad (8.15)$$

j will now be determined by B . It is straightforward to calculate the critical fields at which j changes. The value of the field at which j goes to $j+1$ for even and odd j are respectively given by B_{cr}^{even} and B_{cr}^{odd} .

$$B_{cr}^{\text{even}} = \frac{(1+2\kappa)j}{2} + 1 \quad (8.16)$$

$$B_{cr}^{\text{odd}} = \frac{(1+2\kappa)(j+1)}{2} \quad (8.17)$$

Exactly at B_{cr} , the states having \mathbf{J}^2 eigen value j and $j+1$ are degenerate.

Now we have completely solved the two dimer problem for all values of the magnetic field. The ground state of the full hamiltonian trivially follows from the above solution. It is,

$$... \otimes |j_1, j_1\rangle \otimes |j_2, j_2\rangle \otimes |j_1, j_1\rangle \otimes |j_2, j_2\rangle \otimes ... \quad (8.18)$$

where j_1 and j_2 , depending on B , are determined by Eqs. (8.10), (8.11), (8.16) and (8.17). This state is simultaneously the ground state of h_I , $\forall I$ and hence is the ground state of H .

Exactly at the critical field, the condition for the ground state is that every pair of neighbouring dimers should have total spin j or $j+1$ with corresponding values for j_I . Let j be an even number, say, $2n$. Then for $B < B_{cr}$, all the dimers have $j_I = n$. At $B = B_{cr}$, any state for which $j_I = n$ or $n+1 \forall I$, but with no two neighbouring dimers having $j_I = n+1$, will be a ground state. Thus right at B_{cr} , the ground state has a macroscopic degeneracy.

Let us summarise the results for $\kappa < \frac{1}{2}$. The ground state is the dimer-singlet at $B = 0$. As B is increased, the magnetisation per site goes up in $4s$ equal and discrete steps till it is fully saturated. *i.e.*, there will be plateaus of magnetisation at the fractions,

$$\frac{1}{4s}, \frac{2}{4s}, \dots, 1. \quad (8.19)$$

The dimer lattice can be divided into two sub-lattices. Let A and B denote the sublattices consisting of even and odd dimers respectively. We represent the relevant states as (j_1, j_2) , where j_1 is the magnetisation of A -dimers and j_2 that of B -dimers. Then the sequence in which transition takes place can be represented as,

$$(0, 0) \rightarrow (1, 0) \rightarrow (1, 1) \rightarrow \dots \rightarrow (2s, 2s - 1) \rightarrow (2s, 2s)$$

The critical values of B at which the jumps occur are given by Eqs. (8.16) and (8.17). At successive critical values of the field, the dimers of the two sub-lattices alternately get excited to a spin one unit higher. Exactly at the critical fields, the ground state has a macroscopic degeneracy.

Ground state for $\kappa = \frac{1}{2}$

At $\kappa = \frac{1}{2}$ the two dimer hamiltonian becomes,

$$h = \frac{1}{4} (\mathbf{J}_1 + \mathbf{J}_2)^2 - \frac{B}{2} (J_1^z + J_2^z). \quad (8.20)$$

The minimum energy for a given j is,

$$E = \frac{1}{4} j(j+1) - \frac{B}{2} j. \quad (8.21)$$

As before, B will determine the value of j . Now the eigen value does not depend on j_1 or j_2 . There are numerous ways in which j_1 and j_2 can be chosen to obtain j as the total spin. More precisely, j_1 and j_2 should be such that,

$$|j_1 - j_2| \leq j \leq j_1 + j_2.$$

As the ground state of H , we want to construct a state such that the total spin of any two neighbouring dimers is j . One obvious way of doing this is to choose

$j_1 + j_2 = j$ such that the state is a product of dimer states as before. This can be done in $j + 1$ ways,

$$(j_1, j_2) = (j, 0), (j - 1, 1), \dots, (1, j - 1), (0, j).$$

Thus for a given j , all the states,

$$\dots \otimes |j_1, j_1\rangle \otimes |j_2, j_2\rangle \otimes |j_1, j_1\rangle \otimes |j_2, j_2\rangle \otimes \dots ; \quad j_1 + j_2 = j \quad (8.22)$$

are of minimum energy. The above set of states exhausts all the minimum energy states which are products of dimer states. But there could be other states which have the same energy.

As before, there are further macroscopic degeneracies at B_{cr} owing to local 1-dimer excitations becoming gapless.

Ground state for $\kappa > \frac{1}{2}$

For $\kappa > \frac{1}{2}$, the ground state can no longer be solved using the above method. The ground state of h is then not a product of dimer states and so we cannot construct a state which will simultaneously be the ground state of h_I , $\forall I$.

For the time being, let us assume that at $\kappa = \frac{1}{2}$, those states given in (8.22) are the only ground states and proceed. This assumption, in other words, says that any other state has a finite gap at $\kappa = \frac{1}{2}$.

The hamiltonian (8.4) has the form,

$$H = H_0 + \kappa H_1 - B H_2. \quad (8.23)$$

H_0 , H_1 and H_2 mutually commute and thus the eigen states do not depend on κ or B while the eigen values will be linear functions of κ and B . This fact in conjunction with the above assumption implies that there is a finite neighbourhood around $\kappa = \frac{1}{2}$ where the ground state will be among those at $\kappa = \frac{1}{2}$.

For $\kappa > \frac{1}{2}$ the first term of h in Eq. (8.7) has negative coefficient and thus $[j_1(j_1 + 1) + j_2(j_2 + 1)]$ needs to be maximised. From among the ground states at $\kappa = \frac{1}{2}$, this is satisfied by the choice,

$$j_1 = j, j_2 = 0, \text{ if } j \leq 2s,$$

and,

$$j_1 = 2s, j_2 = j - 2s, \text{ if } j > 2s.$$

The states are,

$$.... \otimes |j, j\rangle \otimes |0, 0\rangle \otimes |j, j\rangle \otimes |0, 0\rangle \otimes; \text{ for } j \leq 2s,$$

and

$$.... \otimes |2s, 2s\rangle \otimes |(j-2s), (j-2s)\rangle \otimes |2s, 2s\rangle \otimes |(j-2s), (j-2s)\rangle \otimes; \text{ for } j > 2s.$$

Thus for $\kappa > \frac{1}{2}$, the magnetisation would still go up by the same set of fractions as in (8.19), but the states and the critical values of the field are now different. In the present case, as B is increased from zero, at successive critical values, the spin of the dimers belonging to one sub-lattice jumps by one unit, while those in the other sub-lattice remain zero. Only when the first sub-lattice has been saturated does the other one start getting magnetized. The sequence of transitions will be,

$$(0, 0) \rightarrow (1, 0) \rightarrow (2, 0) \rightarrow \dots \rightarrow (2s, 0) \rightarrow (2s, 1) \rightarrow \dots \rightarrow (2s, 2s)$$

The critical values of the field at which the total spin of 2 neighbouring dimers goes from j to $j + 1$ is calculated to be,

$$B_{cr} = j + 1, \text{ for } j \leq 2s \quad (8.24)$$

$$B_{cr} = (4\kappa - 1)j + 2s - 4\kappa s + 1, \text{ for } j > 2s. \quad (8.25)$$

The above results crucially rely on the assumption of gap at $\kappa = \frac{1}{2}$. Honecker *et al.* have numerically studied the system for $s = \frac{1}{2}$ [37]. Their results indicate that this assumption is correct except at the critical field at which the system gets fully magnetised, where it becomes gapless. This gapless state corresponds to that for the uniform spin-1 chain above its critical field [47]. Uniform spin-1 chain at zero field has a singlet ground state with a gap to the lowest energy triplet excitations. At a critical field this gap equals the Zeeman gap and the triplets become gapless state.

For $s = \frac{1}{2}$ the magnetisation shows only one plateau - at the fraction $\frac{1}{2}$. For $\kappa > \frac{1}{2}$, the range of B for which the system is gapless widens and we no longer have an abrupt jump from half to full magnetisation. In the range of B for which the system is gapless, magnetisation has an initial jump from $\frac{1}{2}$ to an intermediate value from which it increases smoothly to the saturation value.

The above authors have also studied a three leg ladder for $s = \frac{1}{2}$. In their model the total spin on each rung is conserved. The hamiltonian has the same form as in Eq. (8.5) with,

$$\mathbf{J}_I = \mathbf{S}_{I1} + \mathbf{S}_{I2} + \mathbf{S}_{I3}.$$

For $\kappa < \frac{1}{2}$, there are plateaus corresponding to the fractions $\frac{1}{3}$ and $\frac{2}{3}$. The sequence of transition is then, $(\frac{1}{2}, 0) \rightarrow (\frac{1}{2}, \frac{1}{2}) \rightarrow (\frac{3}{2}, \frac{1}{2}) \rightarrow (\frac{3}{2}, \frac{3}{2})$, where j_1 and j_2 are the magnetisations of the rungs belonging to A and B sub-lattices respectively. In this case too their analysis showed that, at $\kappa = \frac{1}{2}$, the system becomes gapless at the critical values of the field. At the transition point from (j_1, j_2) to $(j_1 + 1, j_2)$, the gapless state is that of the uniform chain consisting of spin- (j_1+1) in one lattice and spin- j_2 in the other.

One can expect a similar scenario for higher spins. *i.e.*, at $\kappa = \frac{1}{2}$, the gapless states set in at the critical values of the field. For $\kappa > \frac{1}{2}$, but not very large, the plateaus may still survive but now there could be gapless phases in between. A more rigorous analysis is required to get the accurate phase diagram for the full range of $\kappa \geq \frac{1}{2}$.

We have argued that there are two different mechanisms for plateau formation depending on the value of κ . This opens up the possibility of a first order transition between two states of same magnetisation, but different ordering pattern.

8.3 Higher dimensional models

The most important feature of the one dimensional model that leads to the formation of magnetisation plateaus is the conservation of total spin of individual dimers. This in turn means that there are spin excitations localised to a dimer. When the field is

high enough to make the ground state unstable to such excitations, a whole lot of them will go up resulting in a macroscopic jump in magnetisation. This mechanism is independent of the number of dimensions and one can expect a similar behaviour for models in higher dimensions which have the property of conserved dimer spins.

Müller-Hartmann *et al.* [36] introduced a generalised Shastry-Sutherland model in two dimensions by introducing extra couplings. At specific values of the couplings the total spin on each dimer is conserved. Sutherland [38] constructed a 3-dimensional version of the Gelfand ladder consisting of edge sharing tetrahedra. Both the above mentioned authors discuss only the $s = \frac{1}{2}$ case. We now generalise the results of the previous section to these models at higher spins. To this end, it is instructive to define a general model consisting of coupled dimers in arbitrary dimension.

8.3.1 A general dimerised model

The system consists of coupled dimers¹ in an arbitrary number of dimensions. The dimers live on some lattice whose sites are labelled by I . The sites within a dimer are labelled by α which takes values 1 or 2. The hamiltonian is,

$$H = \sum_I \frac{1}{2} (\mathbf{S}_{I1} + \mathbf{S}_{I2})^2 + \kappa \sum_{\langle I, J \rangle} (\mathbf{S}_{I1} + \mathbf{S}_{I2}) \cdot (\mathbf{S}_{J1} + \mathbf{S}_{J2}) - B \sum_I (S_{I1}^z + S_{I2}^z), \quad (8.26)$$

where \langle, \rangle indicates nearest neighbours. As before, we define,

$$\mathbf{S}_{I1} + \mathbf{S}_{I2} \equiv \mathbf{J}_I.$$

We can write,

$$\mathbf{J}_I \cdot \mathbf{J}_J = \frac{1}{2} (\mathbf{J}_I + \mathbf{J}_J)^2 - \frac{1}{2} (\mathbf{J}_I^2 + \mathbf{J}_J^2).$$

Then H takes the form,

$$H = \sum_I \frac{1}{2} \mathbf{J}_I^2 + \kappa \sum_{\langle I, J \rangle} \mathbf{J}_I \cdot \mathbf{J}_J - B \sum_I J_I^z, \quad (8.27)$$

¹The model can be defined for any number of sites in one unit, instead of two for the dimer.

Now we write the hamiltonian as a sum over bonds.

$$H = \sum_{[I,J]} h_{IJ} ,$$

where $[,]$ represents a bond between two dimers and,

$$h_{IJ} = \frac{1}{2} \left(\frac{1}{z} - \kappa \right) (\mathbf{J}_I^2 + \mathbf{J}_J^2) + \frac{\kappa}{2} (\mathbf{J}_I + \mathbf{J}_J)^2 - \frac{B}{z} (J_I^z + J_J^z) . \quad (8.28)$$

Here z is the coordination number of the dimer lattice. For the Gelfand ladder $z = 2$. The 2-dimensional model of Müller-Hartmann *et al.* and the 3-dimensional one of Sutherland both have $z = 4$.

Now all the steps for the 1-dimensional case can be exactly repeated. When $\kappa < \frac{1}{z}$, we can construct the ground state from that of the two dimer hamiltonian, provided the dimer lattice is bipartite. As before, magnetisation plateaus occur at the fractions $\frac{n}{4s}$; $n = 1, 2, \dots, 4s$ with dimers of both the sub-lattices going to higher spins in tandem. Extrapolating the $1-d$ result, we can expect gapless states to come into the picture for $\kappa \geq \frac{1}{z}$. The plateaus will still survive, but with gapless states coming in between. The sequence in which the magnetisation of the two sub-lattices goes up will now be different. Dimers of one sub-lattice will get saturated first, only after which, the dimers of the other sub-lattice start getting magnetised.

The results we have derived are independent of the number of dimensions. The only condition is that the dimer lattice be bipartite. So we can construct a large number of models which have the above properties. What is special about the models of Gelfand and Sutherland is that they can be realised such that bonds of equal lengths have the same strength, a physically realistic situation.

Chapter 9

Conclusions

In this thesis we have studied the antiferromagnetic Heisenberg model on various lattices and in different dimensions. In this concluding chapter we summarise and discuss our results.

In the first part we have studied spin chains and their connections with the nonlinear σ model with a topological term. We have analysed the correspondence using $s = \frac{1}{2}$ dimerised spin chain as a prototype. Our aim has been to demonstrate in the case of the $O(3)$ model, the ‘super universal’ features expected of all Grassmann σ models: asymptotic freedom, θ renormalisation and gaplessness at $\theta = \pi$,

- We have done the Haldane mapping for a semi-infinite spin chain. The mapping shows that the correspondence between NLSM and the spin chain is ‘exact’ in the strong coupling limit at quantized values of θ .
- We have analysed the $s = \frac{1}{2}$ spin chain using a real space renormalisation group. The RG confirms that g flows to ∞ and θ renormalises to $2\pi n$.

Our RG analysis could not access the $\theta = \pi$ critical fixed point. For this we need to go to higher orders in perturbation. The next step would then be to do the above and thus obtain a complete picture of the NLSM-spin chain correspondence. Apart from this, our method is a new way to do RG for quantum systems and it will be interesting to apply it to other systems.

- We have obtained effective spin- $\frac{1}{2}$ models for higher spin chains. This enables us to access strong coupling NLSM near $\theta = 2\pi n$, $\forall n$. As a bonus, the effective model also gives a good estimate of the gapless point for the spin-1 chain.
- As the last step, we have derived Grassmann σ models as the long wave-length effective theories for $SU(N)$ spin chains.

This sets us up with lattice models which can be used to access all Grassmann models at strong coupling. The extension of this will be to do RG for dimerised $SU(N)$ spin chains.

In the second part of the thesis we have studied some Majumdar-Ghosh like models for which ground state can be solved exactly.

- We have given a geometric prescription to construct generalised Majumdar-Ghosh models. This can be used to construct a variety of models in *any dimension* with a VBC ground state. In particular, we have applied the prescription to construct a generalised Shastry-Sutherland model in arbitrary dimension. This provides us with an additional calculational tool to probe the two dimensional model which has been experimentally realised in $SrCu_2(BO_3)_2$. We have done a $1/d$ correction to estimate the Nèel-dimer transition.

The model, in the only other physical dimension *i.e.* $d = 3$, has been shown to be experimentally feasible. Thus we have constructed a spin-gapped three dimensional model with an exact ground state which has a realistic lattice structure. The mean field analysis shows that, the Nèel-dimer transition is second order in odd dimensions and first order in even dimensions.

Shastry-Sutherland model in two dimensions is known to have a disordered plaquette phase in between the dimer and the Nèel phases. It will be interesting to see if the d -dimensional model has an analogous phase.

- We have generalised previous models which showed exact magnetisation plateaus for $s = \frac{1}{2}$ to higher spins. Interestingly, there is a fairly large range of the coupling parameter for which the ground state in the presence of an external

magnetic field can be solved exactly for all s . The spin- s model develops $4s$ plateaus. We have argued that, beyond the exact line, the plateau formation is through a different mechanism. This also implies that there is the possibility of a first order transition between two states of same magnetisation but different ordering pattern.

Our analysis has not been rigorous outside the exact regime. A more careful analysis, possibly numerical, is required to get the phase diagram in the full parameter space.

Appendix A

Solid angle for a dimer

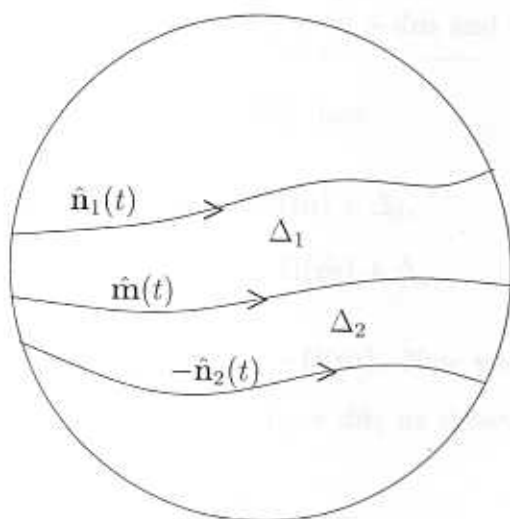


Figure A.1: $\hat{\mathbf{m}}(t)$, $\hat{\mathbf{n}}_1(t)$ and $-\hat{\mathbf{n}}_2(t)$ trace out closed curves on the sphere.

Let $\hat{\mathbf{n}}_1(t)$ and $\hat{\mathbf{n}}_2(t)$ be two unit vectors varying in time. Also let the motion be periodic with period T . Define,

$$\hat{\mathbf{n}}_1 = \sqrt{(1-l^2)} \hat{\mathbf{m}} + \mathbf{l}, \tag{A.1}$$

$$\hat{\mathbf{n}}_2 = -\sqrt{(1-l^2)} \hat{\mathbf{m}} + \mathbf{l}, \tag{A.2}$$

We now calculate the total solid angle subtended by $\hat{\mathbf{n}}_1(t)$ and $\hat{\mathbf{n}}_2(t)$ during one period. Let, $\Omega(\hat{\mathbf{n}}_\alpha)$ be the solid angle subtended by $\hat{\mathbf{n}}_\alpha(t)$ during one period. Then we can write $\Omega(\hat{\mathbf{n}}_\alpha)$ as the sum of $\Omega((-1)^\alpha \hat{\mathbf{m}})$ and the area of the strip between

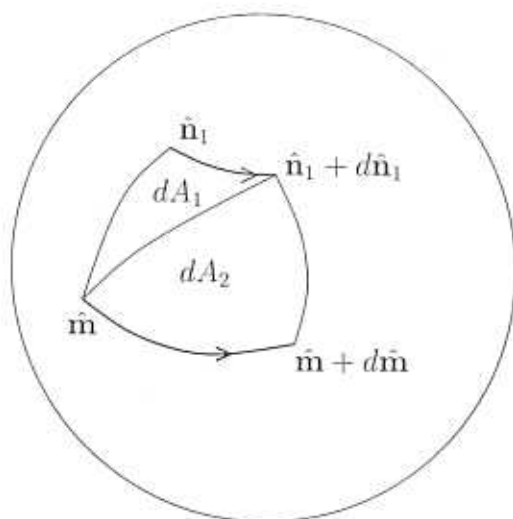


Figure A.2: The area swept as $\hat{\mathbf{m}} \rightarrow \hat{\mathbf{m}} + d\hat{\mathbf{m}}$ and $\hat{\mathbf{n}}_1 \rightarrow \hat{\mathbf{n}}_1 + d\hat{\mathbf{n}}_1$

$\hat{\mathbf{m}}(t)$ and $\hat{\mathbf{n}}_\alpha(t)$, say, Δ_α (see Fig. A.1). We have,

$$\Omega(\hat{\mathbf{n}}_1) = \Omega(\hat{\mathbf{m}}) + \Delta_1, \quad (\text{A.3})$$

$$\Omega(\hat{\mathbf{n}}_2) = -\Omega(\hat{\mathbf{m}}) + \Delta_2, \quad (\text{A.4})$$

where we have used the result $\Omega(-\hat{\mathbf{m}}) = -\Omega(\hat{\mathbf{m}})$. Now we triangulate the strip of area swept as $\hat{\mathbf{m}} \rightarrow \hat{\mathbf{m}} + d\hat{\mathbf{m}}$ and $\hat{\mathbf{n}}_1 \rightarrow \hat{\mathbf{n}}_1 + d\hat{\mathbf{n}}_1$ as shown in Fig. A.2. We then have,

$$\Delta_1 = \int_0^T (dA_1 + dA_2) \quad (\text{A.5})$$

dA_1 , the area of the triangle formed by $\hat{\mathbf{m}}$, $\hat{\mathbf{m}} + d\hat{\mathbf{m}}$ and $\hat{\mathbf{n}}_1 + d\hat{\mathbf{n}}_1$, can be calculated as follows (see Fig. A.2 and Fig. A.3).

$$\begin{aligned} dA_1 &= \left(d\hat{\mathbf{m}} \times \frac{1}{l} \cdot \hat{\mathbf{m}} \right) \left(\frac{1}{l} \right) s \\ &= \frac{1 \cdot \hat{\mathbf{m}} \times d\hat{\mathbf{m}}}{l^2} (1 - \sqrt{1 - l^2}). \end{aligned} \quad (\text{A.6})$$

Now define (see Fig. A.3),

$$\mathbf{k} \equiv \hat{\mathbf{m}} - \sqrt{1 - k^2} \hat{\mathbf{n}}_1 \quad (\text{A.7})$$

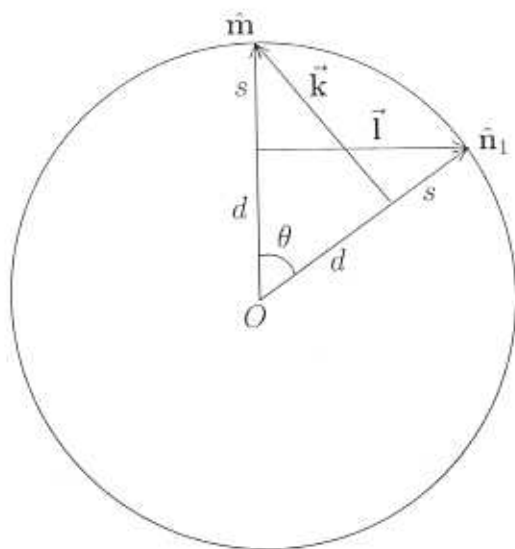


Figure A.3: Here $d \equiv \sqrt{1-l^2}$ and $s \equiv 1 - \sqrt{1-l^2}$.

Then the area of the triangle formed by $\hat{\mathbf{m}}$, $\hat{\mathbf{n}}_1$ and $\hat{\mathbf{n}}_1 + d\hat{\mathbf{n}}_1$ is,

$$\begin{aligned} dA_2 &= -\frac{\mathbf{k} \cdot \hat{\mathbf{n}}_1 \times d\hat{\mathbf{n}}_1}{k^2} \left(1 - \sqrt{1-k^2}\right) \\ &= \frac{1}{l^2} \left(1 - \sqrt{1-l^2}\right) \left[\sqrt{1-l^2} \mathbf{l} \cdot \hat{\mathbf{m}} \times d\hat{\mathbf{m}} + \mathbf{l} \cdot \hat{\mathbf{m}} \times d\mathbf{l}\right], \end{aligned} \quad (\text{A.8})$$

where we have used Eqs. (A.1) and (A.7) for $\hat{\mathbf{n}}$ and \mathbf{k} respectively. Substituting Eqs. (A.6) and (A.8) in Eq. (A.5) we get,

$$\Delta_1 = \int_0^T dt \left(\mathbf{l} \cdot \hat{\mathbf{m}} \times \partial_t \hat{\mathbf{m}} + \frac{(1 - \sqrt{1-l^2})}{l^2} \mathbf{l} \cdot \hat{\mathbf{m}} \times \partial_t \mathbf{l} \right). \quad (\text{A.9})$$

To obtain Δ_2 , we replace $\hat{\mathbf{m}}$ with $-\hat{\mathbf{m}}$ in the above expression.

$$\Delta_2 = \int_0^T dt \left(\mathbf{l} \cdot \hat{\mathbf{m}} \times \partial_t \hat{\mathbf{m}} - \frac{(1 - \sqrt{1-l^2})}{l^2} \mathbf{l} \cdot \hat{\mathbf{m}} \times \partial_t \mathbf{l} \right). \quad (\text{A.10})$$

Finally we get the total solid angle subtended by $\hat{\mathbf{n}}_1$ and $\hat{\mathbf{n}}_2$ by adding Eqs. (A.3) and (A.4), and using Eqs. (A.9) and (A.10).

$$\Omega(\hat{\mathbf{n}}_1) + \Omega(\hat{\mathbf{n}}_2) = 2 \int_0^T dt (\mathbf{l} \cdot \hat{\mathbf{m}} \times \partial_t \hat{\mathbf{m}}). \quad (\text{A.11})$$

Appendix B

Dimer perturbation theory to all orders

In this appendix we calculate the free energy for the dimer to all orders in κ . We also calculate the effective hamiltonian to all orders for the case in which the time derivatives are neglected.

B.1 Free Energy

The partition function for the dimer is,

$$Z = \text{Tr} \left[T \left(\exp - \int_0^\beta d\tau (h + \kappa h_{int}) \right) \right] \equiv e^{-F}, \quad (\text{B.1})$$

where,

$$h_0 = \frac{J}{2} (\mathbf{S}_1 + \mathbf{S}_2)^2, \quad (\text{B.2})$$

$$h_{int} = \mathbf{S}_1 \cdot \mathbf{m}_2(\tau) + \mathbf{S}_2 \cdot \mathbf{m}_1(\tau). \quad (\text{B.3})$$

Now we do a cumulant expansion for the free the Free energy.

$$F = \sum_n \frac{\kappa^n}{n!} \frac{\partial^n F}{\partial \kappa^n} \bigg|_{\kappa=0}, \quad (\text{B.4})$$

where,

$$\begin{aligned}
\frac{1}{n!} \frac{\partial^n F}{\partial \kappa^n} &= \frac{(-1)^n}{n!} \int \prod_{m=1}^n d\tau_n \langle T \left(\prod_{m=1}^n H_{int}(\tau_m) \right) \rangle_{conn} \\
&= (-1)^n \int_{-\infty}^{\infty} d\tau_1 \int_{-\infty}^{\tau_1} d\tau_2 \langle 0 | n^a(\tau_1) S^{b_2}(\tau_2) \dots S^{b_{n-1}}(\tau_{n-1}) n^c(\tau_n) | 0 \rangle \\
&\quad \times m^a(\tau_1) M^{b_2}(\tau_2) \dots M^{b_{n-1}} m^c(\tau_n) \quad (B.5)
\end{aligned}$$

The vacuum expectation value is,

$$\langle 0 | n^a(\tau_1) S^{b_2}(\tau_2) \dots S^{b_{n-1}}(\tau_{n-1}) n^c(\tau_n) | 0 \rangle = \frac{1}{4} \langle 0 | A_a(\tau_1) S^{b_2} \dots S^{b_{n-2}} i\epsilon^{b_{n-1}cc'} A_{c'}^\dagger(\tau_n) | 0 \rangle,$$

where A_a and A_a^\dagger are defined in Eqs. (4.20) and (4.21). Let $T_{bc}^a \equiv i\epsilon_{abc}$. Then,

$$\langle 0 | n^a(\tau_1) S^{b_2}(\tau_2) \dots S^{b_{n-1}}(\tau_{n-1}) n^c(\tau_n) | 0 \rangle = \frac{1}{4} e^{-(\tau_1 - \tau_2)} (T^{b_{n-1}} \dots T^{b_2})_{ca} \quad (B.7)$$

Using Eq. (B.7), we get

$$\begin{aligned}
\frac{1}{n!} \frac{\partial^n F}{\partial \kappa^n} &= \int_{-\infty}^{\infty} d\tau_1 \int_{-\infty}^{\tau_1} d\tau_n \frac{1}{(n-2)!} \int_{\tau_n}^{\tau_1} \prod_{m=2}^{n-1} d\tau_m T \left(\prod_{m=2}^{n-1} \text{T.M}(\tau_m) \right) \\
&\quad \times \frac{1}{4} e^{-(\tau_1 - \tau_n)} m^a(\tau_1) m^c(\tau_n)
\end{aligned}$$

Next we calculate the nth derivative of free energy at $\kappa = 0$.

$$\begin{aligned}
\left. \frac{1}{n!} \frac{\partial^n F}{\partial \kappa^n} \right|_{\kappa=0} &= \int_{-\infty}^{\infty} d\tau_1 \int_{-\infty}^{\tau_1} d\tau_2 \frac{1}{4} e^{-(\tau_1 - \tau_2)} m^a(\tau_1) \\
&\quad \times \frac{1}{(n-2)!} \int_{\tau_2}^{\tau_1} \prod_{m=1}^{n-2} d\tau'_m T \left(\prod_{m=1}^{n-2} \text{T.M}(\tau'_m) \right) m^c(\tau_2)_{ac}
\end{aligned}$$

We get the final expression for free energy as,

$$\begin{aligned}
F &= 1 + \kappa^2 \int_{-\infty}^{\infty} d\tau_1 \int_{-\infty}^{\tau_1} d\tau_2 \frac{1}{4} e^{-(\tau_1 - \tau_2)} m^a(\tau_1) \\
&\quad \times \sum_{n=0}^{\infty} \frac{\kappa^n}{n!} \int_{\tau_2}^{\tau_1} \prod_{m=1}^n d\tau'_m T \left(\prod_{m=1}^n \text{T.M}(\tau'_m) \right) m^b(\tau_2)_{ab}
\end{aligned}$$

In a more compact notation,

$$\begin{aligned}
F &= 1 + \kappa^2 \int_{-\infty}^{\infty} d\tau_1 \int_{-\infty}^{\tau_1} d\tau_2 \frac{1}{4} e^{-(\tau_1 - \tau_2)} m^a(\tau_1) \\
&\quad T \left(e^{\kappa \int_{\tau_2}^{\tau_1} d\tau' \text{T.M}(\tau')} \right) m^b(\tau_2)_{ab} \quad (B.8)
\end{aligned}$$

B.2 Effective hamiltonian

Next we calculate the effective hamiltonian in the case where the time derivatives are neglected. Then we can do the τ_2 integrals in the expansion for the free energy.

$$F = 1 + \kappa^2 \int_{-\infty}^{\infty} d\tau \sum_{n=0}^{\infty} \kappa^n c_n \quad (\text{B.9})$$

where,

$$\begin{aligned} c_n &= \frac{1}{4} m^a(\tau) \left(\mathbf{T} \cdot \mathbf{M}(\tau) \right)_{ab}^n m^b(\tau) \\ &= \frac{-1}{4} (A_a^\dagger - A_a) \left(\frac{\mathbf{T} \cdot \mathbf{S}}{2} \right)_{ab}^n (A_a^\dagger - A_b). \end{aligned}$$

Now $S^a A_b = 0$ and $A_a^\dagger S^b = 0$. Therefore,

$$\begin{aligned} c_n &= \frac{1}{4} A_a \left(\frac{\mathbf{T} \cdot \mathbf{S}}{2} \right)_{ab}^n A_b^\dagger \\ T_{ab}^c S^c A_b^\dagger &= -\epsilon_{cab} \epsilon_{cbd} A^{d\dagger} \end{aligned}$$

Thus,

$$\left(\mathbf{T} \cdot \mathbf{S} \right)_{ab} A_b^\dagger = 2A_a^\dagger \quad (\text{B.10})$$

Except for $n = 0$, we get,

$$c_n = \frac{1}{4} A_a A_b^\dagger = \frac{3}{4} \left(\frac{1}{4} - \mathbf{S}_1 \cdot \mathbf{S}_2 \right) \quad (\text{B.11})$$

and

$$c_0 = \frac{1}{4} m^a m^a = \left(\frac{3}{8} - \frac{1}{2} \mathbf{S}_1 \cdot \mathbf{S}_2 \right) \quad (\text{B.12})$$

Finally we have the effective hamiltonian as,

$$F = 1 + \kappa^2 \int_{-\infty}^{\infty} d\tau \left[\left(\frac{3}{8} - \frac{1}{2} \mathbf{S}_1 \cdot \mathbf{S}_2 \right) + \sum_{n=1}^{\infty} \kappa^n \frac{3}{4} \left(\frac{1}{4} - \mathbf{S}_1 \cdot \mathbf{S}_2 \right) \right] \quad (\text{B.13})$$

Thus under RG, κ flows to

$$\kappa' = \frac{\kappa^2}{2} + \frac{3\kappa}{4(1-\kappa)} \quad (\text{B.14})$$

Solving for $\kappa' = \kappa$, we get the fixed points as $\kappa^* = 0$ and 0.61 .

Bibliography

- [1] C. Waldtmann *et al.*, *Eur. Phys. J. B* **2**, 501 (1998).
- [2] R. Chitra *et al.*, *Phys. Rev. B* **52**, 6581 (1995).
- [3] S. Pati *et al.*, *Europhys. Lett.* **33**(9), 707 (1996).
- [4] C. K. Majumdar and D. K. Ghosh, *J. Math. Phys.* **10**, 1388 (1969).
- [5] C. K. Majumdar, *J. Phys. Condens. Matter* **3**, 911 (1969).
- [6] H. A. Bethe, *Z. Phys.* **71**, 205 (1931).
- [7] F. D. M. Haldane, *Phys. Lett.* **93A**, 464 (1983).
- [8] F. D. M. Haldane, *Phys. Rev. Lett.* **50**, 1153 (1983).
- [9] A. M. Polyakov, *Phys. Lett. B* **59**, 79 (1975).
- [10] E. Brezin and J. Zinn-Justin, *Phys. Rev. B* **14**, 3110 (1976).
- [11] I. Affleck, T. Kennedy, E. H. Lieb and H. Tasaki, *Commun. Math. Phys.* **115**, 477 (1988).
- [12] I. Affleck. *Fields, Strings and Critical Phenomena - Les Houches 1988*, North-Holland (1990).
- [13] M. A. Delgado *et al.*, *Phys. Rev. Lett.* **77**, 3443 (1996).
- [14] H. Levine, S. Libby and A. M. M. Pruisken, *Nucl. Phys. B* **240** [FS12] 30, 49, 71 (1984).

- [15] H. Levine, S. Libby and A. M. M. Pruisken, *Phys. Rev. Lett.* **51**, 20 (1983).
- [16] A. M. M. Pruisken, *Phys. Rev. Lett.* **61** 1297 (1988).
- [17] E. Witten, *Nucl. Phys. B* **235** 277 (1979).
- [18] A. M. M. Pruisken, *Phys. Rev. B* **32** 2636 (1985).
- [19] M. A. Baranov, A. M. M. Pruisken and B. Škorić, *Phys. Rev. B* **60** 16821 (1999).
- [20] A. M. M. Pruisken, B. Škorić and M. A. Baranov, *Phys. Rev. B* **60** 16838 (1999).
- [21] Th. Jolicoeur and J. C. Le Guillou, *Phys. Rev. B* **40** 2727 (1989).
- [22] B. S. Shastry and B. Sutherland, *Physica* **108B**, 1069 (1981).
- [23] A. Laeuchli, S. Wessel and M. Sigrist, *Phys. Rev. B* **66**, 014401 (2002).
- [24] A. Koga and N. Kawakami, *Phys. Rev. Lett.* **82**, 4461 (2000).
- [25] M. Albrecht and F. Mila, *Europhys. Lett.* **34**, 145 (1996).
- [26] Z. Weihong, J. Oitmaa and C. J. Hamer, *Phys. Rev. B* **65**, 014408 (2002).
- [27] H. Kageyama *et al.*, *Phys. Rev. Lett.* **82**, 3168 (1999).
- [28] S. Miyahara and K. Ueda, *Phys. Rev. Lett.* **82**, 3701 (1999).
- [29] K. Hida, *J. Phys. Soc. Japan* **63**, 2359 (1994).
- [30] K. Okamoto, *Solid State Comm.* **98**, 245 (1995).
- [31] T. Tonegawa, T. Nakao and M. Kaburagi, *J. Phys. Soc. Japan* **65**, 3317 (1996).
- [32] Y. Narumi *et al.*, *Physica B* **246-247**, 509 (1998).
- [33] M. Oshikawa, M. Yamanaka and I. Affleck *Phys. Rev. Lett.* **78**, 1984 (1997).
- [34] T. Momoi and K. Totsuka, *Phys. Rev. B* **61**, 3231 (2000).

- [35] T. Momoi and K. Totsuka, *Phys. Rev. B* **62**, 15067 (2000).
- [36] E. Müller-Hartmann, R. R. P. Singh, C. Knetter and G. S. Uhrig, *Phys. Rev. Lett.* **84**, 1808 (2000).
- [37] A. Honecker, F. Mila and M. Troyer, *Eur. Phys. J. B* **15**, 227 (2000).
- [38] B. Sutherland, *Phys. Rev. B* **62**, 11499 (2000).
- [39] E. Fradkin. *Field Theories of Condensed Matter Systems*, Addison-Wesley (1991).
- [40] A. Perelemov. *Generalised Coherent States and their applications*, Springer-Verlag (1986).
- [41] R. Shankar and N. Read, *Nucl. Phys. B* **336**, 457 (1990).
- [42] H. Georgi, *Lie Algebras in Particle Physics*, The Benjamin/Cummings publishing company, Inc. (1982).
- [43] I. Kanter, *Phys. Rev. B* **39**, 7270 (1989).
- [44] B. S. Shastri and B. Sutherland, *J. Stat. Phys.* **33**, 477 (1983).
- [45] S. Miyahara and K. Ueda, *Phys. Rev. B* **61**, 3417 (2000).
- [46] M. P. Gelfand, *Phys. Rev. B* **43**, 8644 (1991).
- [47] I. Affleck, *Phys. Rev. B* **41**, 6697 (1990).